

25682



National Library
of Canada

Bibliothèque nationale
du Canada

CANADIAN THESES
ON MICROFICHE

THÈSES CANADIENNES
SUR MICROFICHE

NAME OF AUTHOR/NOM DE L'AUTEUR Thomas Walter Mojelsky

TITLE OF THESIS/TITRE DE LA THÈSE Kinetic, Theoretical and Stereochemical Aspects
of Nitrogen Radical Reactions

UNIVERSITY/UNIVERSITÉ Simon Fraser University

DEGREE FOR WHICH THESIS WAS PRESENTED/
GRADE POUR LEQUEL CETTE THÈSE FUT PRÉSENTÉE Ph.D.

YEAR THIS DEGREE CONFERRED/ANNÉE D'OBTENTION DE CE DEGRÉ 1975

NAME OF SUPERVISOR/NOM DU DIRECTEUR DE THÈSE Dr. Y. L. Chow

Permission is hereby granted to the NATIONAL LIBRARY OF
CANADA to microfilm this thesis and to lend or sell copies
of the film.

The author reserves other publication rights, and neither the
thesis nor extensive extracts from it may be printed or other-
wise reproduced without the author's written permission.

*L'autorisation est, par la présente, accordée à la BIBLIOTHÈ-
QUE NATIONALE DU CANADA de microfilmer cette thèse et
de prêter ou de vendre des exemplaires du film.*

*L'auteur se réserve les autres droits de publication; ni la
thèse ni de longs extraits de celle-ci ne doivent être imprimés
ou autrement reproduits sans l'autorisation écrite de l'auteur.*

DATED/DATE Feb. 24, 1975 SIGNED/SIGNÉ _____

PERMANENT ADDRESS/RÉSIDENCE FIXE _____

KINETIC, THEORETICAL AND STEREOCHEMICAL
ASPECTS OF NITROGEN RADICAL REACTIONS

by

THOMAS WALTER MOJELSKY

M. Sc., University of Alberta, 1968

A DISSERTATION SUBMITTED IN PARTIAL FULFILLMENT
OF THE REQUIREMENTS FOR THE DEGREE OF
DOCTOR OF PHILOSOPHY
in the Department
of
Chemistry

© THOMAS WALTER MOJELSKY, 1975

SIMON FRASER UNIVERSITY

February 1975

All rights reserved. This thesis may not be
reproduced in whole or in part, by photocopy
or other means, without permission of the author.

APPROVAL

Name: Thomas Walter Mojelsky

Degree: Doctor of Philosophy

Title of Thesis: Kinetic, Theoretical and Stereochemical
Aspects of Nitrogen Radical Reactions.

Examining Committee:

Dr. Y. L. Chow
Senior Supervisor

Dr. K. U. Ingold
External Examiner
National Research
Council, Ottawa

Dr. C. H. W. Jones
Examining Committee

Dr. A. C. Oehlschlager
Examining Committee

Dr. K. E. Rieckhoff
Examining Committee

Date Approved:

February 3, 1975

PARTIAL COPYRIGHT LICENSE

I hereby grant to Simon Fraser University the right to lend my thesis or dissertation (the title of which is shown below) to users of the Simon Fraser University Library, and to make partial or single copies only for such users or in response to a request from the library of any other university, or other educational institution, on its own behalf or for one of its users. I further agree that permission for multiple copying of this thesis for scholarly purposes may be granted by me or the Dean of Graduate Studies. It is understood that copying or publication of this thesis for financial gain shall not be allowed without my written permission.

Title of Thesis/Dissertation:

Kinetic, Theoretical and Stereochemical Aspects of
Nitrogen Radical Reactions

Author:

(signature)

Thomas Walter Mojelsky

(name)

Feb. 24, 1975

(date)

ABSTRACT

KINETIC, THEORETICAL AND STEREOCHEMICALASPECTS OF NITROGEN RADICAL REACTIONS

This work can be partitioned into three sections.

1) Polar Effects of Piperidinium Radical Addition to Substituted Styrenes

In the competitive photoaddition of N-nitrosopiperidine to a binary system of styrenes, an electron-donating substituent facilitates the piperidinium radical addition. A series of eight para- and meta-substituted styrenes were found to give a better correlation with Hammett σ rather than with σ^+ constants and to give a ρ value of -1.34 which was among the larger ρ values of various known radical addition reactions. The polar effects observed were interpreted in terms of ground state electrostatic attraction between the positive charge of the aminium radical and the π electrons of the styrenes rather than resonance stabilization at the transition state. The quantum yield of the N-nitrosopiperidine photoaddition was dependent on the nitrosamine concentration but not on the styrene concentration thus suggesting the occurrence of radical chain processes.

2) Calculations of the Σ - Π Electronic States of Amido Radicals

INDO SCF MO calculations were performed on selected conformers of a number of variously substituted amido and closely related radicals. An N-methyl substituent conferred Π electronic

ground state character to the amido radical, whereas an N-hydrogen substituent conferred Σ electronic state character. Substituents at the carbonyl carbon had no effect upon the radical electronic state. Imido radicals were all shown to be Σ . On the basis of limited experimental data from the literature and from the calculations done, it is postulated that those amido radicals possessing Σ electronic states undergo addition to olefins whereas those radicals of Π character abstract hydrogen preferentially.

3) Transition State Geometry in Intramolecular Hydrogen Abstraction by Amido Radicals

Amido radicals generated from photolysis of N-bromamides can undergo either intra- or intermolecular hydrogen abstraction. The six atoms participating in the transition state of intramolecular hydrogen abstraction can assume either a hexagonal or a pentagonal geometry. Calculations suggest that coplanarity of the six atomic centres favours the hydrogen transfer process. The requirements of coplanarity of the intramolecular hydrogen transfer were tested using carboxamido radicals generated from photolysis of N-bromo-trans-4-t-butyl-cis-2-methyl-N-t-butyl-cyclohexanecarboxamide and of the corresponding trans-trans compound. The conformation energy facilitates the attainment of coplanarity in the cis isomer but inhibits in the trans. From experiment it was found that the cis radical gave the greater amount of intramolecular hydrogen abstraction product.

To those who toil like Sisyphus
without the prospect of fame or recompense
in pursuit of the reification of ephemeral ideas
this work is respectfully dedicated.

ACKNOWLEDGEMENTS

The author wishes to express sincere gratitude to Dr. Y. L. Chow for his informative discussions, for his sagacious chemical counsel and for his genuine interest in the research progress. He also wishes to thank his graduate student colleagues, especially R. A. Perry and K. S. Pillay, for their countless beneficial suggestions, discussions and general assistance. The contributions of Drs. K. Hanaya, T. Tezuka, A. C. Oehlschlager, P. Perkins and M. Tichy to the successful completion of the graduate requirements and research is gratefully acknowledged. Finally, without the labours of the technical and support staff of Simon Fraser University, this project would have amounted to naught.

7

CONTENTS

PART A		<u>Page</u>
<u>Chapter 1</u>	<u>Introduction</u>	1
<u>Chapter 2</u>	<u>Results</u>	
2-1	General	
2-1-1	Preparation of Styrenes	7
2-1-2	Photoaddition of NNP to Styrenes	7
2-1-3	Kinetic Monitoring of Photoaddition of NNP to Styrenes	8
2-2	Quantum Yield Determinations	11
2-3	Effects of Altering Concentration of Reactants	11
2-4	Relative Reactivities	13
2-5	Complex Formation Between <i>p</i> -Methoxystyrene and NNP	18
2-6	Some Preliminary Ground State INDO Calculations	18
2-7	Competition Between Diazenium Salt and NND as Substrates	21
2-8	Some Properties of Other Aminium Radicals	
2-8-1	Photoaddition of N-Nitroso-N-Methylbenzylamine to Styrene	21
2-8-2	Competition Between Intra- and Intermolecular Addition	22
<u>Chapter 3</u>	<u>Discussion</u>	
3-1	General	23
3-2	Polar Effects	24
3-3	Quantum Yields	29
3-4	Qualitative Ranking of Nitrosamine Reactivity	29

3-5	The Photophysical Process of Nitrosamine Photolysis	30
<u>Chapter 4</u>	<u>Experimental</u>	
4-1	General Techniques	32
4-2	Materials	33
4-3	Preparation of Substituted Styrenes	33
4-3-1	Synthesis of <u>p</u> -Methylstyrene (5-2)	34
4-3-2	Synthesis of <u>p</u> -Chlorostyrene (5-3)	34
4-3-3	Synthesis of <u>p</u> -Methoxystyrene (5-4)	35
4-3-4	Synthesis of <u>p</u> -Cyanostyrene (5-5)	35
4-3-5	Synthesis of <u>m</u> -Methylstyrene (5-6)	36
4-3-6	Synthesis of <u>m</u> -Methoxystyrene (5-7)	37
4-3-7	Synthesis of <u>m</u> -Acetamidostyrene (5-8)	37
4-3-8	Synthesis of <u>m</u> -Bromostyrene (5-9)	39
4-4	General Conditions for Preparative Photolysis	39
4-5	General Procedure for Kinetic Study of NNP Photoaddition to Substituted Styrenes	40
4-6	Quantum Yield Determinations	42
4-7	Spectroscopic Attempt to Detect Complex Formation	44
4-8	INDO Molecular Orbital Calculations	44
4-9	Other Nitrosamines Investigated	
4-9-1	Preparation of N-Nitroso-N-Methylbenzylamine <u>7</u>	45
4-9-2	Photoaddition of <u>7</u> to Styrene	45
4-9-3	Competitive Intra- and Intermolecular Photo- addition	46
4-10	Competitive Photoaddition Between NNP and Diazenium Salt (<u>6</u>) to Styrene	47

PART B

<u>Chapter 5</u>	<u>Introduction</u>	
5-1	General	48
5-2	General Objectives	49
5-3	Experimental Investigations of Amido Radicals	50
5-3-1	Amido Radicals	51
5-3-2	Structurally Related Radicals	52
5-4	Chemical Reactivity of Amido Radicals	53
5-4-1	Amido Radicals	55
5-4-2	Imido Radicals	56
5-5	The INDO MO Method	57
<u>Chapter 6</u>	<u>Results</u>	
6-1	General	59
6-2	Allyl Radical	61
6-3	Amido Radicals	
6-3-1	N-Methylacetamido Radical	66
6-3-2	Other Amido Radicals	72
6-4	Imido Radicals	75
6-5	Carbomethoxyamino Radicals	77
6-6	Urea Radicals	79
<u>Chapter 7</u>	<u>Discussion</u>	
7-1	General	81
7-1-1	Orbital Occupancy	83
7-1-2	Other Calculated Parameters	83
7-2	Structure, Configuration and Reactivity Relationships	

7-2-1	Qualitative Features of Amido Radical Structure and Configuration	86
7-2-2	Reactivities of Σ - Π Radicals	88
PART C		
<u>Chapter 8</u>	<u>Introduction</u>	
8-1	Transition States for Hydrogen Abstraction	90
8-2	Examples of 1,5-Intramolecular Hydrogen Transfer	91
8-3	Geometry of Transition States	91
8-4	Objective	93
8-5	The Cyclohexane Ring System	95
<u>Chapter 9</u>	<u>Results</u>	
9-1	Interatomic Distances for Intramolecular Hydrogen Abstraction	99
9-2	Physical Properties of N-Haloamides	
9-2-1	Preparation of N-Bromamides	99
9-2-2	Spectroscopic Properties of N-Haloamides	101
9-3	Photolysis of N-Bromamides	
9-3-1	Photolysis of Rigid N-Bromamides - N-Bromo- toluamide	104
9-3-2	Photolysis of Semi-Rigid N-Bromamides	
9-3-2-1	Photolysis of <u>trans</u> -N-Bromo-4- <u>t</u> -Butyl- <u>trans</u> - 2-Methyl-N- <u>t</u> -Butylcyclohexanecarboxamide (26-3)	105
9-3-2-2	Photolysis of <u>trans</u> -N-Bromo-4- <u>t</u> -Butyl- <u>cis</u> - 2-Methyl-N- <u>t</u> -Butylcyclohexanecarboxamide (27-3)	106

9-4	Competitive Intra- and Intermolecular Hydrogen Abstraction Processes	107
<u>Chapter 10</u>	<u>Discussion</u>	
<u>Chapter 11</u>	<u>Experimental</u>	
11-1	General Techniques	114
11-2	Preparation of Reagents	
11-2-1	Preparation of N- <u>t</u> -Butylacetamide	114
11-2-2	Preparation of <u>t</u> -Butylhypobromite	114
11-2-3	Preparation of <u>t</u> -Butylhypochlorite	114
11-2-4	Preparation of N- <u>t</u> -Butyltoluamide (<u>29-1</u>)	115
11-2-5	Preparation of <u>trans</u> -4- <u>t</u> -Butyl- <u>trans</u> -2- Methyl-N- <u>t</u> -Butylcyclohexanecarboxamide (<u>26-2</u>)	115
11-2-6	Preparation of <u>trans</u> -4- <u>t</u> -Butyl- <u>cis</u> -2-Methyl- N- <u>t</u> -Butylcyclohexanecarboxamide (<u>27-2</u>)	115
11-3	General Procedure for N-Halogenation	
11-3-1	Preparation of N-Chloramides	116
11-3-2	Preparation of N-Bromamides	116
11-4	Spectroscopic Investigations of Substituted N-Haloacetamides	117
11-4-1	Infrared Determinations	117
11-4-2	Nuclear Magnetic Resonance Investigations	118
11-4-3	Raman Investigations	118
11-4-4	Ultraviolet Spectral Studies	118
11-5	Photolysis of Substituted Toluamines	
11-5-1	Photolysis of N-Bromo-N-Methyltoluamide (<u>28-2</u>)	119

11-5-2	Photolysis of N-Bromo-N- <u>t</u> -Butyltoluamide (<u>29-2</u>)	120
11-6	Photolyses of Isomeric Cyclohexanecarboxamides	
11-6-1	Photolysis of <u>trans</u> -Bromamide <u>26-3</u>	121
11-6-2	Photolysis of <u>cis</u> -Bromamide <u>27-3</u>	122
11-7	Quantitative Aspects of Isomeric N-Bromo- cyclohexanecarboxamide Photolysis	
11-7-1	General Procedure	124
11-7-2	Quantitative Analysis	
11-7-2-1	Photolysis of <u>trans</u> -Bromamide <u>26-3</u>	124
11-7-2-2	Photolysis of <u>cis</u> -Bromamide <u>27-3</u>	125
11-7-3	Solvents Used in the Photolyses	125
	<u>References</u>	126

LIST OF TABLES

Table		Page
2-1	The Yields and Physical Data of the Substituted α -Piperidinoacetophenone Oximes	9
2-2	The Photoaddition of NNP (0.04M) to Styrenes (0.04M)	12
2-3	Variation of Concentrations in the Photoaddition of NNP to Styrene	14
2-4	The Competitive Photoaddition of NNP to Styrenes	16
2-5	INDO Open Shell Calculations of Selected Geometries of Dimethylaminium Radical	19
2-6	INDO Closed Shell Calculations of Various Forms of N-Nitroso-N,N-Dimethylamine	20
3-1	The ρ -Values of Some Radical Addition Reactions	26
5-1	Radical Structures and Configurations Assigned from ESR Data	54
6-1	Calculated Energies of Allyl Radical Conformers	62
6-2	Spin Densities of Allyl Radical Conformers	62
6-3	Eigenvalues of Two Allyl Radical Conformers	65
6-4	Calculated Energies of N-Methylacetamido Radical Conformers	68
6-5	Spin Densities of N-Methylacetamido Radical Conformers	70
6-6	Eigenvalues of Two N-Methylacetamido Radical Conformers	71
6-7	Calculated Energies and Spin Densities of Other Amido Radicals	73

6-8	Calculated Energies and Spin Densities of Imido Radicals	76
6-9	Calculated Energies and Spin Densities of Carbo-methoxyamino Radicals	78
6-10	Calculated Energies and Spin Densities of Urea Radicals	80
9-1	Calculated Carbon-Nitrogen Interatomic Distances of Model Radicals	100
9-2	Infrared and Raman Absorptions of N-Haloamides	102
9-3	Nuclear Magnetic Resonance Chemical Shifts in N-Haloamides	103
9-4	Ultraviolet Absorption Properties of N-Haloamides	103
9-5	Solvent Composition and Hydrogen Abstraction Products	109

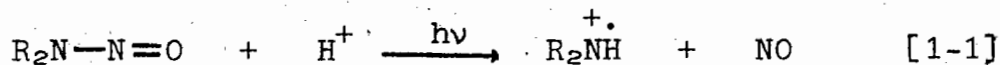
LIST OF FIGURES

FIGURE		<u>Page</u>
2-1	The relative reactivities of substituted styrenes toward the piperidinium radical addition as a function of substituent constant.	17
6-1	Total energy and nuclear repulsion energy as a function of degrees methylene rotation.	63
6-2	Total energy and nuclear repulsion energy as a function of degrees of conformer rotation.	69
8-1	The qualitative potential energy curve of cyclohexane as a function of the dihedral angle.	97

PART A

CHAPTER 1INTRODUCTION

The photochemistry of nitrosamines is inextricably associated with the reactivity and reactions of aminium radicals. In the presence of dilute acid, N-nitrosamines rapidly undergo homolysis prior to subsequent photoreactions (1,2) and generate the aminium radical and NO.



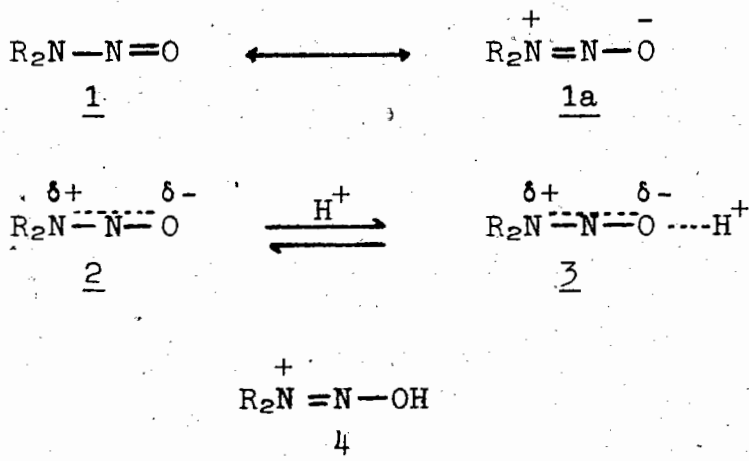
The flash excitation technique has been employed to establish the identity of the species of the primary photoprocess (3) depicted in [1-1].

Since the initial description of nitrosamine photochemistry (1,4), much effort has been expended to determine the mechanism, the scope and limitation, and the reactivity of aminium radicals (3,5). Misisci and co-workers (5) have generated aminium radicals by photolyzing N-chloramines in concentrated sulphuric acid-acetic acid medium. Reaction species likely involving aminium radicals can also be found in metal ion (Fe^{+2} or Tl^{+3}) reactions with N-haloamines (6,7) or from the reaction of metal ions with hydroxylamine (8), hydroxylamine-O-sulphonic acid (9) or tertiary amine oxides (10).

The reactivity of the aminium radicals resembles that of

uncharged radicals in many ways. The aminium radical may undergo addition to olefins (3) or addition to aromatic nuclei (5,11). Alternately the aminium radical may abstract a hydrogen atom from substituted toluenes (12) or from a hydrogen-donating solvent (3). They may also undergo disproportionation (13), termination (14) and chain propagation (15) reactions.

In the presence of dilute acid, N-nitrosodialkylamines rapidly undergo photoaddition to olefins (1). Experimental evidence suggests that the intermediate of this reaction is the positively charged aminium radical (16). This radical and the concomitantly generated nitric oxide add to the double bond of olefins to form, after tautomerization, the appropriate α -amino-oxime. SCF calculations on ground state nitrosamine (17) suggest that there is a 48% contribution of polar resonance form 1a. The proton coordinates with the more electron rich nitroso-



oxygen atom as in 3. At low concentrations of acid (pH > 1) association takes place through hydrogen bonding while at higher concentrations of acid (> 2M H₂SO₄) the nitrosamine is proton-

ated as in 4 (18). The fully protonated nitrosamine does not undergo photoaddition (19).

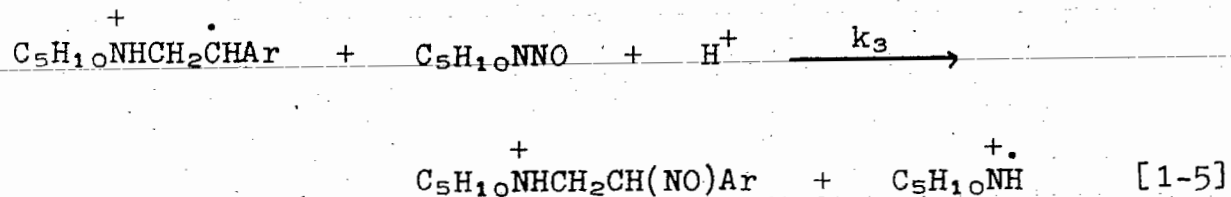
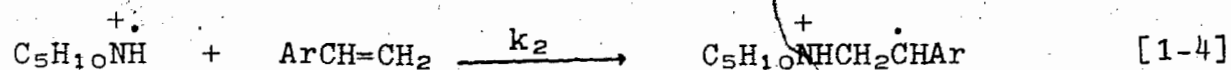
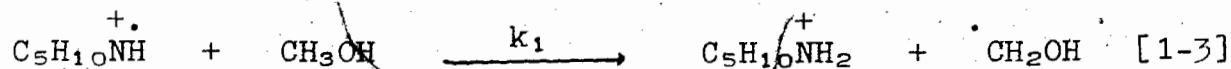
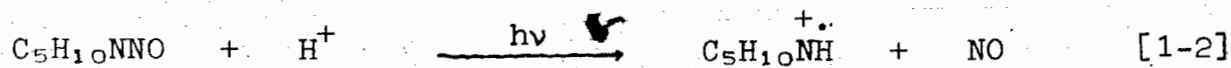
Flash photolysis studies of acidified N-nitrosopiperidine (16) have resulted in the detection of a transient having identical absorption characteristics to that generated from N-chloropiperidine. Piperidinium radical has been established (20) as the intermediate in the photolysis of N-chloropiperidine.

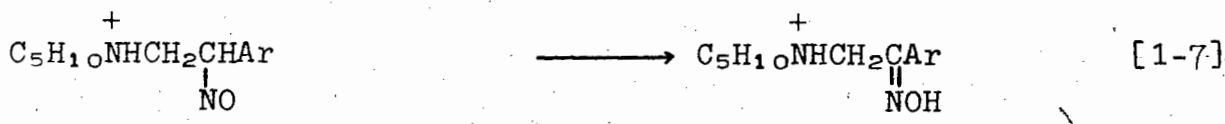
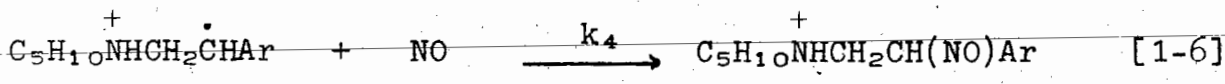
The piperidinium radical obtained from nitrosamine flash photolysis was unaffected by the presence of oxygen or by the band of irradiation ($n \rightarrow \pi^*$ or $\pi \rightarrow \pi^*$ excitation). The piperidinium radical decays with first order rate constant of $1.85 \times 10^4 \text{ sec}^{-1}$ (3). Based upon the transient reaction rates in acidified aqueous methanol and in cyclohexene, piperidinium undergoes photoaddition to cyclohexene about 5000 times faster than it abstracts a hydrogen atom from methanol (16).

Since the aminium radical carries a positive charge (3,5,12), there is good reason to suspect that it is an electrophilic species. Neale and Gross (12) have studied the relative reactivities of the substituted toluenes toward hydrogen abstraction by piperidinium radical generated from N-chloropiperidine photolysis in 2M H_2SO_4 in acetic acid. They concluded that the presence of a positive charge on the piperidinium radical did not lead to an unusually enhanced polar effect at the transition state for hydrogen abstraction. In general competitive hydrogen abstractions from m- and p-substituted toluenes have been widely utilized successfully to obtain Hammett correlations (21). However, in contrast, there are only a few reported studies in

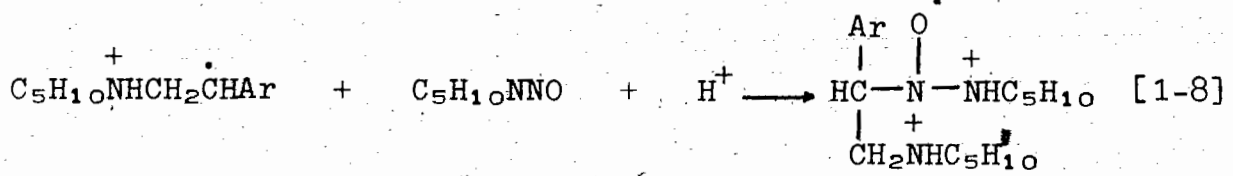
the literature of similar correlation of radical addition to m- and p-substituted styrenes and stilbenes (22,23,24). All the reported radicals studied in these hydrogen abstraction and addition reactions gave negative reaction constants ($-\rho$ values) of varying magnitude. Generally the correlation has been found to result in a better fit with σ^+ substituent constants than with σ constants.

In this section the addition of photochemically generated aminium radicals to variously m- and p-substituted styrenes will be discussed. The medium conditions used were dilute acid and methanol. The competitive addition reactivities of the piperidinium radical will be compared with those obtained from the radical generated under strongly acidic conditions (5,12). Under steady state irradiation, N-nitrosopiperidine (NNP) photolysis in methanol and in the presence of dilute hydrochloric acid and styrene is believed to follow the mechanism shown below (3,13,25,26).





From flash photolysis studies (16) it has been shown that the observed decay rate of the piperidinium radical is proportional to the concentration of the olefin but is independent of the concentration of NNP. In this experiment very high concentrations of aminium radicals and NO are produced. As a result under these conditions equation [1-5] is probably rather unimportant. However, under the regular photolytic conditions it is assumed that the propagation step of the above mechanistic scheme (k_3) is rate determining and is, hence, slower than the addition step (k_2). Equation [1-5] may in fact represent a sequence of events. It is conceivable that the adduct of equation [1-8] formed analogously to amino radical addition to



2-nitroso-2-methylpropane (27) is a short-lived intermediate. The chain length of the photoaddition process will be given by equation [1-9].

$$\text{chain length} = \frac{k_3[C_5H_{10}NNO]}{k_4[NO]} \quad [1-9]$$

The determined quantum yield of NNP disappearance represented the

minimum chain length of the photoaddition process.

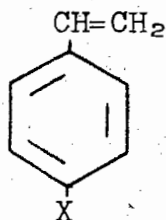
The reactivity of styrenes in terms of their absolute rate constants toward the piperidinium radical is estimated¹ to be 10^7 to $10^8 \text{ M}^{-1} \text{ sec}^{-1}$. Since the rate of combination of organic free radicals is of the order 10^8 to $10^9 \text{ M}^{-1} \text{ sec}^{-1}$ (28), the differences of the free energies of activation of addition of the styrenes will be fairly small. The competitive addition to two styrenes, one substituted and the other not, in equimolar initial concentrations is utilized to obtain the reactivity ratio k_x/k_H . The k_x and k_H are the observed pseudo-first order rate constants of the piperidinium radical addition to X-substituted and to styrene respectively. This ratio is a measure of the partition of the piperidinium radical reaction toward the styrenes and is proportional to the two different activation free energies of the addition reaction.

¹ From flash photolysis of NNP in the presence of trans-1,3-pentadiene, it was shown that the aminium radical reacted with the diene with the bimolecular rate constant of $6.25 \times 10^7 \text{ M}^{-1} \text{ sec}^{-1}$. (A. J. Cessna, unpublished results.)

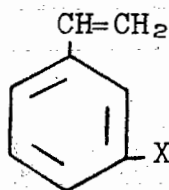
CHAPTER 2

RESULTS2-1 General2-1-1 Preparations of Styrenes

All the styrenes except 5-3 and 5-7 used in this project were synthesized by way of dehydration of the appropriate carbinols which in turn were formed from either Grignard condensation of CH_3MgBr with the appropriate aldehyde or from NaBH_4 reduction of the substituted acetophenone. The dehydration step was achieved using KHSO_4 and relatively high temperatures (approximately 200°C). Even the presence of hydroquinone in the flask was unable to inhibit completely the polymerization of the formed styrenes which were isolated



5-1 X = H
5-2 X = CH_3
5-3 X = Cl
5-4 X = OCH_3
5-5 X = CN



5-6 X = CH_3
5-7 X = OCH_3
5-8 X = NHCOCH_3
5-9 X = Br

in 30 to 50% yield. The p-methoxystyrene 5-3 was formed by thermal decarboxylation of p-methoxycinnamic acid. The m-acetamidostyrene 5-7 was synthesized by the reductive acetylation of m-nitrostyrene.

2-1-2 Photoaddition of NNP to Styrenes

In methanolic solution containing dilute hydrochloric

acid, N-nitrosopiperidine (NNP) photolytically added to styrene to give very high yields of syn- and anti- α -piperidinoacetophenone oximes. In Table 2-1 are listed the styrenes used and the yields of the expected oximes along with some of their physical properties. The total percentage yield of syn- and anti-oximes in each photoaddition indicated that these styrenes react very efficiently with the piperidinium radical. The exception to the observed trend was p-cyanostyrene. The drastically reduced reactivity of this styrene was demonstrated by the low yield of the corresponding oxime and by the isolation of N-piperidinoformamide which is a photoreduction product of piperidinium radical reaction with methanol (13). There was no experimental evidence to suggest that the piperidinium radical had added to any aromatic nuclei of the styrenes or that there was any hydrogen abstraction from any of the substituents.

2-1-3 Kinetic Monitoring of Photoaddition of NNP to Styrene

For the purpose of kinetic investigation, the initial concentrations of hydrochloric acid, NNP and styrenes were fixed at 0.04 M each in methanol unless specified otherwise. The substituted styrenes possessed no absorption greater than 300 nm and, hence, were stable under the adopted photolysis conditions. The eight chosen styrenes of both meta- and para-substitution had suitably different σ constants.

Table 2-1

The Yields and Physical Data of the Substituted α -Piperidinoacetophenone Oximes

Substituent	Crude Oximes				Syn-Oxime	
	Yield (%)	Ratio (syn:anti)	ν -C-CH ₂ -N (r value) ^b	IR (cm ⁻¹)	M. P. (°C)	Analysis ^c C H N
H	90	9:1	6.25(1.8) 6.65(0.2)	3150 979 940	117- 117.5	- - -
p-OCH ₃	80	9:1	6.25(1.8) 6.70(0.2)	3400 1075 835	108	67.97 8.25 11.38 (67.72 8.12 11.28)
p-CH ₃	91	85:15	6.30(1.7)	3400 995 825	144- 145	72.68 8.75 12.18 (72.48 8.68 12.06)
p-Cl	85	85:15	6.30(1.7) 6.65(0.3)	3160 1090 1070 835	137- 138	61.89 6.84 11.29 (61.78 6.78 11.08)
p-CN ^d	47	8:2	6.30(1.6) 6.70(0.4)	3250 2230 985 825	141- 144	- - -

Table 2-1 (continued)

Substituent	Crude Oximes			Syn-Oxime			
	Yield (%)	Ratio (syn:anti) (τ value)	$\nu_{\text{C-CH}_2\text{-N}}$ IR (cm^{-1})	M. P. ($^{\circ}\text{C}$)	Analysis ^c		
m-Br	93	10:0	3310 1050	102- 103	C 52.47 52.54	H 5.86 5.77	N 9.26 9.43
m-OCH ₃	81	8:2	3280 1035	98- 99	C 67.97 67.72	H 8.20 8.12	N 11.36 11.28
m-CH ₃	81	10:0	3300 1035	92.5- 93	C 72.33 72.38	H 8.72 8.68	N 11.94 12.06
m-NHCOCH ₃	85	95:5	3310 985	157- 158	C 65.49 65.43	H 7.61 7.69	N 15.40 15.26

a The percentages are isolated yields of the mixture of the syn- and anti-oximes and represent the lower limit since thorough extraction gives additional product (5-10%).

b The chemical shifts of the α -methylene protons (singlets) in the mixture of the syn- and anti-oximes isolated from the photoaddition. The integration is given in the parenthesis.

c The calculated % are given in the parenthesis below the corresponding "found" values.

d The sample was contaminated with a trace amount of the bromide compound.

2-2 Quantum Yield Determinations

The quantum yields of NNP disappearance (ϕ_N) and the pseudo-first order rate constants of the styrene disappearance (k_x) were determined under the identical conditions used in kinetic studies except that only one styrene was present in the photolysis solution. As shown in Table 2-2, ϕ_N varied between 6 and 10 and irregularly with respect to the nature of the substituent. Since the product analysis showed that the yields of the oximes were nearly quantitative, the ϕ_N probably will represent the chain length of the addition reaction provided radical recombination is minimal. In the photoaddition to the much less reactive *p*-cyanostyrene, the piperidinium radical also underwent reaction with methanol. Therefore, ϕ_N represented the sum of the quantum yields of both addition and reduction processes. Under identical irradiation conditions, the observed rate constants (k_x) varied without a discernible general trend. The rate constants were the products of two variables, the bimolecular rate constant (k_2) and the steady-state concentration of the piperidinium radical. To obtain relative reactivities it was, therefore, necessary to perform the competitive addition reaction experiments.

2-3 Effects of Altering Concentration of Reactants

In order to examine the effects of the reactant concentrations on the addition mechanism, quantum yields, ϕ_N , and the pseudo-first order rate constant, k_H , under varying

Table 2-2The Photoaddition of NNP (0.04M) to Styrenes (0.04M)

<u>XC₆H₄CH = CH₂</u>	<u>k_x x 10⁴</u> <u>(sec⁻¹)</u>	<u>φ_N</u>
p-OCH ₃	0.77	6.2
p-CH ₃	0.72	7.1
<u>m</u> -CH ₃	1.13	7.5
H	1.36	8.0
p-Cl	0.69	10.1
<u>m</u> -Br	1.05	7.4
p-CN	0.64	10.1

conditions were investigated. A four-fold variation of NNP concentration was used as well as a three-fold variation of styrene concentration. The good linear relationship of the plot of k_H and ϕ_N against time verified that up to 100 minutes reaction time, the reaction pattern was not affected by the length of photolysis nor the concentration of the reactants.

From Table 2-3 it can be seen the ϕ_N remained constant as long as the NNP concentration was kept constant but increased when the NNP concentration was increased. The chain length however is inversely proportional to the unknown NO concentration. It is believed that the steady state concentration of the aminium radical was increased concomitantly with ϕ_N . This in turn increased the magnitude of the observed rate constant for styrene addition since $k_H = k_2[C_5H_{10}NH^+]$. In the presence of higher concentrations of styrene, the lowering of k_H (Table 2-3) was to be expected since the steady state concentration of $[C_5H_{10}NH^+]$ was reduced. These measurements ascertained that the analytical procedures were satisfactory and established the general conditions for the competitive reaction of the piperidinium radical with the styrenes.

2-4 Relative Reactivities

Styrene was chosen as the standard substrate in the determination of relative reactivities. The competitive addition of the piperidinium radical was carried out in the presence of one of the para- or meta-substituted styrenes.

Table 2-3

Variation of Concentrations in the Photoaddition
of NNP to Styrene

<u>Concentration (M)</u> <u>NNP</u>	<u>Styrene</u>	$k_H \times 10^4$ <u>(sec⁻¹)</u>	ϕ_N
0.04	0.04	1.36	8.0
0.08	0.04	1.84	9.1
0.12	0.04	2.22	10.1
0.16	0.04	2.29	12.1
0.04	0.08	0.52	7.6
0.04	0.12	0.46	7.9

In each run the pseudo-first order rate constants of the addition to styrene (k_H) and that of substituted styrene were calculated. The results are given in Table 2-4. In the p-methoxystyrene - styrene experiment, the piperidinium radical underwent addition exclusively with the more electron-rich olefin, the p-methoxystyrene. Conversely, in the p-cyanostyrene - styrene experiment, styrene was consumed exclusively. These results unambiguously indicated that the aminium radical attack was electrophilic in nature and the relative reactivities in these couples were too far apart to be measured experimentally. The reactivity of p-methoxystyrene was subsequently determined relative to p-methylstyrene and normalized to give the k_X / k_H relationship shown in Figure 2-1. The p-cyanostyrene was not appreciably attacked by piperidinium radical even in competition with m-bromostyrene. Estimating that even 5% reaction of p-cyanostyrene had occurred, k_{CN} / k_H is still less than 0.085.

The plot of $\log k_X / k_H$ against σ constant values is shown in Figure 2-1. The reaction constant (ρ value) was computed using a least squares method to give -1.34 with r (correlation coefficient) of 0.978. When σ^+ values of the substituents were used, the relative reactivity of p-methoxystyrene and, to a lesser extent, that of p-methylstyrene deviated from the linearity established by the other points. Relatively wider scatter of points occurred when σ^+ was used, even when p-methoxystyrene was excluded. The resulting ρ value was found to be -1.04 with $r = 0.957$.

Table 2-4

The Competitive Photoaddition of NNP to Styrenes^a

$\text{XC}_6\text{H}_4\text{CH} = \text{CH}_2$ (0.04M)	$k_x \times 10^5$ (sec^{-1})	$\text{XC}_6\text{H}_4\text{CH} = \text{CH}_2$ (0.04M) ^d	$k_H \times 10^4$ (sec^{-1})	k_x/k_H
<u>p</u> -CH ₃	10.39	H	5.70	1.82
	7.82		4.04	1.93
<u>p</u> -Cl	6.89	H	8.95	0.77
	4.45		6.72	0.66
	3.16		7.22	0.44
	3.21		5.70	0.57
<u>p</u> -OCH ₃	4.95	<u>p</u> -CH ₃	3.09 ^b	1.99
	6.82		4.18 ^b	2.05
<u>m</u> -CH ₃	4.10	H	3.21 ^b	1.28
	3.67		2.42 ^b	1.51
	6.55		4.94	1.32
<u>m</u> -OCH ₃	5.47	H	5.14 ^b	1.06
	5.31 ^b		4.86 ^b	1.12
	4.09 ^b		3.67 ^b	1.09
<u>m</u> -NHCOCH ₃	2.34	H	3.98 ^b	0.58
	1.39		2.72 ^b	0.55
<u>m</u> -Br	2.87 ^b	H	8.09	0.356
	2.57 ^b		7.22	0.356
<u>p</u> -CN	-	<u>m</u> -Br	-	(0.085) ^c

- a Concentration of NNP and hydrochloric acid were 0.04M.
- b Except for the calculation of these rate constants, the correlation coefficients (r) were better than 0.985.
- c This ratio was estimated assuming 5% p-cyanostyrene had reacted after 100 minutes.
- d The standard styrene used in the particular experiments.

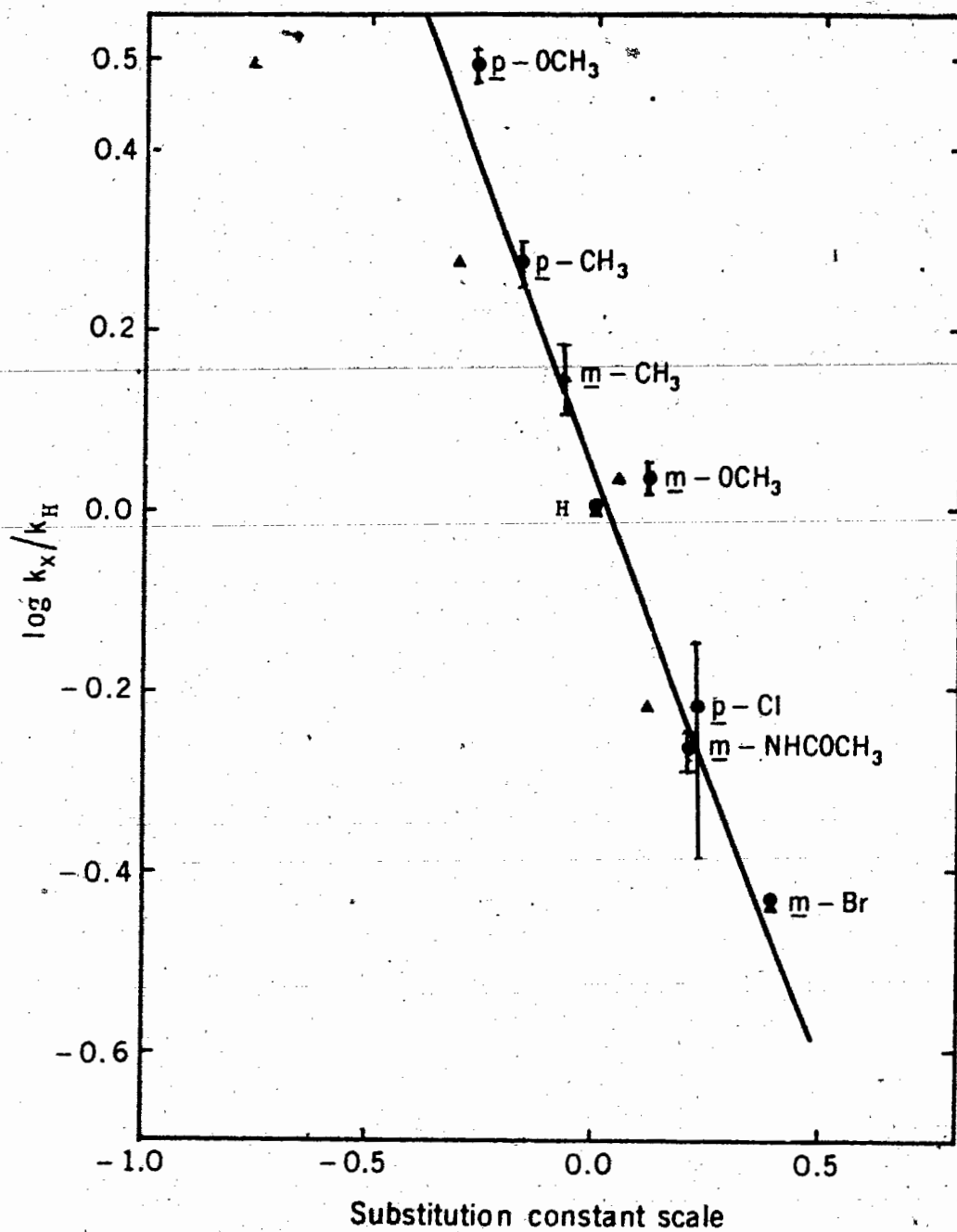


Figure 2-1 The relative reactivities of substituted styrenes toward the piperidinium radical addition as a function of substituent constant σ (•) and σ^+ (▲).

2-5 Complex Formation Between p-Methoxystyrene and NNP

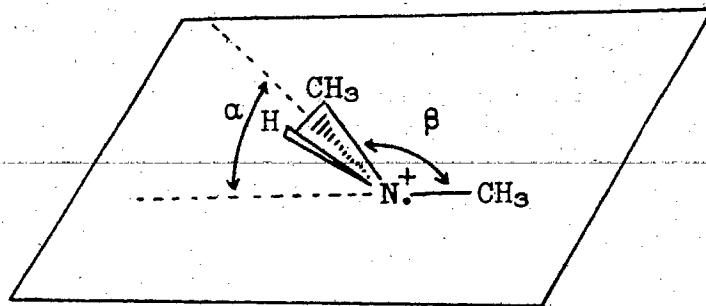
Ultraviolet spectroscopy was used to check for the presence of any charge transfer complex formation occurring in the ground state in a mixture of p-methoxystyrene and NNP, with and without the presence of dilute acid. Using special double-compartment corex cuvettes, no new absorption band was detected.

2-6 Some Preliminary Ground State INDO Calculations

Assuming that the chemical properties of N-nitrosodimethylamine (NND) and NNP are similar, some INDO SCF MO calculations were performed on the aminium radical generated from NND. In Table 2-5 are shown some representative calculation results. The results are preliminary in that no attempt was made to find the energy minimum with respect to changes of all the geometrical variables. The results indicated that the planar form of the aminium radical with the bond angle between the methyl groups of 120° was the most stable. This prediction has been reinforced in a recently appearing communication (29). The calculated nitrogen hyperfine coupling constant (16.44) compared reasonably well with the observed value of 19.28 (29).

In Table 2-6 are listed some INDO closed shell calculations of properties of NND and protonated NND. Structure B has depicted fully protonated alkyl nitrogen while in structure C the nitroso oxygen is shown to be fully protonated. Structure C is shown by calculation to be more stable by about 16 kcal/mol.

Table 2-5

INDO Open Shell Calculations of Selected Geometriesof Dimethylaminium Radical

α = angle of departure from planarity

β = CNC bond angle

Structure	Calculated Energy (atomic units)	Calculated Nitrogen Hyperfine Coupling Constant
$\alpha = 71^\circ$ $\beta = 109^\circ$ (tetrahedral)	-29.886	38.57
$\alpha = 55^\circ$ $\beta = 109^\circ$	-29.907	22.30
$\alpha = 0^\circ$ $\beta = 109^\circ$ (planar)	-29.911	16.77
$\alpha = 0^\circ$ $\beta = 120^\circ$ (planar)	-29.918	16.44

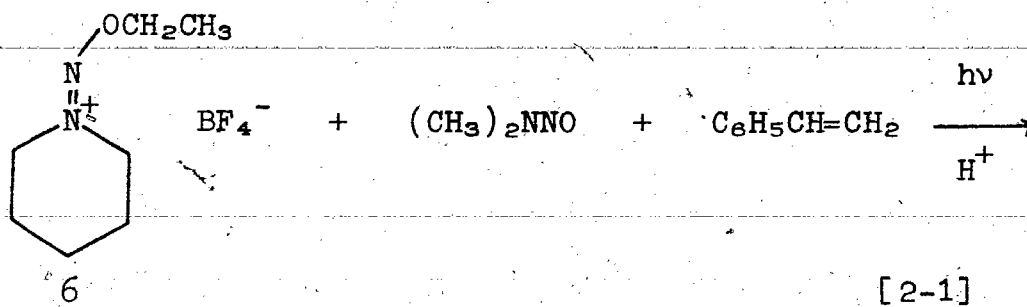
Table 2-6

INDO Closed Shell Calculations of Various
Forms of N-Nitroso-N,N-Dimethylamine

<u>Structure</u> <u>(all planar)</u>	<u>Calculated Energy</u> <u>(atomic units)</u>	<u>Calculated</u> <u>Electron Densities</u>
A 	-57.631	$N_1 = 5.0894$ $N_2 = 4.8397$ $O = 6.2670$
B 	-58.134	$N_1 = 4.8415$ $N_2 = 4.8224$ $O = 6.0426$
C 	-58.160	$N_1 = 4.8837$ $N_2 = 4.7477$ $O = 6.1064$

2-7 Competition Between Diazenium Salt and NND as Substrates

In order to ascertain whether a fully oxygen protonated nitrosamine such as structure C of Table 2-6 is involved in the photoaddition mechanism, a model ether, 2-ethoxy-1,1-pentamethylene diazenium tetrafluoroborate, 6, was prepared. In the competitive reaction represented by [2-1], the diazenium salt

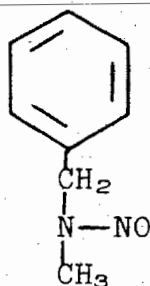
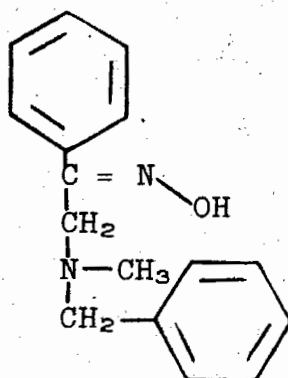
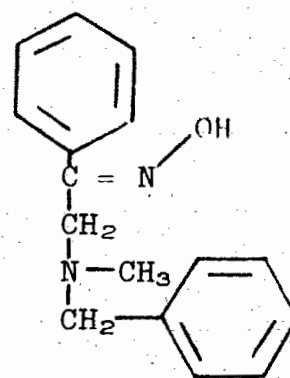


did not undergo photoaddition. The only oxime isolated was from NND addition to styrene. The diazenium salt was unable to initiate or to participate in the chain propagation step of the photoaddition.

2-8 Some Properties of Other Aminium Radicals

2-8-1 Photoaddition of N-Nitroso-N-Methylbenzylamine to Styrene

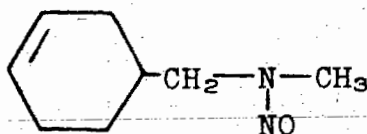
The N-nitroso-N-methylbenzylamine, 7, under the typical photoaddition conditions, resulted only in partial photoaddition to an equimolar concentration of styrene. Approximately 45% of the total product isolated was an equal mixture of the corresponding syn- and anti-oximes (8-1 and 8-2) as estimated

78-18-2

from the singlet nmr absorptions at τ 6.2 and τ 6.4 of the $-CCH_2N-$ protons of the oximes. About 35 % of the total product resulted from photo-induced decomposition of 7 and gave benzaldehyde and benzylamine. The remainder of the product corresponded most probably to α -benzylic hydrogen elimination and subsequent oxime formation.

2-8-2 Competition Between Intra- and Intermolecular Addition

The N-nitroso-N-methyl-3-cyclohexene-1-methylamine 9 underwent intramolecular photoaddition upon photolysis in the presence of an equimolar concentration of styrene. From vapour phase chromatography there was no indication that any styrene was consumed in the reaction.

9

CHAPTER 3DISCUSSION3-1 General

Basic factors which determine the reactivity of free radicals toward reactive substrates include such components as the polar, resonance and steric effects, the dissociation energy of the bond (in abstraction reactions) and the nature of the atomic centre associated with the unpaired electron. Not all of these parameters are mutually independent. By the judicious choice of experimental conditions and reactants, all but the polar and resonance factors have been standardized by the use of substituted styrenes as substrates in the photo-addition experiments. The polar and resonance effects caused by substituents can be measured using the Hammett correlation equation.

The Hammett equation was originally formulated from data obtained from heterolytic reactions. The relationship gives the ratio of rate or equilibrium constants for the reactions of substituted benzene derivatives in terms of para- and meta- substituent σ constants (30). The proportionality constant is

$$\log_{10} k_X / k_H = \sigma \rho \quad [3-1]$$

ρ . The polar effect of the substituent is transmitted through the sigma bond system (inductive effect) and through the pi bond system (resonance effect) (31). In reactions where an

electron deficient intermediate is formed, substituents which are in direct conjugation through the benzene ring with the reactive centre will display enhanced σ values. Brown and Okamoto (32) have termed this enhanced substituent constant as σ^+ . In some cases the substituent may be able to interact via resonance directly with the reactive centre. If this extended conjugation affects only one side of a thermodynamic equilibrium or one of the ground or transition states of a kinetic equilibrium, a new substituent constant, σ_p^o , has been proposed (33,34).

The Hammett ρ value is an indicator of the transition state structure. When formation of the transition state involves donation of electron density to the reaction site, the reaction is accelerated by electron donors and ρ is negative (35). The size of ρ is a measure of the extent of charge development at the reaction centre adjacent to the ring when the reaction coordinate passes from the ground to the transition state.

3-2 Polar Effects

It is expected that the presence of the positive charge in the aminium radical renders electrophilic character to this transient intermediate. At which stage of the reaction coordinate this effect will be greatest is uncertain. It is also suspected that reactions of this radical may have quite different electronic requirements from those of neutral electrophilic radicals such as $\cdot\text{Cl}$, $\cdot\text{OC}(\text{CH}_3)_3$, $\cdot\text{Br}$ and $\cdot\text{CCl}_3$. In an exhaustive compilation of free radical substitution reactions (31), it was found that $\rho \leq 0$ for all such reactions. A qualitative

dependence of ρ on the electronegativity of the free radical was observed. The absolute value of ρ increased (31) in the series $\cdot\text{CH}_3 < \cdot\text{C}_6\text{H}_5 < \text{HOOCCH}_2\cdot < \cdot\text{CCl}_3, \cdot\text{Br}$ in the same direction as the electronegativity of these radicals.

In Table 3-1 are listed some relevant ρ values. For comparison those of the piperidinium radical hydrogen abstraction from toluenes (12), amino radical hydrogen abstraction from toluenes (37), acid catalyzed hydration of styrenes (38) and polymerization of styrene (39,40) are also listed. Although paucity of data does not allow a systematic discussion of the polar effects on radical addition reactions, the following observations can be mentioned. Firstly, among the limited number of studies available, the ρ value of the piperidinium radical addition is the largest in the absolute sense and exhibits greater dependency on electron affinity than neutral radical additions. The ρ value of piperidinium radical addition is not exceptionally large when compared with that of the protonation of styrenes where considerable electropositive character at the benzylic position is developed in the transition state (38). Secondly, while almost all of the neutral radical additions correlate better with σ^+ constants, the piperidinium radical addition is a rare exception in that the relative reactivities exhibit better correlation with σ constants.

The lack of correlation with the σ^+ constants (32) is particularly obvious when the extreme electron-donating and electron-withdrawing p-methoxystyrene and p-cyanostyrene respectively are considered. The σ^o (34) value of p-methoxy

Table 3-1

The ρ -values of Some Radical Addition Reactions

Reactions	Temp.	Solvent	ρ	Ref.
1) $\cdot\text{CCl}_3 + \text{ArCH}_2\text{CH}=\text{CH}_2$	70°		-0.29	36
2) $\cdot\text{CCl}_3 + \text{Ar}(\text{CH}_2)_2\text{CH}=\text{CH}_2$	70°		-0.20	36
3) $\cdot\text{CCl}_3 + \text{C}_6\text{H}_5\text{CH}=\text{CHAr}$	105°	CBrCl ₃	-0.7	23
4) $\cdot\text{CCl}_3 + \text{ArC}(\text{CH}_3)=\text{CH}_2$	105°	CBrCl ₃	-0.7 ^a	23
5) $\text{HOOCCH}_2\text{S}\cdot + \text{ArCH}=\text{CHPh}$	105°	HSCH ₂ COOH	-0.4	23
6) $\text{CH}_3\text{O}_2\text{CCH}_2\text{S}\cdot + \text{ArC}(\text{CH}_3)=\text{CH}_2$	105°	HSCH ₂ CO ₂ CH ₃	-0.52 ^{ac}	23
7) $\text{RO}_2\cdot + \text{ArCH}=\text{CH}_2$	60°	C ₆ H ₆	-0.3	24
8) $\cdot\text{CCl}_3 + \text{ArCH}=\text{CH}_2$	80°	C ₆ H ₆	-0.42	22
9) $\text{C}_5\text{H}_{10}\text{NH}^{\cdot+} + \text{ArCH}=\text{CH}_2$	20°	CH ₃ OH	-1.34 ^c	this work
10) $\text{C}_5\text{H}_{10}\text{HN}^{\cdot+} + \text{ArCH}_3$	20°	2MH ₂ SO ₄ , AcOH	-1.21 ^b	12
11) $\text{H}^{\cdot+} + \text{ArCH}=\text{CH}_2$	25°	H ₂ O	-3.42	38
12) $-\text{CH}_2\dot{\text{C}}\text{HPh} + \text{ArCH}=\text{CH}_2$	60°		0.51	39
13) $-\text{CH}_2\dot{\text{C}}\text{HPh} + \text{ArCH}=\text{CH}_2$	60°		0.60	40
14) $(\text{CH}_3)_2\text{N}\cdot + \text{ArCH}_3$	136°	ArCH ₃	-1.08	37

a These figures were calculated from the data given in ref. 23.

b This value is calculated from the data given in ref. 12.

c For these two ρ -values better correlations were obtained with σ constants. For the other ρ -values, σ^+ constants were used to give better correlation.

d The reaction was run in 3.83M aqueous HClO₄ solution.

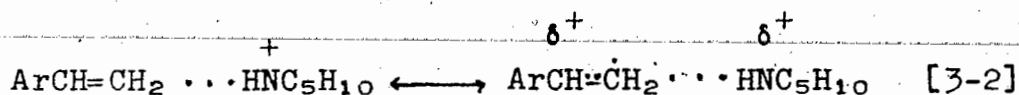
is -0.12 and does not improve the correlation either. Thirdly, the present σ_p relationship is correlated by a single line for both para- and meta-substituted styrenes without showing enhanced reactivities for the para substituents as was observed in trichloromethyl radical additions to styrenes (22). However, in the event that p-methoxystyrene is reacting at or near the diffusion controlled rate of addition, the results are more difficult to interpret. It is the p-methoxy substituent which is the best criterion for distinguishing between correlation with σ or σ^+ .

If the p-methoxystyrene reactivity is slower than the rate of diffusion, the unique features described above appear to arise from the reaction mode rather than from the attacking cationic species. A recalculation² of Neale's results (12) on the piperidinium radical abstraction reaction from toluenes gave the relative reactivities correlating better with σ^+ values (p-methoxytoluene was not used as a substrate) and with $\rho = -1.21$ which is not significantly different from the corresponding bromine atom and trichloromethyl radical abstraction reactions (31).

² Neale and Gross (12) have plotted $\log [\text{ArCH}_2\text{Cl}]/[\text{PhCH}_2\text{Cl}]$ against σ^+ constant by assuming a pseudo-zero order reaction. However, a first order kinetic plot must be employed,

$$k_X/k_H = \frac{\log \frac{[\text{ArCH}_3]_1}{[\text{ArCH}_3]_f}}{\log \frac{[\text{PhCH}_3]_1}{[\text{PhCH}_3]_f}}$$

Accepting the validity of the σ correlation, the results suggest that in the piperidinium radical addition to styrenes, the benzylic carbonium ion character is not developed to any significant extent at the transition state. The following transition state structure for the process can, therefore, be ruled out.



The results unambiguously show that electron-donating substituents on styrene facilitate reaction with piperidinium radicals. The observed ρ value probably reflects the ground state electronic interaction between the cationic radical and the π electron cloud of the olefinic moiety of the styrenes. Efforts, however, to detect the presence of a charge transfer complex between p-methoxystyrene and NNP by uv spectroscopy were not successful.

Solvent has a large effect on the magnitude of ρ but has, generally, little influence on σ values (41). In different solvent systems the behaviour of the piperidinium radical may be modified considerably. Consequently the ρ value of Neale (12) which was taken in strongly acid conditions (2M H_2SO_4 in acetic acid) cannot safely be compared with the value obtained in this work. Unfortunately, under strongly acidic conditions NNP is completely protonated and is not photolabile (19). This prevents extending the present photoaddition study to a higher acidity region. Photodecomposition of N-chloramine at a lower

acidity region suffers from various side reactions (12) and is not readily adaptable for kinetic study. Recently Malatesta and Ingold (14) have demonstrated the increased stability of aminium radicals along with increases in solvent acidity at the -H₀ range of 3 to 11. Although the factors controlling the moderation of the reactivity are unknown, the aminium radicals are no doubt less reactive and hence more selective at higher acidity.

3-3 Quantum Yields

The quantum yield measurements indicate that the NNP photoaddition to styrene follows a short chain process with chain lengths of at least 6 to 10. The reasonable constancy of ϕ_N with changing styrene concentration indicates that every piperidinium radical reacts with styrene. The ϕ_N is proportional to the rate of the propagation step as experimentally demonstrated by its proportional increase with the increase in NNP concentration. For this step to be efficient, the free energy of activation must be very small, but larger than that required in the addition step.

3-4 Qualitative Ranking of Nitrosamine Reactivity

It was observed that when the structure of the nitrosamine was chosen (9) in such a manner where intramolecular addition is facile, the intramolecular addition proceeded to the exclusion of photoaddition to a reactive substrate such as styrene. In a competitive situation, the benzylic nitrosamine 7 underwent bi-

molecular photoaddition to styrene in approximately the same proportion as it underwent unimolecular elimination, presumably through an iminium intermediate. Benzylic nitrosamine 7 also underwent intramolecular oxime formation in competition with the other photoprocesses, but less efficiently.

3-5 The Photophysical Process of Nitrosamine Photolysis

A truly interesting feature of nitrosamine photochemistry is the actual mechanism involved in the generation of the aminium radical prior to its addition to a suitable substrate. INDO SCF MO closed shell calculations suggest that the oxygen of NND is the electron rich atom in the molecule. This has been confirmed experimentally by the x-ray diffraction observation that copper bonds to nitrosamine via the oxygen atom (42). The uv spectra of acidified nitrosamine solutions change as a function of the hydrogen ion concentration (18). The calculations performed also indicate that the most stable protonated form of NND is planar and the proton is bonded to the oxygen atom.

INDO open shell calculations also demonstrate that the aminium radical is more stable in the planar form with CNC bond angle of 120° . The reported INDO energy minimized structure of the dimethylaminium radical had CNC bond angle of 126° (29).

The proton is indispensable to the photoaddition. The actual stepwise involvement of the proton, however, from its associated status in the pre-photolysis complex to its full proton status in the aminium radical is not known. One fact is

obvious. The nitroso oxygen must be "free" since the diazenium salt 6 of the nitrosamine is unable to initiate or to propagate the chain transfer process of the photoaddition.

TL

CHAPTER 4EXPERIMENTAL4-1 General Techniques

Unless otherwise specified the following experimental conditions prevailed. Nuclear magnetic resonance (nmr) spectra were recorded with a Varian A 56/60 spectrometer in CDCl_3 solution using TMS as the internal standard. The coupling patterns of nmr signals were presented as d (doublet), t (triplet), s (singlet), q (quartet), b (broad) and m (multiplet). D_2O exch signified that the proton was exchangeable with added D_2O . A Perkin-Elmer RMU-6E mass spectrometer was used to record mass spectra. Infrared (ir) spectra were recorded on a Perkin-Elmer 457 spectrophotometer as a nujol mull, KBr pellet, liquid/film or CHCl_3 solution. An Unicam SP-800 UV-Visible spectrophotometer was used to follow the course of the photoaddition reactions. A Cary 14 Spectrophotometer was utilized to monitor the kinetic disappearance of N-nitrosopiperidine. The vapour phase chromatography (vpc) was performed on a Varian 1200 flame ionization chromatograph using a 20% SE - 30 10' x 1/8" stainless steel column. The recorder was equipped with a Disc Chart Integrator (model 244). The photochemical kinetic experiments were executed on a merry-go-round apparatus. The least squares statistical analysis was performed on a programmable Monroe Calculator 1670.

Thin layer chromatography (tlc) was performed on alumina or silica gel plates (0.2 to 0.3 mm in thickness). The ad-

sorbant was impregnated with a uv indicator which permitted the examination of the plates by uv light or iodine vapour development. Chromatography was also accomplished using columns packed with Brockman neutral alumina, activity 1, 80-200 mesh or Mallinckrodt silicic acid (100 mesh). Melting points were determined on a Fisher-Johns hot stage or a Gallenkamp heating block apparatus. The melting or boiling points were reported uncorrected. Elemental analyses were performed on a Perkin-Elmer 240 Microanalyzer by Mr. M. K. Yang, Biosciences Department, Simon Fraser University.

In general the combined organic extracts were dried with anhydrous magnesium sulphate and filtered. Organic solvents were removed by evaporation under reduced pressure using a rotary evaporator.

4-2 Materials

Commercially obtained styrene was distilled under reduced pressure immediately before use. The *p*- and *m*-substituted styrenes were synthesized and distilled immediately before use. Purity as evaluated by vpc analysis. The N-nitroso-piperidine was obtained commercially and used without further purification. Bromobenzene was distilled prior to use as an internal standard for the quantitative analysis of the styrenes in the photoaddition reactions.

4-3 Preparation of Substituted Styrenes

The substituted styrenes used in this study were prepared

by KHSO_4 mediated dehydration of the appropriately substituted phenylmethylcarbinols. Due to a more satisfactory yield, p-methoxystyrene was prepared by the decarboxylation of p-methoxycinnamic acid. The substituted phenylcarbinols were prepared either by NaBH_4 reduction of the appropriate acetophenone or by CH_3MgBr condensation with the required benzaldehyde.

4-3-1 Synthesis of p-Methylstyrene (5-2)

The Grignard reagent prepared from 21.0 g CH_3Br was treated with 24.0 g p-tolualdehyde. On work-up of this reaction mixture, there was obtained an oil, p-methylphenylcarbinol (19.4 g, 71.5%): b. p. 74-75°/1.8 mm Hg, reported (43) b. p. 108°/14 mm; ir (film) 3340, 1085, 1065 cm^{-1} ; nmr τ 2.98 (2H,s), 5.4 (1H, q (J=6.5 cps)), 7.05 (1H, b, D_2O exch), 7.75 (3h,s), 8.75 (2H, d (J=6.5 cps)).

Five grams of the carbinol was dehydrated according to the procedure of Brooks (44), using 75 mg KHSO_4 , 75 mg hydroquinone and a temperature of 200-210° at 100-120 mm Hg pressure. Following work-up the residual oil (2.3 g, 52 %) of 5-2 was distilled: b. p. 56-58°/ 12 mm Hg, reported (45) b. p. 81°/ 41 mm Hg; ir (film) 3090, 3050, 3020, 3005, 1625 cm^{-1} ; nmr τ 2.9 (4H, A_2B_2 pattern), 3.15-4.0 (3H, ABC pattern), 7.75 (3H, s).

4-3-2 Synthesis of p-Chlorostyrene (5-3)

The Grignard reagent prepared from 21.0 g CH_3Br was treated with 28.0 g p-chlorobenzaldehyde. On work-up p-chlorophenylmethylcarbinol (26.7 g, 86 %) was distilled: b. p. 93-94°/ 4 mm Hg, reported (44) b. p. 87-89°/ 2 mm; ir (film) 3350, 1085, 1015

cm^{-1} ; nmr τ 2.8 (4H, s), 5.4 (1H, q ($J=6.5$ cps)), 6.5 (1H, b, D_2O exch), 8.72 (3H, d ($J=6.5$ cps)).

Five grams of the carbinol was dehydrated (44) in the presence of 50 mg KHSO_4 and 50 mg hydroquinone. After work-up an oil was distilled to give 5-3 (1.6 g, 36 %): b. p. $49^\circ/3.2$ mm Hg, reported (44) b. p. $53-54^\circ/3$ mm; ir (film) 3090, 3070, 3040, 3010, 1630 cm^{-1} ; nmr τ 2.8 (4H, s), 3.4 (1H, ABC pattern), 4.7 (2H, ABC pattern).

4-3-3 Synthesis of p-Methoxystyrene (5-4)

The p-methoxycinnamic acid, synthesized in 85 % yield by the Perkin condensation of p-methoxybenzaldehyde and malonic acid (46), was decarboxylated according to a method suggested by Kitchen and Pollard (47). Five grams of the cinnamic acid was heated together with 20 g quinoline and 0.5 g copper powder until decarboxylation was effected. After work-up the resulting oil was distilled to give 5-4 (1.6 g, 41 %): b. p. $92-93^\circ/13$ mm Hg, reported (48) b. p. $90-91^\circ/13$ mm; ir (film) 3090, 3060, 3040, 3005, 1625 cm^{-1} ; nmr τ 3.0 (4H, A_2B_2 pattern), 3.15-4.1 (3H, ABC pattern), 6.3 (3H, s).

4-3-4 Synthesis of p-Cyanostyrene (5-5)

The p-cyanoacetophenone was prepared in 71 % yield from p-bromoacetophenone as reported by Friedman and Shechter (49). Following reduction of 10.6 g p-cyanoacetophenone by 1.5 g NaBH_4 and subsequent work-up, p-cyanophenylmethylcarbinol (8.4 g, 83%)

was collected: b. p. 131-133°/2 mm Hg, reported (50) b. p. 136-140°/5 mm; ir (film) 3420, 2230, 1085, 1010 cm^{-1} ; nmr τ 2.48 (4H, A_2B_2 pattern), 5.1 (1H, q ($J=6.5$ cps)), 6.55 (1H, b, D_2O exch), 8.65 (3H, d ($J=6.5$ cps)).

Dehydration of 5.3 g of the carbinol was carried out using a suggested modification (50). Following customary work-up, a yellowish liquid was distilled to give 5-5 (450 mg, 10 %): b. p. 95-96°/20 mm Hg, reported (50) b. p. 102-104°/29 mm; ir (film) 3090, 3070, 3040, 3010, 2230, 1630 cm^{-1} ; nmr τ 2.5 (4H, A_2B_2 pattern), 3.05-4.75 (3H, ABC pattern).

4-3-5 Synthesis of m-Methylstyrene (5-6)

m-Toluic acid (25 g) was reduced with 7.5 g $LiAlH_4$ and upon subsequent work-up gave m-methylbenzyl alcohol (20 g, 90 %): b. p. 162-163°/20 mm Hg, reported (51) b. p. 217°; ir (film) 3300, 1015 cm^{-1} ; nmr τ 2.9 (4H, m), 5.45 (2H, s), 7.5 (1H, b, D_2O exch), 7.7 (3H, s).

The m-methylbenzyl alcohol was oxidized with active manganese dioxide prepared according to a method of Pratt (52). Following work-up there was isolated an oily residue of m-tolualdehyde (20 g, 100 %); ir (film) 2810, 2715, 1695 cm^{-1} ; nmr τ 0.1 (1H, s), 2.5 (4H, m), 7.6 (3H, s).

The Grignard reagent prepared from 17.5 g CH_3Br was treated with 20.0 g m-tolualdehyde. On work-up m-toluylmethylcarbinol (9.4 g, 42 %) was collected: b. p. 113-114°/20 mm Hg, reported (43) b. p. 104-105°/12 mm; ir (film) 3330, 1065, 1025 cm^{-1} ; nmr τ 2.9 (4H, m), 5.25 (1H, q ($J=6.5$ cps)), 7.45 (1H, b, D_2O exch),

7.68 (3H, s), 8.55 (2H, d (J=6.5 cps)).

Five grams of the carbinol was dehydrated according to (44) using 1.0 g KHSO₄ and 0.4 g hydroquinone. Following work-up, an oil (1.8 g, 29 %) of 5-6 was collected: b. p. 53-55°/10 mm Hg, reported (53) b. p. 61-62°/18 mm; ir (film) 3090, 3050, 3030, 1630 cm⁻¹; nmr τ 2.85 (4H, m), 3.34 (1H, ABC pattern), 4.6 (2H, ABC pattern), 7.68 (3H, s).

4-3-6 Synthesis of m-Methoxystyrene (5-7)

m-Methoxyacetophenone (15.0 g) was reduced with 1.7 g NaBH₄. After work-up there was obtained m-methoxyphenylmethylcarbinol (13.5 g, 90 %): b. p. 79-80°/0.3 mm Hg, reported (48) b. p. 132-133°/12 mm; ir (film) 3400, 1045, 1015 cm⁻¹; nmr τ 3.0 (4H, m), 5.25 (1H, q (J=6.5 cps)), 6.25 (3H, s), 7.4 (1H, b, D₂O exch), 8.55 (3H, d (J=6.5 cps)).

The carbinol was dehydrated (44) with the assistance of 1.0 g KHSO₄ and 0.4 g hydroquinone. Following work-up there was obtained 5-7 (1.2 g, 23 %): b. p. 79-80°/15 mm Hg, reported (48) b. p. 77-78°/12 mm; ir (film) 3090, 3050, 3005, 1600 cm⁻¹; nmr τ 3.1 (4H, m), 4.38 (1H, dd (J=10.5 cps)), 4.76 (1H, dd (J=10.5 cps)), 6.22 (3H, s).

4-3-7 Synthesis of m-Acetamidostyrene (5-8)

Commercial m-nitroacetophenone (16.4 g) was reduced by 1.9 g NaBH₄. Following work-up there was obtained m-nitrophenylmethylcarbinol (15.2 g, 92 %): m. p. 59-60°, reported (54) m. p. 60-61°; ir (film) 3350, 1525, 1350, 1065, 1015 cm⁻¹; nmr τ 2.1

(4H, m), 5.0 (1H, q ($J=6.5$ cps)), 7.15 (1H, b, D_2O exch), 8.5 (3H, d ($J=6.5$ cps)).

The carbinol was dehydrated by heating a mixture of 7.5 g alcohol, 2.0 g $KHSO_4$ and 0.5 g hydroquinone to 220° at 20 mm Hg. Following customary work-up of the distillate, there was obtained a yellow oil, m-nitrostyrene (3.3 g, 49 %): b. p. $111-112^\circ/12$ mm Hg, reported (55) b. p. $106-107^\circ/8$ mm; ir (film) 3080, 3070, 3010, 1630, 1525, 1350 cm^{-1} ; nmr τ 2.1 (4H, m), 3.2 (1H, ABC pattern), 4.35 (2H, ABC pattern).

The m-acetamidostyrene was prepared directly from m-nitrostyrene using a modification of a procedure of Landesberg (56). A mixture of 1.0 g m-nitrostyrene, 29 ml glacial acetic acid, 29 ml acetic anhydride and 2.0 g sodium acetate was reductively acetylated by the drop-wise addition of 3.4 g Zn powder. After stirring the resulting solution for 2 h at 20° and filtering the solid, the filtrate was concentrated. The oily residue was washed with 34 ml dilute NH_4OH solution. After filtration and washing with H_2O , 0.44 g of a semi-solid was subjected to column chromatography using 10 g neutral alumina as adsorbant and petroleum ether 30:60 as the eluting solvent. The desired compound was finally eluted with a mixture of 25 % ether:75 % petroleum ether to give 0.27 g solid. Recrystallization of the compound from benzene:petroleum ether 30:60 gave white crystals of 5-8 (0.2 g): m. p. $72-73^\circ$, reported (57) m. p. $74-75^\circ$; ir ($CHCl_3$) 3090, 1680 cm^{-1} ; nmr τ 1.85 (1H, b), 2.65 (4H, m), 3.35 (1H, ABC pattern), 4.5 (2H, ABC pattern), 7.9 (3H, s).

4-3-8 Synthesis of m-Bromostyrene (5-9)

m-Bromoacetophenone (15.0 g) was reduced by 1.25 g NaBH₄. After work-up there was isolated m-bromophenylmethylcarbinol (12.1 g, 80 %): b. p. 79-81°/0.5-0.6 mm Hg, reported (58) b. p. 136-140°/20 mm; ir (film) 3560, 3340, 1065, 1010 cm⁻¹; nmr τ 2.7 (4H, m), 5.15 (1H, q (J=6.5 cps)), 7.15 (1H, b, D₂O exch), 8.5 (3H, d (J=6.5 cps)).

Dehydration of 6.0 g carbinol by 1.0 g KHSO₄ and 0.4 g hydroquinone was accomplished by a known procedure (44). After work-up the resulting oil was distilled to give 5-9 (2.9 g, 55%): b. p. 79-81°/20 mm Hg, reported (58) b. p. 90-94°/20 mm; ir (film) 3090, 3060, 3010, 1625 cm⁻¹; nmr τ 2.5 (4H, m), 3.3 (1H, ABC pattern), 4.6 (2H, ABC pattern).

4-4 General Conditions for Preparative Photoaddition

The photoadditions of N-nitrosopiperidine to substituted styrenes were carried out in a manner similar to that reported (24, 59).

To 0.01 moles of each substituted styrene in 250 ml CH₃OH was added 0.01 moles NNP and 0.84 ml conc. HCl. The solution was poured into the photo-cell and purged with nitrogen gas throughout the photolysis. The source of irradiation was a medium pressure 200 watt Hanovia lamp 654A36. A nonex filter was used to cut off irradiation below 340 nm. The entire photo-cell was immersed in an ice-bath. Cold water was circulated through the cooling jacket encircling the lamp. The progress of the photolysis was followed by withdrawing a 1.0 ml aliquot

of the mixture, diluting to 10.0 ml with CH_3OH and observing the decrease of the 350 nm absorption of NNP. The photoadditions were generally complete after 1 to 1.5 h irradiation.

After completion of the photoreaction, the CH_3OH was removed on the rotary evaporator until about 40 ml volume was left. This solution was diluted with 40 ml H_2O and the resulting turbid mixture was extracted with ether (2 x 40 ml). The ether extracts were combined, dried (MgSO_4) and concentrated prior to analysis. The aqueous solution was made basic ($\text{pH} \sim 10$) by the dropwise addition of saturated Na_2CO_3 solution. The precipitated amino-oximes were isolated by filtration and dried over P_2O_5 in a vacuum dessicator. The filtrate was extracted with CH_2Cl_2 (2 x 40 ml). In the latter extract the photodecomposition products of NNP and small quantities of amino-oximes appeared.

The physical properties and yields of the amino-oximes obtained are given in Table 2-1.

4-5 General Procedure of Kinetic Study of NNP Photoaddition to Substituted Styrenes

For all kinetic studies of the photoaddition of NNP to a substituted styrene, a solution of 10^{-3} moles styrene, 10^{-3} moles substituted styrene, 10^{-3} moles NNP, 0.085 ml conc. HCl and sufficient CH_3OH to make 25.0 ml was prepared. Aliquots of 3.0 ml were pipetted into the photolysis tubes fitted with a gas purging device. Nitrogen was bubbled through each solution for 90 to 120 seconds. Each tube after being purged with nitrogen was sealed.

Five tubes containing the solutions were placed into the slots of the merry-go-round apparatus which was immersed in a bath thermostated at 20°C. The source of irradiation was a medium pressure 450 watt Hanovia lamp 679A36. A nonex filter was inserted into the centrally located cold finger of the apparatus. For each run, the lamp was warmed up for 20 minutes prior to irradiation of the samples. The sixth tube was protected from light with Al foil and served as the control. At each 20 minute interval, one tube was removed from the merry-go-round and stored in the dark. At the 100 minute interval when the last tube was withdraw, generally 50 to 52 % of the NNP had reacted.

To each tube of the experiment, 0.5 ml of a bromobenzene solution (0.534 g in 10.0 ml CH₃OH) was added. For uv analysis 1.0 ml of each solution was diluted to 5.0 ml with CH₃OH. The quantity of NNP consumed in the photolysis was calculated from the decrease of the 350 nm absorption band.

The remainder of the irradiated solution was used directly for vpc analysis. For each styrene a calibration curve plotting the ratios of bromobenzene to the styrene integration reading was constructed prior to the analysis. The areas of each peak were obtained from the integrator attached to the recorder. The amount of unreacted styrene in the photolysate could then be readily calculated. The data obtained was found to obey first order disappearance of the styrene (k_H) and of the substituted styrene (k_X). The first order rate constant and the correlation coefficient were obtained from a least squares

analysis of the data.

For each substituted styrene, the measurement of k_x / k_H was repeated two or more times to give the average ratios listed in Table 2-4. Competitive photoaddition between p-methoxystyrene and p-methylstyrene was carried out because the former reacted exclusively in the competition with styrene. The ratio of the rate constants obtained this way was normalized by multiplying $k_{\text{p-CH}_3} / k_H$ by $k_{\text{p-OCH}_3} / k_{\text{p-CH}_3}$ to obtain $k_{\text{p-OCH}_3} / k_H$.

In the competitive photoadditions of p-cyanostyrene in the presence of either styrene or m-bromostyrene, no addition to p-cyanostyrene had occurred. Assuming that even 5% p-cyanostyrene had reacted during photolysis, $k_{\text{p-CN}} / k_H$ was estimated to be 0.085. The plot of the measured $\log k_x / k_H$ against σ values is shown in Figure 2-1.

4-6 Quantum Yield Determinations

A potassium ferrioxalate actinometry solution (3.0 ml) as described by Hatchard and Parker (60) was placed into the photocell and irradiated for 5 minutes under the same conditions as discussed for the photoaddition. This operation was repeated several times at 15 minute intervals. The actinometry solutions were processed as described (60) and the photon count was determined to be $1.44 (\pm 0.03) \times 10^{15}$ quanta/sec and was reproducible.

To compensate for the unutilized photons due to the decrease in the nitrosamine 350 nm absorbance as the photolysis proceeded, a calibration curve was constructed to provide the appropriate correction factors. This was done by measuring the light fil-

tered through solutions containing 0.04, 0.032, 0.024, 0.02 and 0.016 moles/liter of NNP and styrene and striking 3.0 ml solutions of potassium ferrioxalate. The correction factor was defined as the ratio of the photon count striking the actinometry solution for the unfiltered light and that for the reaction solution filtered light.

For determination of the quantum yields a 0.04 M solution in each of NNP, the styrene and HCl in CH_3OH was irradiated in the merry-go-round apparatus as described. At each 20 minute interval, one tube was withdrawn for analysis. The 3.0 ml solution of the actinometer was irradiated for 5 minutes only. The quantities of NNP and styrene consumed were determined by analysis. The calculated quantum yields of NNP disappearance (ϕ) and the pseudo-first order rate constants of the styrene reaction are given in Table 2-2.

Keeping the concentration of styrene at 0.04 M, the concentrations of NNP and HCl were varied successively by four-fold. The quantum yield (ϕ_N) and the pseudo-first order rate constant (k_H) were determined and listed in Table 2-3. At a higher concentration of NNP the photolysate was suitably diluted for uv spectrophotometry. Any dilution errors will, of course, affect the accuracy of ϕ_N values. In all the k_H plots, reasonable straight lines could be drawn with the points up to 100 minutes irradiation.

In the next set of experiments, the concentration of NNP and HCl were fixed at 0.04 M and the concentration of styrene was varied from 0.04 to 0.12 M. Similar determinations of the

quantum yields and the pseudo-first order rate constants were carried out. Again most of the experimental points obtained up to 100 minutes irradiation gave reasonable linear plots except for the k_H determination with 0.12 M styrene. In this case, relatively small decreases of styrene with respect to the high concentration of styrene decreased the vpc accuracy. The data is summarized in Table 2-3.

4-7 Spectroscopic Attempt to Detect Complex Formation

Double compartment silica cells were used in an attempt to detect any complex that may be formed between p-methoxystyrene and NNP both with and without an equivalent of HCl. Initially 8×10^{-5} moles/liter p-methoxystyrene in CH_3OH was added to one compartment and NNP of similar concentration to the other. The spectrum was scanned from 3400 to 2200 A° . The solutions in the two compartments were mixed and the scan was repeated. No difference in the resulting spectra was detected.

An analogous experiment was performed using 8×10^{-2} moles/liter each of NNP and p-methoxystyrene. The spectrum was scanned from 7000 to 4000 A° . Again no new absorptions appeared.

4-8 INDO Molecular Orbital Calculations

The INDO SCF MO method was based on the formulation of Pople (61). The INDO calculations were performed using a standard programme (62) on the IBM 370 155 computer. Standard bond lengths and bond angles (63,64) were employed for the geometrical parameters, except those altered to achieve the

desired molecular geometry.

4-9 Other Nitrosamines Investigated

4-9-1 Preparation of N-Nitroso-N-Methylbenzylamine (7)

To a 200 ml round bottom flask was added 22.6 g^v (0.22 moles) benzylamine and 23 ml (0.27 moles) conc. HCl in 25 ml H₂O. The flask was cooled to 5°. To the magnetically stirred solution was added (2h) through a dropping funnel a solution of 17.0 g. (0.25 moles) NaNO₂ in 50 ml H₂O. The mixture was permitted to stir overnight and was then extracted with CH₂Cl₂ (2 x 50 ml). The organic extract was dried (MgSO₄) and concentrated. The residue was distilled (b. p. 136°/11 mm Hg, reported (65) b. p. 158°/26 mm) to give 7 (23.8 g, 74 %): ir (film) 3090, 3070, 3030, 1600, 1495, 1445 cm⁻¹; nmr τ 2.75 (5H, m), 5.3 (2H, s), 7.2 (3H, s).

4-9-2 Photoaddition of 7 to Styrene

A solution of 1.04 g (0.01 moles) styrene, 1.51 g (0.01 moles) 7, 0.84 ml conc. HCl in 230 ml CH₃OH was subjected to irradiation by the 200 watt Hanovia lamp through the nonex filter. The photolysis was complete in 1 h as noted by the disappearance of the 350 nm absorption peak. The reaction solution was concentrated to 25 ml and diluted with 25 ml H₂O. The resulting turbid solution was extracted with ether (2 x 50 ml). After drying (MgSO₄) and concentrating, 0.80 g residue

resulted from this acid extract. The aqueous phase was made basic (pH ~ 10) by the dropwise addition of saturated Na_2CO_3 solution. The precipitate was filtered and dried over P_2O_5 in a vacuum dessicator to give 0.82 g solid. The filtrate was extracted (2 x 50 ml) with CH_2Cl_2 . The combined CH_2Cl_2 extracts were dried (MgSO_4) and then concentrated to give 0.23 g residue.

The acid extract (0.80 g) gave: ir (CHCl_3) 3380, 3090, 3070, 3030, 2740, 1700 cm^{-1} ; nmr τ -0.1 (s), 1.8-2.8 (m); vpc on 20 % SE-30 column gave three peaks having the same retention time as styrene, benzaldehyde and benzylamine.

The solid (0.82 g) material gave 8-1 and 8-2: ir (CHCl_3) 3200, 3070, 3000, 1630 cm^{-1} ; nmr τ -1.0 (1H, b, D_2O exch), 2.6 (10H, m), 6.2 (~1H, s), 6.4 (~1H, s), 7.78 (3H, s), 7.95 (2H, s); ms m/e (%) 254 (M, 21), 237 (M-17, 27).

The CH_2Cl_2 extract (0.23 g) gave product: ir (CHCl_3) 3420, 3200, 3070, 1630, 1155, 1120, 1080 cm^{-1} ; nmr τ 2.1 (b, D_2O exch); 2.6 (m), 7.78 (s); ms m/e (%) 150 (M, 95), 134 (13), 133 (M-17, 17). This material was suspected to be the oximes of N-methylbenzamide.

4-9-3 Competitive Intra- and Intermolecular Photoaddition

The N-nitroso-N-methyl-3-cyclohexene-1-methylamine³ 9 (0.152 g, 0.001 moles), styrene (0.105 g, 0.001 moles) and 0.085 ml conc. HCl were dissolved in sufficient CH_3OH to make 25.0 ml

³ This compound was kindly furnished by R. A. Perry.

solution. Aliquots of 3.0 ml were added to 5 reaction vessels and purged with nitrogen for about 120 seconds. One tube prepared in the same manner served as a control. The tubes were placed in the merry-go-round apparatus and were irradiated through a nonex filter with the 450 watt Hanovia medium pressure lamp. One flask was removed at every 20 minute interval. To each flask was added 0.5 ml bromobenzene solution (0.534 g in 10.0 ml CH₃OH). The contents were analyzed by vpc for the amount of unreacted styrene. Styrene was not consumed during the photo-reaction but 9 had reacted as shown by the decrease in the uv absorption.

4-10 Competitive Photoaddition Between NNP and Diazenium Salt (6) to Styrene

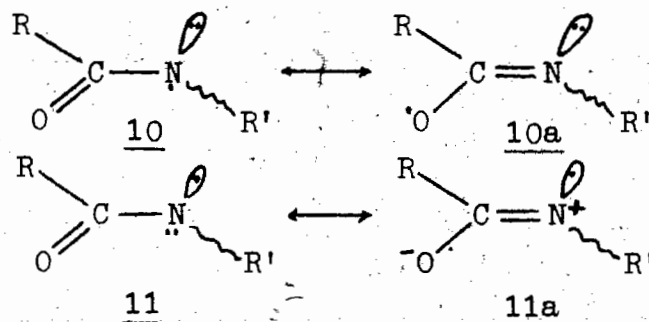
The 2-ethoxy-1,1-pentamethylene diazenium tetrafluoroborate 6 was prepared according to the published procedure (66). The diazenium salt (1.19 g, 0.005 moles), NND (0.37 g, 0.005 moles), styrene (1.05 g, 0.010 moles), conc. HCl (0.42 ml) and sufficient CH₃OH to make 250 ml solution were irradiated with the 200 watt Hanovia lamp through a nonex filter. From uv spectroscopy the disappearance of NND was essentially complete after 1 h irradiation. The work-up procedure was as described for the other photoadditions. A crude oxime was isolated, N,N-dimethylaminoacetophenone oxime (0.65 g): ir (CHCl₃) 3300, 3170, 3050, 1660, 1305, 1260 cm⁻¹; nmr τ -0.6 (1H, b, D₂O exch), 2.5 (5H, m), 6.25 (2H, s), 7.6 (6H, s). From nmr spectroscopy there was no evidence for the presence of the piperidiny1 oxime.

PART B

CHAPTER 5
INTRODUCTION

5-1 General

Transient amido radicals possess the capability of accommodating the unpaired electron in one of two different molecular orbitals. The ground state of the radical may assume either a Π (structure 10) or a Σ (structure 11) electronic configuration. In both examples an sp^2 hybridization at nitrogen is assumed.



In the Π radical the unpaired electron can resonate between the nitrogen and oxygen atoms (10 \longleftrightarrow 10a) by way of the p_z orbitals. In the Σ radical the unpaired electron remains localized in the nitrogen sp^2 hybrid orbital and the lone pair is involved in the resonance delocalization (11 \longleftrightarrow 11a). Which electronic configuration of the amido radical will prevail is governed, at least in part, by the energy differences of the two states. There is a balance between the energy needed to promote an electron in a hybrid orbital to a p orbital and the energy difference resulting from resonance delocal-

ization of the electron pair of 11 over a single electron in a p orbital of 10 (67). The results of N,O-diacylhydroxamine photolysis (68) and of very simple molecular orbital considerations (69) have been interpreted in favour of a Σ configuration for the amido radical. More recently Danen and Gillert (70) have obtained electron spin resonance (esr) evidence which is consistent with a Π radical configuration.

Electron spin resonance spectroscopy parameters have been used to differentiate between Σ and Π radicals. Nevertheless, controversy has flared in the literature. Some investigators would assign a certain configuration to a putative radical (71) only to be repudiated shortly later by a second group of workers (for example (72)) who would suggest an alternative structure or configuration to fit the data. Part of the difficulty lies in the method of radical generation. In high energy bombardment with x-rays (73-75) and with γ -rays (72, 76, 77) the fragmentation pattern of the precursor molecule is not always known with certainty (72).

5-2 General Objectives

In this investigation the chemical reactions of the various amido radicals, when known, will be discussed to see if there is any discernible trend which will differentiate between the reactivity of Σ and Π radicals. However, such a task is fraught with difficulties. The available data is limited and subject to divergent interpretation both as to radical structure and to mechanism of radical reactivity. An

encouraging fact, however, is that predictions of the INDO SCF MO theory support esr data in assigning Π configuration to N-t-butyl acetamido (70), N-hydroxyformamido (78), N-methoxy-N-methylamino (79) and Σ configuration to iminoyl (80) and benzoyl (81) radicals. In this study the INDO method will be employed to investigate the effects of conformation and of substitution on the Σ - Π character of a series of related amido radicals.

5-3 Experimental Investigations of Amido Radicals

Although some degree of uncertainty still remains, the Σ - Π nature of radicals can best be characterized from esr data. The Σ radical has the unpaired electron localized in an sp^2 hybrid orbital. Because of the s orbital component, this hybrid orbital has non-vanishing amplitude of electron density at the nucleus. Electron density at the nucleus is essential in order to give rise to hyperfine splitting (82). Pure atomic p and d orbitals and molecular π orbitals will result in no esr spectrum being observed (82). The hyperfine coupling constant of a radical, therefore, is directly dependent upon the amount of s character of the orbital. The Σ radicals also have a lower proportionality constant, g, values than that of the unbound electron (81). The Π radicals on the other hand will have lower hyperfine coupling constants and a larger g value than that of the unbound electron.

5-3-1 Amido Radicals

Danen and Gillert (70) have reported the first unequivocal identification of a simple amido radical which had esr parameters in agreement with a Π radical ground state. They observed a nitrogen hyperfine coupling constant, α^N , of 15.0 G and a g value of 2.0053 (70). Earlier French workers (83, 84) had erroneously reported the esr observance of the Π ground state of N-methylacetamido radical, α^N of 6.9 G. What they had observed in fact was the acyl nitroxide radical (70).

Smith and Wood (71) have claimed the generation of OCHNH from formamide using a flow technique of $\cdot\text{OH}$ produced from titanous chloride and H_2O_2 . Based on esr data, $\alpha^N = 21.65$ G and $g = 2.0016$, they (71) concluded that the radical had the Π electronic configuration. Other workers (85) observed the same esr parameters when the precursor was OCHND_2 and concluded that the radical structure was CONH_2 . Symons (72) bombarded formamide with γ -rays and concluded from the esr data that the resultant product, CONH_2 , had Σ configuration.

Cyr and Lin (75) have reported that the radical, $\text{H}_2\text{NCOCH}_2\text{CONH}$, resulting from x-ray irradiation of malonamide had an unusually large ^1H hyperfine coupling constant and was Σ in nature. There was support for this assignment (73) and disagreement from Symons (86) who reviewed the published data and suggested the radical to be Π . Lin and co-workers (76) subsequently modified their structural assignment to the imino radical, $\text{H}_2\text{NCOCH}_2\text{CH}=\text{N}\cdot$, which is structurally related to the iminoxy radical, $\text{R}_2\text{C}=\text{N}-\text{O}\cdot$, which is known to have the

Σ electronic configuration (87).

5-3-2 Structurally Related Radicals

Controversy also exists as to the structures of the related hydrazide radicals. In x-ray irradiated cyanoacetohydrazide, Lin (88, 89) assigned the structure, $\text{NCCH}_2\text{CONH}\dot{\text{N}}\text{H}$ to the resultant radical. From consideration of the direction of the nitrogen and proton tensors, it was concluded that the unpaired electron was in a delocalized π molecular orbital (88). This assignment has been challenged by Muszkat (77) who carried out γ -irradiation of a single crystal of cyanoacetohydrazide and suggested the structure of the radical to be $\text{NCCH}_2\text{CON}\dot{\text{N}}\text{H}_2$. One of the reasons for this conclusion was the similarity of the a_{β}^{N} of 2.0 to 5.0 G with those observed in free radicals of the type $\text{RN}_\beta\text{HCHCOOH}$. Radical $\text{NCCH}_2\text{CON}\dot{\text{N}}\text{H}_2$ was stated to be Π (77).

The urea radicals have been the subject of similar confusion. Studies of the x-ray irradiation of single crystals of hydroxyurea ($\text{H}_2\text{NCONHOH}$) and N-methylurea (90) led to the incorrect assignment of structures $\text{H}_2\text{NCON}\dot{\text{H}}$ and $\text{H}_2\text{NCONHCH}_2$ respectively. Lau and Lin (74) x-irradiated cyanoacetylurea and obtained two radicals. One was a Π radical, $\text{NCCHCONHCON}\dot{\text{H}}_2$; the other a Σ radical, $\text{NCCH}_2\text{CONHCON}\dot{\text{H}}$. The radical obtained from hydroxyurea has been reinvestigated (91) and found to be the nitroxide, $\text{H}_2\text{NCONHO}\cdot$, which was of Π configuration. Recently the radical obtained from γ -ray bombardment of urea at 77°K has been stated to be of Π character (72).

Irradiation with γ -rays at 77°K of N-chlorosuccinimide gave radicals which were interpreted (92) as having an unpaired electron predominantly in a N-halogen σ^* orbital. The radicals were stated to be the radical anions of the imide. It may be postulated that outside the confines of the matrix, the imide radicals would be Σ in nature.

Thermal decomposition of N-nitrosohydroxylamine derivatives gave as intermediates, the N-alkoxyamido radicals (78). This radical had α^N of 10.5 G and was stated to possess Π electronic configuration (78). Photolysis of ethyl N-ethoxy t-butyl carbamate resulted in the formation of N-alkoxy-N-carboethoxy-amino radical (67) which had an α^N of 10.8 G and the species was characterized as a Π radical.

In Table 5-1 are summarized some of the radical structures and configurations reported in the literature.

5-4 Chemical Reactivity of Amido Radicals

Free radicals generally undergo four main types of reactions - hydrogen abstraction, addition to unsaturated linkages, dimerization and disproportionation. The former two processes are most characteristic of amido and related radicals. In these types of reactions conclusions concerning the possible involvement of radicals must be drawn with great care. It is imperative to establish that the radicals are indeed involved and that the observed products are not the result of ionic processes. Touchard and Lessard (93) have shown that N-bromoacetamide (NBA) under photolytic conditions

Table 5-1

Radical Structures and Configurations Assigned from ESR Data

Source	Structure	Assigned Configuration	Reference
OHCNH ₂	OHCNH ^{••}	Π	71
	CONH ₂ [•]	Σ	72
OHCND ₂	OCND ₂ [•]	Π	85
H ₂ NCOCH ₂ CONH ₂	H ₂ NCOCH ₂ CONH [•]	Σ	72,75
	H ₂ NCOCH ₂ CH=N [•]	Σ	76
NCCH ₂ CONHNH ₂	NCCH ₂ CONHNH [•]	Π	88,89
	NCCH ₂ CONNH ₂ [•]	Π	77
H ₂ NCONHOH	H ₂ NCONH [•]	Π	90
	H ₂ NCONHO [•]	Π	91
H ₂ NCONH ₂	H ₂ NCONH [•]	Π	72
CH ₃ NHCONH ₂	[•] CH ₂ NHCONH ₂	Π	90
R'CON(NO)OR	R'CONOR [•]	Π	78
CH ₃ CONCl(CH ₃)	CH ₃ CONCH ₃ [•]	Π	70
(CH ₃ CONCH ₃) ₂ N ₂	CH ₃ CONCH ₃ [•]	Π	83

undergoes addition to cyclohexene in 25% yield by a radical pathway. Wolf and Awang (94) have demonstrated that in refluxing CCl_4 NBA decomposed to give N,N-dibromoacetamide as the intermediate which underwent ionic addition to give 2-bromo-N-bromoacetamides. Recently (95) it has been shown that NBA added smoothly to 2,3-unsaturated nitro sugars in aqueous acetone solution in an ionic manner.

5-4-1 Amido Radicals

The amido radical can react as a N-radical (10, 11, 11a) or as an O-radical (10a). The reactivities will be controlled by the spin density at each heteroatom and by other factors which influence radical reactions. Amido radicals derived from N-halocarboxamides (96) typically undergo intramolecular rearrangement reactions. In such structures as N-halo-N-methylacetamide where intramolecular hydrogen transfer is not possible, the radical intermediate generally will abstract an allylic hydrogen intermolecularly (97) but addition is limited to special cases such as intramolecular addition or addition to norbornene. When photolyzed, N-chloro-N-methylacetamide only abstracted a hydrogen atom from cyclohexene solvent (93) but did add to norbornene which lacks labile hydrogens. On the other hand, N-bromo-N-methylacetamide when photolyzed even at -70° gave no addition product with any reactive olefins (97). There are two examples in the literature (98, 99) where N-methylamido radicals have undergone intramolecular addition to a double bond. In both cases the structures were

very favourable for intramolecular additions.

The N-haloacetamides under photolytic conditions do add to olefins (93). The yield of the 1,2 adduct is remarkably increased when the temperature is lowered and when α -halogens on the carbonyl methyl are present (97). The N-chloro-trifluoroacetamide gave only cis-1,2 adduct in 97% yield (97). The addition reactivity was suppressed by the presence of an N-methyl substituent. Primary amides in the presence of iodine, an oxidizing agent and irradiation result in the spontaneous formation of 2-iminotetrahydrofuran (100), most probably via an amido radical intermediate.

5-4-2. Imido Radicals

The imido radicals undergo reactions similar to those of the amido radicals. The N-acyl-N-chlorocarboxamides under photolytic conditions undergo intramolecular hydrogen transfer (101). Bromination of the allylic position on an olefin using N-bromosuccinimide (NBS) has been established to follow a free radical mechanism (102). Generally, the bromination reaction proceeds very efficiently to form the bromo-alkene and succinimide. The latter is formed from preferential hydrogen abstraction. NBS has been found, however, to give 1,2 adducts with dihydropyran (103) and with 3-butenitrile (104), though in low yield. NBS with dihydropyran in refluxing CCl_4 gave a 7% yield of adduct (103) and with 3-butenitrile and dibenzoyl peroxide in refluxing CCl_4 gave a 2% yield of adduct (104). NBS has also been shown to give 1,2 adducts

with double bonds in about 20 % yield of several unsaturated nitriles and acetylenes (105). In these examples, however, it has not been established unequivocally that the succinimido radical is indeed involved.

5-5 The INDO MO Method

The INDO MO method (61) takes into account the interaction between two orbitals on the same atom as opposed to the complete neglect of differential overlap (CNDO) (106). To make calculations on large molecules more manageable, interatomic interactions are given empirical values. For equation [5-1] INDO computes the value

$$\psi_i = \sum_{\mu} c_{\mu i} \phi_{\mu} \quad [5-1]$$

of each molecular orbital, eigenvalue and eigenvector, $c_{\mu i}$, which is related to the contribution that each atomic orbital ($2s$, $2p_x$, $2p_y$, $2p_z$) makes toward the composition of the molecular orbital. For radicals unrestricted wavefunctions are utilized. In essence this means that two completely independent sets of molecular orbitals ψ_1^{α} , ψ_2^{α} and ψ_1^{β} , ψ_2^{β} are used (63). An eigenvalue is calculated for each molecular orbital having spin α and spin β . One eigenvalue of spin α and one of spin β will naturally make up one molecular orbital. The eigenvalues of spin α and spin β must be very similar for a correct match.

The total energy, E , of the system for a given set of inter-nuclear distances is given by

$$E = e + \sum_{A < B} e^2 Z_A Z_B r_{AB}^{-1} \quad [5-2]$$

where ϵ is the electronic energy and the second term of [5-2] is the electrostatic internuclear repulsion energy (63). Both the total and the electronic energies are calculated while the difference of these terms will give the nuclear repulsion energy.

In a Π radical the molecular orbital containing the unpaired electron will have contributions from the p_z eigenvectors of all atomic centres, but no contributions from the other eigenvectors. For Σ radicals the molecular orbital localizing the unpaired electron will have no p_z contribution but only contributions from atomic s , p_x and p_y orbitals which constitute the sp^2 hybrid orbital.

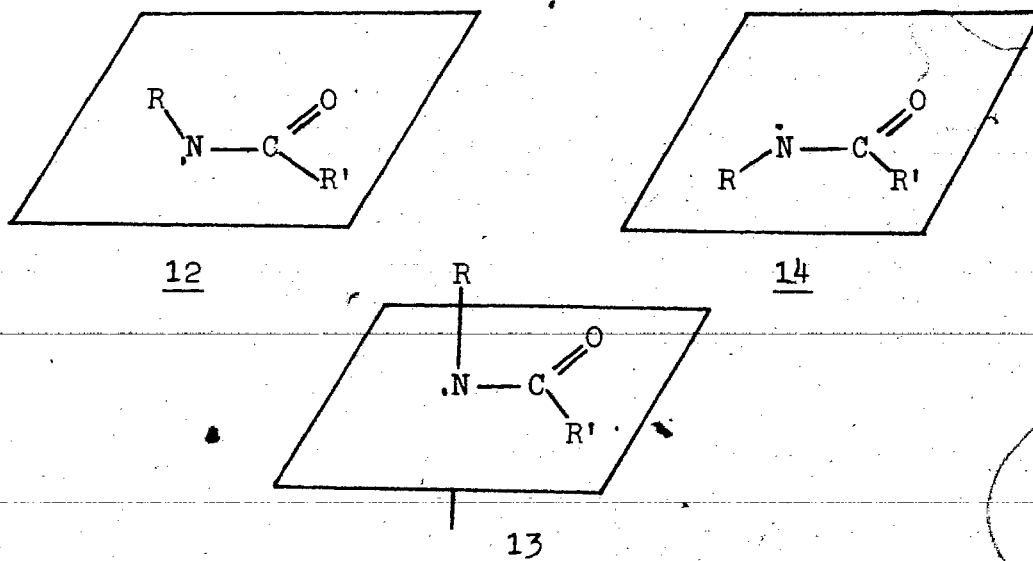
The INDO programme, where applied, has been very successful in predicting Σ or Π character of radicals. Results from INDO calculations (83) and from esr data (70) of N-substituted acetamido have agreed that the radical is Π . Calculations on formamido radical have shown it to be Σ (107) and this is consistent with esr data (72). The N-methoxy-N-methylamino radical has been studied by both esr and INDO with complete accord as to the Π character of the radical (79). Iminoyl free radical, $R-C=N-R'$, had low g value (2.0016) and small β -hydrogen hyperfine interaction (80) which are characteristic of Σ radicals. INDO calculations supported this assignment (80). In the following chapter the Σ and Π electronic configurations of various conformations and structures of amido and related radicals will be considered by the INDO method.

CHAPTER 6RESULTS6-1 General

In all the following calculations on nitrogen centred radicals, the INDO SCF MO programme was used. The open shell option with the unrestricted method of calculating the eigenvalues of both alpha (α) and beta (β) spins was utilized. The only input necessary for the programme was the cartesian coordinates and the atomic number of each atom of the radical. The geometry of the radical chosen was based on the appropriate ground state precursor molecule. No attempt was made to minimize the total energy of the radical with respect to variation of all bond lengths, bond angles and dihedral angles. Of prime interest in this investigation were the spin densities in the various orbitals. From preliminary calculations it was observed that electron distributions were not influenced or affected by minor geometrical alterations.

Throughout the following sections the influence of changes in conformation on calculated radical spin densities, total energies and eigenvalues of the highest occupied molecular orbitals (HOMO) will be considered. The general procedure followed was to investigate the trans, cis and orthogonal conformations of amido and related radicals. For the orthogonal conformer, the NCOC plane was rotated by 90° as shown in 13. Structures 12, 13 and 14 represent the trans, orthogonal

and cis conformers respectively. The effect on the calculated



properties of allyl radical by such procedures was first considered. Subsequently this method will be applied to the nitrogen centred radicals of interest. All energies are given in atomic units (1 a. u. = 627.7 kcal/mole). Where indicated relative energies, in kcal/mole, are given in parentheses in the tables. The convention followed was to affix a negative sign to a relative energy which was more stable than the standard taken.

The bond lengths, bond angles and dihedral angles used as input parameters were generally expressed to three significant figures. From the rules governing the proper retention of significant figures (108), the calculated energies must be expressed also in three significant figures. The results under this criterion are then at best significant to ± 0.05 atomic units or ± 31.4 kcal/mole. In spite of this, however, generally at least four significant figures were retained in the following tables. Because of the semi-empirical nature of INDO, the accuracy of the

computed results are suspect. The precision of the results for the various manipulations will be high due to the rather stringent convergence criterion (10^{-6} atomic units) of the programme.

6-2 Allyl Radical

The allyl radical was taken to be planar with the p orbitals perpendicular to this plane of carbon and hydrogen bonds. The



methylene carrying the unpaired electron and consisting of the plane containing the HCH atoms, was rotated through various angles up to 90° for the calculation. The latter conformation resulted in the p orbital containing the unpaired electron being orthogonal to the remaining p orbitals of the radical, 16.

The calculated results for such an operation are given in Table 6-1 and are shown graphically in Figure 6-1. Progressive rotation of the methylene group increased the total energy of the conformation, as would be intuitively expected, due to the removal of the p orbital from conjugative resonance stabilization with the p orbitals of the double bond. Such rotation, however, decreased the nuclear repulsion contributing to the total energy (the solid line of Figure 6-1).

In Table 6-2 are listed the calculated spin densities of each orbital of the three carbon atoms. Carbon 3 accommodated the original unpaired electron in a p orbital. As can be seen from Table 6-2 the spin density in the p_z orbital decreased with

Table 6-1

Calculated Energies of Allyl Radical Conformers

CH ₂ =CHCH ₂ 1 2 3 Radical Conformer	Electronic Energy ^a	Total Energy ^a	Nuclear Repulsion ^a
0°	-59.079 (0)	-24.050 (0)	35.028 (0)
45°	-59.042 (23.0)	-24.043 (4.3)	34.999 (-18.3)
60°	-59.026 (33.3)	-24.040 (6.3)	34.985 (-27.0)
90°	-59.010 (42.9)	-24.038 (7.5)	34.972 (-35.5)

^a Energies are in atomic units with relative energies (kcal/mol) given in parentheses.

Table 6-2

Spin Densities of Allyl Radical Conformers

Orbital	Conformer				
	0°	45°	60°	90°	
C ₁	s	0.02	0.02	0.02	0.01
	p _x	0.01	0.02	0.02	0.01
	p _y	0.01	0.01	0.01	0.0
	p _z	0.36	0.21	0.11	0.02
C ₂	s	-0.02	-0.02	-0.02	-0.02
	p _x	-0.01	-0.02	-0.02	-0.02
	p _y	-0.02	-0.03	-0.03	-0.03
	p _z	-0.21	-0.13	-0.08	-0.02
C ₃	s	0.05	0.05	0.05	0.05
	p _x	0.03	0.36	0.55	0.73
	p _y	0.03	0.13	0.18	0.24
	p _z	0.83	0.47	0.25	0.03

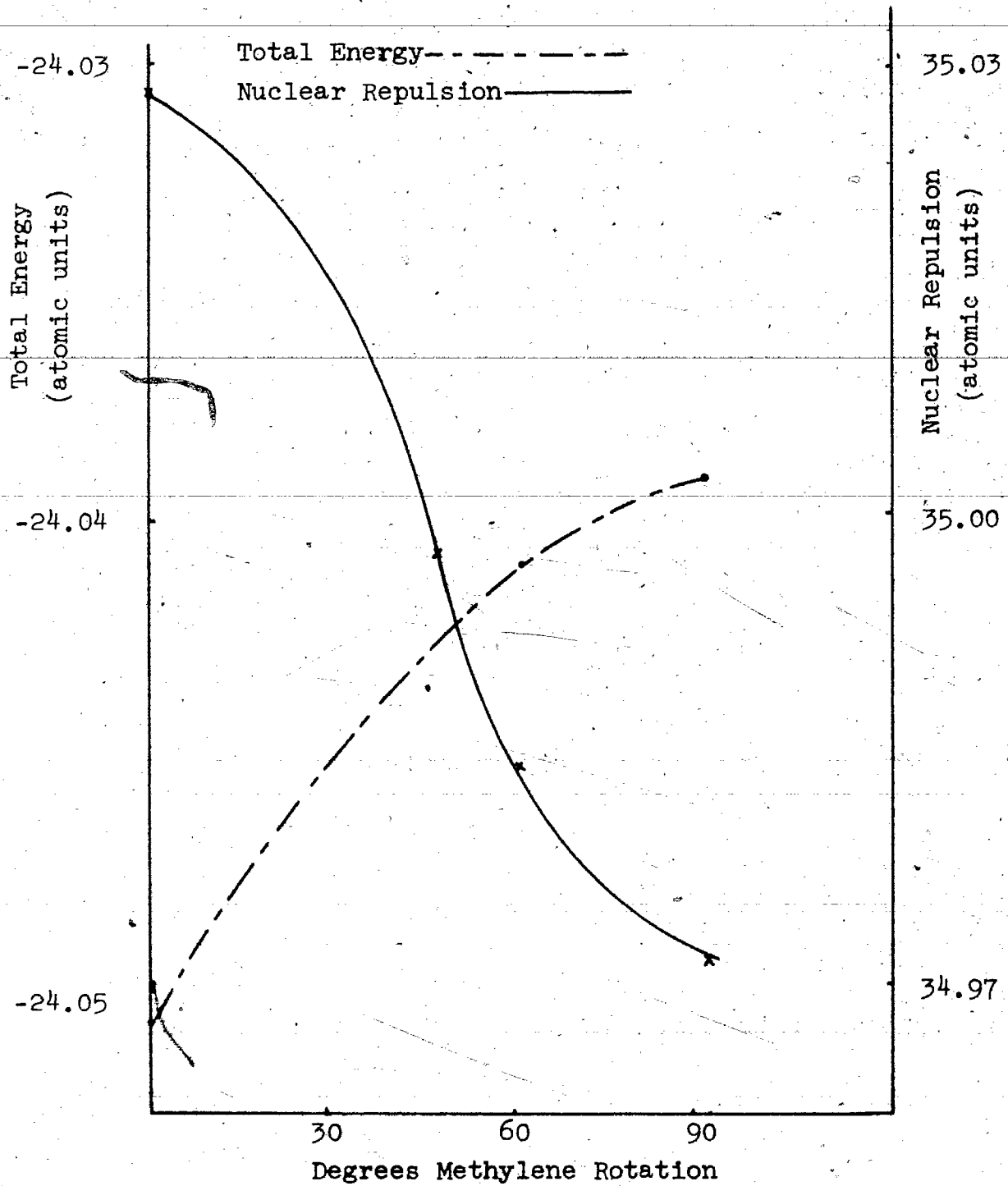


Figure 6-1 Total Energy and Nuclear Repulsion Energy as a Function of Degrees Methylene Rotation

the degree of methylene rotation. In the orthogonal conformer, the p_z spin density on carbon 3 had virtually disappeared as would be expected when the orbital is perpendicular to the remaining p orbitals of the radical.

Experimentally in the allyl radical the spin densities at carbons 1 and 3 were found to be 0.594 and at carbon 2, -0.189 (109). In the present calculation the terminal spin densities were unequal.

The allyl radical has 17 valence electrons which are shown in Table 6-3 to be distributed over 9 orbitals of α spin and 8 orbitals of β spin. The HOMO is shown at the top of the series of eigenvalues or molecular orbital energies. The π eigenvalues had only p_z eigenvectors or orbital coefficients, the square of which indicated the contribution of the particular atomic orbital to the molecular orbital. Those eigenvalues labelled σ had zero contribution from p_z eigenvectors. In Table 6-3 for the 0° rotation conformer of allyl radical, eigenvalue 6 of α spin (α_6) and eigenvalue 7 of β spin (β_7) were both π . The three circles below each eigenvalue represent the phases of the p_z eigenvectors of each of the 3 carbon atoms of allyl radical.

Hence, eigenvalue α_6 and eigenvalue β_7 have the same symmetry and must be components of the same molecular orbital. Eigenvalue α_9 was of π character and had no matching β eigenvalue of the same symmetry. The odd electron was then localized in a π orbital of the 0° rotation (normal) allyl radical. This was, of course, in harmony with the spin density data of

Table 6-3Eigenvalues of Two Allyl Radical Conformers0° Conformer90° Conformer

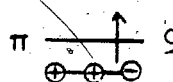







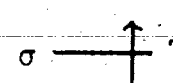

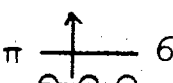



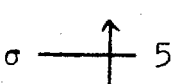

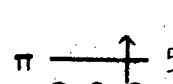
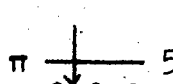
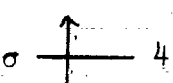
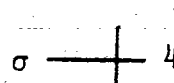

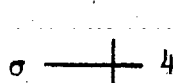


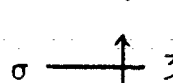

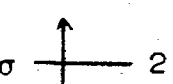
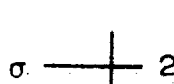

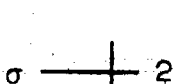


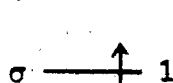

<u>α Spin</u>		<u>β Spin</u>		<u>α Spin</u>		<u>β Spin</u>	
π				σ			
σ		σ		π		π	
σ		π		σ		σ	
π		σ		σ		σ	
σ		σ		π		π	
σ		σ		σ		σ	
σ		σ		σ		σ	
σ		σ		σ		σ	
σ		σ		σ		σ	

Table 6-2. In the 90° conformer, both α and β eigenvalues in orbital 5 and 8 had π character. The phases of the carbon eigenvectors are shown below each orbital in Table 6-3. Eigenvalues α_5 and α_8 are of complementary symmetry to eigenvalues β_5 and β_8 . Complementary symmetry is taken here to mean the matching of plus with minus symmetry phase elements. The unpaired electron was in a σ orbital. Again this was in agreement with the data of Table 6-2 which showed no spin density in the p_z orbital. Conformers of 45 and 60 degree methylene rotation gave eigenvalues whose eigenvectors could not be matched with respect to symmetry elements.

The results for the allyl radical corroborated quantitatively what would be anticipated in qualitative terms if the stated operations were performed on the radical. Thus the INDO programme is capable of yielding information with regard to orbital occupancy and electron unpaired spin distribution. The study can then be extended with reasonable confidence to a similar analysis of amido and related radicals.

6-3 Amido Radicals

6-3-1 N-Methylacetamido Radical

Due to the very interesting properties of N-methylacetamido radical, several conformations were considered. Beginning with the trans conformation, the plane incorporating the NCOCH_3 atoms was rotated through 60, 70, 80, 90, 120 and 180 degrees analogously to the process represented by structure 13. The 180° conformer, of course, corresponded to cis-N-methylacetamido radical. The

values of the calculated total energies and nuclear repulsions are tabulated in Table 6-4. The total energy of Figure 6-2 (dashed line) showed a minimum at 80° rotation. In Figure 6-2 the solid line represented the nuclear repulsion is shown to mirror the curve of the total energy. The minimum occurred at 70° rotation. The nuclear-nuclear repulsion was greatest at the cis conformer as would be intuitively expected.

In Table 6-5 are tabulated the spin densities of the unpaired electron at each orbital centred on the nitrogen and oxygen atoms. It can be seen that in the trans conformer of N-methylacetamido radical the spin density is localized in the p_z orbitals of nitrogen and oxygen. This was indicative of a Π radical. However, as the angle of rotation increased, the spin densities in the p_z orbitals rapidly decreased and the unpaired electron density was transferred to the nitrogen p_x and p_y orbitals. The radical became Σ .

In Table 6-6 are shown the distributions of the 29 valence electrons of N-methylacetamido radical into 15 orbitals of α spin and 14 orbitals of β spin. Each eigenvalue of π symmetry is so labelled. Adjacent to each π eigenvalue are five interconnected circles representing the p orbitals of the five atoms of the skeleton. Each circle bears the phase of the contributing π eigenvector.

It can be seen that in the trans radical conformer, α_5 and β_6 had the same symmetry. Eigenvalues α_9 and β_9 had complementary symmetry. Eigenvalues α_{11} and β_{12} had the same symmetry. Eigenvalue α_{14} was of π character but had no corresponding eigenvalue

Table 6-4

Calculated Energies of N-Methylacetamido Radical Conformers

<u>CH₃NCOCH₃</u> <u>Radical</u> <u>Conformer</u>	<u>Electronic Energy^a</u>	<u>Total Energy^a</u>	<u>Nuclear Repulsion^a</u>
0° (trans)	-147.722 (282)	-53.741 (-25.9)	93.980 (-303)
60°	-147.416 (474)	-53.742 (-24.7)	93.674 (-494)
70°	-147.406 (480)	-53.742 (-23.9)	93.663 (-501)
80°	-147.418 (473)	-53.743 (-23.9)	93.675 (-493)
90°	-147.457 (448)	-53.743 (-23.8)	93.714 (-471)
120°	-147.713 (287)	-53.739 (-21.4)	93.974 (-307)
180° (cis)	-148.170 (0)	-53.705 (0)	94.465 (0)

^a Energies are in atomic units with relative energies (kcal/mol) given in parentheses.

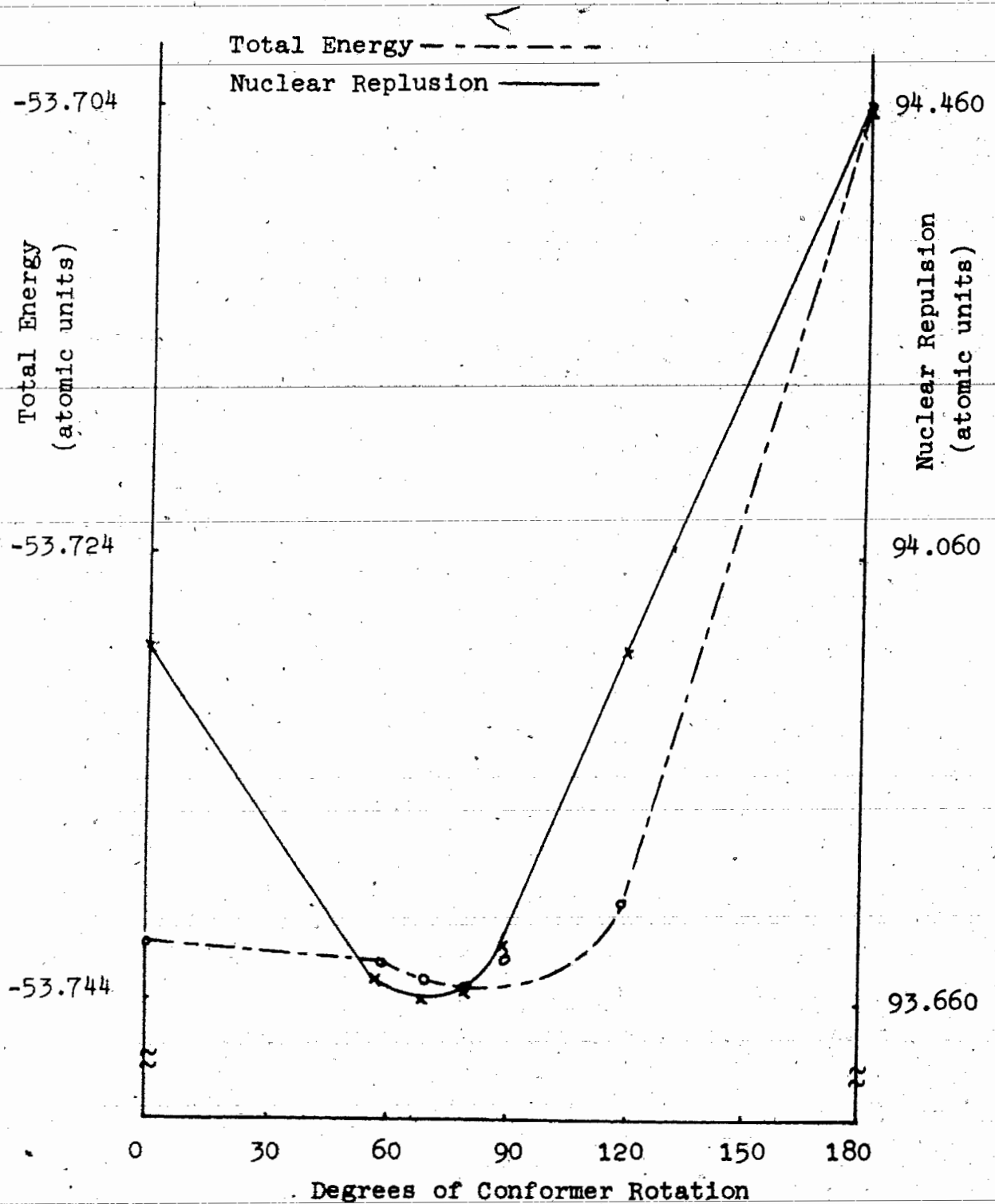
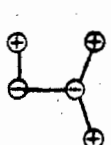

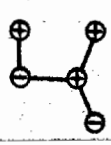
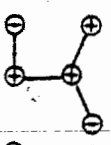

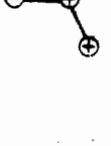
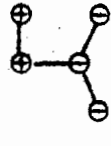
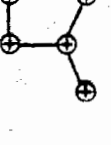
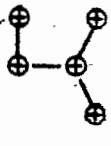

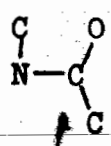


Figure 6-2 Total Energy and Nuclear Repulsion Energy as a Function of Degrees of Conformer Rotation

Table 6-6

Eigenvalues of Two N-Methylacetamido Radical Conformers

<u>trans Conformer</u>			<u>cis Conformer</u>		
<u>α Spin</u>		<u>β Spin</u>	<u>α Spin</u>		<u>β Spin</u>
	σ ↑ 15			π ↑ 15	
	π ↑ 14	σ ↓ 14		σ ↑ 14	
	σ ↑ 13	σ ↓ 13		σ ↑ 13	σ ↓ 13
	σ ↑ 12			σ ↑ 12	σ ↓ 12
	π ↑ 11	π ↓ 12		π ↑ 11	π ↓ 11
	σ ↑ 10	σ ↓ 11		σ ↑ 10	σ ↓ 10
	π ↑ 9			π ↑ 9	π ↓ 9
	σ ↑ 8	σ ↓ 10		σ ↑ 8	σ ↓ 8
	σ ↑ 7	σ ↓ 9		σ ↑ 7	σ ↓ 7
	σ ↑ 6			σ ↑ 6	σ ↓ 6
	π ↑ 5	π ↓ 7		π ↑ 5	π ↓ 5
	σ ↑ 4	σ ↓ 6		σ ↑ 4	σ ↓ 4
	σ ↑ 3	σ ↓ 5		σ ↑ 3	σ ↓ 3
	σ ↑ 2	σ ↓ 4		σ ↑ 2	σ ↓ 2
	σ ↑ 1	σ ↓ 3		σ ↑ 1	σ ↓ 1
		σ ↓ 2			σ ↓ 2
		σ ↓ 1			σ ↓ 1

 = 

of β spin. An examination of the σ character eigenvalues α_{13} , α_{15} , β_{13} and β_{14} showed that eigenvalues α_{15} and β_{14} had eigenvectors of the same sign and magnitude. Eigenvalues α_{13} and β_{13} were of similar magnitude but of complementary phase. Hence, the unpaired electron in the trans N-methylacetamido radical occupied a π MO but this orbital was the second highest occupied. Spin density data from Table 6-5 also suggested that this radical was of Π configuration.

In the cis-N-methylacetamido radical given in Table 6-6, the 29 electrons were again distributed into α and β spin eigenvalues. From the symmetry phase properties of the π molecular orbitals, it can be seen that α_5 and β_5 had identical symmetry while α_9 and β_9 , α_{11} and β_{11} , and α_{15} and β_{14} had complementary phased eigenvectors which were taken to represent the same molecular orbitals. The eigenvectors of σ eigenvalues α_{13} and β_{13} were similar. The unpaired electron in the cis conformer must reside in σ orbital α_{14} which was the second highest occupied. The calculated spin densities from Table 6-5 were also in agreement with the cis conformer being of Σ type. For the orthogonal conformer such analysis could not be done because all the eigenvectors had numerical value and no symmetry.

6-3-2 Other Amido Radicals

The pertinent information for the other amido radicals is summarized in Table 6-7. The cisoid and transoid conformers of formamido and acetamido radicals and 2-pyrrolidinone had the unpaired spin density concentrated in either the p_x or p_y orbitals

Table 6-7

Calculated Energies and Spin Densities of Other Amido Radicals

Radical	Calculated Energies			Spin Densities								
	Conformer	Electronic ^a	Total ^a	Nuclear ^a	Nitrogen			Oxygen				
			Repulsion ^a	s	P _x	P _y	P _z	s	P _x	P _y	P _z	
HCONH	transoid	-71.99	-36.77	35.13	-0.01	0.09	0.05	-0.02	0.02	0.01	0.86	0.02
	orthogonal	-71.85	-36.79	35.05	0.04	0.69	0.26	0.01	0.0	0.05	0.0	0.0
	cisoid	-71.73	-36.77	34.96	-0.01	0.02	0.07	-0.02	0.02	0.0	0.86	0.02
FCONCH ₃	trans	-163.46	-70.99	92.47	0.03	0.02	0.01	0.75	0.01	0.01	0.01	0.46
	orthogonal	-163.32	-70.99	92.32	0.04	0.02	0.01	0.85	0.0	0.01	0.02	0.0
	cis	-164.02	-71.00	93.02	0.03	0.02	0.01	0.74	0.01	0.01	0.0	0.46
CH ₃ NCHO	trans	-107.80	-45.29	62.51	0.03	0.02	0.01	0.73	0.01	0.0	0.01	0.50
	orthogonal	-106.83	-45.29	61.54	0.04	0.02	0.01	0.85	0.0	0.0	0.01	0.02
	cis	-106.27	-45.29	60.98	0.03	0.02	0.01	0.73	0.01	0.01	0.0	0.50
CH ₃ CONH	transoid	-107.43	-45.22	62.20	-0.01	0.12	0.02	-0.02	0.02	0.68	0.19	0.02
	orthogonal	-107.40	-45.25	62.15	0.04	0.02	0.94	0.01	0.0	0.02	0.03	0.0
	cisoid	-107.48	-45.22	62.26	-0.01	0.10	0.01	-0.02	0.02	0.64	0.24	0.02

Table 6-7 (continued)

Calculated Energies and Spin Densities of Other Amido Radicals

Radical	Calculated Energies			Nuclear Repulsion ^a	Spin Densities							
	Conformer	Electronic ^a Total	s		p _x	p _y	p _z					
2 Pyrol- lidinbno			-0.01	0.11	0.04	-0.02	0.02	0.62	0.26	0.02		
CH ₃ ONCOCH ₃	trans	-201.70	-71.41	130.29	0.03	0.01	0.01	0.66	0.01	0.0	0.01	0.46
	orthogonal ^b	-201.33	-71.38	132.96	0.08	0.04	0.35	0.19	0.0	0.0	0.08	0.08
	cis	-201.30	-71.40	129.91	0.03	0.0	0.01	0.61	0.01	0.0	0.01	0.46

^a Energies are in atomic units.

^b Programme did not converge to the 10⁻⁶ atomic unit limit.

of the oxygen atom. The orthogonal conformers of formamido and acetamido radicals had the unpaired spin density concentrated on the nitrogen p_x or p_y orbitals. All these radicals were of Σ electronic configuration.

In the cisoid and transoid conformers of formamido and acetamido radicals, the HOMO was of π character. The HOMO of β spin was of π character with eigenvectors corresponding to those of the HOMO of α spin. The unpaired electron was localized in the second HOMO of σ character. In 2-pyrrolidinono radical the HOMO of α spin localized the unpaired electron and was of σ character.

From Table 6-7 it can be seen that all the conformers of N-methylfluoroformamido and N-methylformamido radicals localized the unpaired spin density on the nitrogen p_z orbital. The cis and trans conformers of N-methoxyacetamido radical had the unpaired electron density in the p_z orbital system of the oxygen and nitrogen atoms. The data convincingly demonstrated that these radicals were of Π configuration.

Only in trans-N-methoxyacetamido radical was the unpaired electron in the α spin HOMO of π character. In all the other radical conformers of N-methylfluoroformamido, N-methylformamido and N-methoxyacetamido, the second HOMO of α spin was of π character and localized the unpaired electron.

6-4 Imido Radicals

From the data of Table 6-8 it can be seen that the syn and anti conformers of N-formylformamido and N-formylacetamido radicals and that of succinimido have the unpaired spin density

Table 6-8

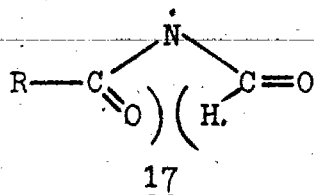
Calculated Energies and Spin Densities of Imido Radicals

Radical	Conformer	Electronic Total ^a	Nuclear Repulsion ^a	Nitrogen			Oxygen				
				P _x	P _y	P _z	s	P _x	P _y	P _z	
OHCNCHO	syn	-139.17	78.01	0.11	0.17	0.53	0.03	0.0	0.01	0.0	-0.01
	anti	-140.99	79.83	0.0	0.01	0.07	-0.02	0.02	0.0	0.85	0.02
OHCNCOCH ₃	syn	-183.97	114.36	0.10	0.19	0.52	0.03	0.0	0.01	0.0	-0.02
	anti	-188.51	118.89	0.10	0.70	0.02	0.03	0.0	0.06	0.02	-0.01
Succinimido				0.10	0.71	0.01	0.03	0.0	-0.01	-0.01	-0.03

^a Energies are in atomic units.

centred predominantly on either nitrogen p_x or p_y orbitals. The radicals were unmistakably of Σ electronic configuration.

The calculated energies demonstrated that both anti conformers experienced the greater nuclear-nuclear repulsion. This can be seen from the structural formula of an anti conformer, 17,



which experienced an oxygen-hydrogen interaction.

Succinimido was a well-behaved Σ radical with the unpaired electron occupying the HOMO of σ character. In both N-formylformamido and N-formylacetamido radicals, the second HOMO of α spin was of σ character and localized the unpaired electron.

6-5 Carbomethoxyamino Radicals

The spin densities of the trans and cis conformers of carbomethoxyamino and of all the three conformers of N-methyl-N-carbomethoxyamino radicals were restricted to the p_z orbitals as shown in Table 6-9. The radicals were of Π electronic configuration. Only the orthogonal conformer of the carbomethoxyamino radical was Σ .

In all conformers the unpaired electron was found in the second π HOMO of α spin.

Table 6-9

Calculated Energies and Spin Densities of Carbomethoxyamino Radicals

Radical	Conformer	Calculated Energies	Electronic Total ^a	Nuclear Repulsion ^a	Nitrogen			Oxygen					
					s	p _x	p _y	p _z	s	p _x	p _y	p _z	
HNCOOCH ₃	transoid	-158.26	-62.89	95.38	0.03	0.02	0.0	0.79	0.01	0.0	0.01	0.01	0.56
	orthogonal	-158.26	-62.88	95.38	0.04	0.02	0.94	0.01	0.0	0.04	0.01	0.01	0.0
	cisoid	-158.37	-62.89	95.48	0.03	0.03	0.01	0.80	0.01	0.0	0.01	0.01	0.55
CH ₃ NCOOCH ₃	trans	-202.83	-71.36	131.47	0.03	0.02	0.01	0.74	0.01	0.01	0.01	0.01	0.49
	orthogonal	-202.86	-71.36	131.50	0.04	0.02	0.01	0.85	0.0	0.01	0.01	0.02	0.01
	cis	-203.75	-71.36	132.38	0.03	0.02	0.01	0.74	0.01	0.01	0.01	0.0	0.50

^a Energies are in atomic units.

6-6 Urea Radicals

The cis and trans conformers of N-methylurea and of urea exhibited spin density in the p_z orbitals of both nitrogen and oxygen atoms as shown in Table 6-10. Both orthogonal conformers localized the spin density in the nitrogen p_y orbital. In the urea radicals the orthogonal conformers were Σ while the remaining conformers were of Π electronic configuration.

In both radicals the second HOMO of α spin was π in nature and localized the unpaired electron.

Table 6-10

Calculated Energies and Spin Densities of Urea Radicals

Radical	Calculated Energies				Spin Densities							
	Conformer	Electronic ^a	Total ^a	Nuclear ^a Repulsion ^a	Nitrogen			Oxygen				
			s		p _x	p _y	p _z	s	p _x	p _y	p _z	
HNCONH ₂	transoid	-111.46	-48.81	62.65	0.03	0.02	0.01	0.80	0.01	0.0	0.01	0.56
	orthogonal	-111.42	-48.81	62.61	0.04	0.02	0.94	0.01	0.0	0.04	0.02	0.0
	cisoid	-111.50	-48.81	62.69	0.03	0.03	0.01	0.80	0.01	0.0	0.01	0.55
CH ₃ NCONH ₂	trans	-151.21	-57.27	93.94	0.04	0.02	0.0	0.77	0.01	0.0	0.01	0.51
	orthogonal	-150.94	-57.27	93.67	0.04	0.02	0.88	0.01	0.0	0.03	0.02	0.0
	cis	-151.65	-57.27	94.38	0.03	0.03	0.01	0.76	0.01	0.0	0.01	0.52

^a Energies are in atomic units.

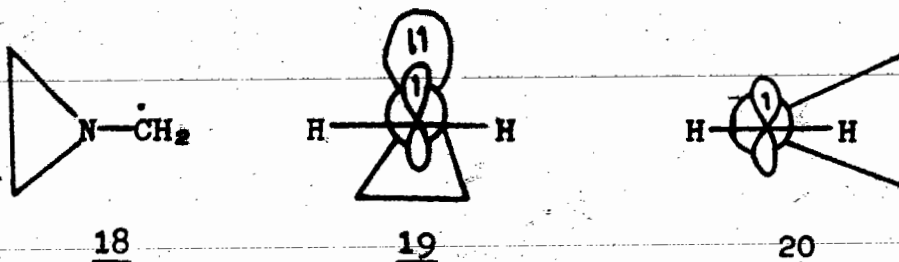
CHAPTER 7DISCUSSION7-1 General

One of the most productive applications of a theoretical computation is the study of a system whose properties cannot be measured or observed readily if at all. Such a rationale was adopted in employing the INDO method to the examination of various ground state conformations of amido and related radicals. Three conformations of each radical were generally considered and from the computed total energies, relative stabilities were obtained. In most of the radicals investigated, the orthogonal conformer had the lowest energy. There is no experimental evidence, however, either to confirm or to disclaim the intermediacy of a free radical with orthogonal conformation in chemical transformations.

There are other reports of a theoretical nature which suggest that orthogonal conformers are more stable than planar species (110, 111) of molecules and reactive intermediates. Cramer and Drago (110) have used extended Huckel calculations to compute some of the molecular properties of benzaldoximes. They found that the anti-benzaldoxime was 17.4 kcal/mol more stable when the plane of the phenyl ring and the plane of the -CHNO group were orthogonal than when the molecule was completely planar. The syn isomer, however, was more stable in the planar form. In some preliminary ab initio calculations, Rauk (111) has found that the carbene species (HCCH) and the

neutral isoelectronic system (HCBH_2) preferred the perpendicular conformation by 63 and 120 kcal/mol respectively. The nitrenium species (HCN) was more stable when planar (111).

In an investigation of 1-aziridylcarbinyl radical 18, Danen and West (109) have interpreted from esr evidence the radical to have the conformation shown in 19. INDO calculations



(112) exhibited an energy minimum for this conformation. The analogous cyclopropyl carbinyl radical was found to prefer conformation 20 (112). No doubt 19 is stabilized from resonance interaction of the unpaired radical electron and the nitrogen lone pair. In the CH_2OH radical (113) the most stable conformation obtained by INDO was the one where the hydroxylic proton was perpendicular to the carbon $2p_z$ axis.

In the allyl radical conformations investigated, the orthogonal conformer was the least stable. In the amido radicals by contrast, the orthogonal conformer was generally the most stable. The $\text{N}p_z$ orbital orientation in both orthogonal conformers had been disturbed. This may mean that in amido radicals there is much less resonance stabilization than there is in allyl radicals. The orthogonal conformers generally were also found to have the least nuclear-nuclear repulsion between the nitrogen substituent and the carbonyl oxygen or the

carbon substituent. It is very likely that this decrease in the nuclear repulsion contribution to the total energy in amido radicals may be in large measure responsible for the greater stability of the orthogonal amido radical.

7-1-1 Orbital Occupancy

The general trend in the acyclic radicals was for the HOMO of α spin to have opposing π or σ symmetry from that shown in the calculated spin densities. In other words, for the characterization of the electronic configuration of the radical, the symmetry of the α spin HOMO was opposite to the orbital which localized the unpaired spin density. This may be an idiosyncrasy of the programme. Koenig (114) in a footnote has suggested that the INDO ordering of energies is not necessarily the correct one. In a subsequent paper Koenig (112) using an altered INDO programme has shown that in formamido but not in N-methylformamido radical the electronic state is dependent upon the geometrical parameters chosen. Of the cyclic radicals investigated, all had the same symmetry for both the HOMO and the radical.

7-1-2 Other Calculated Parameters

The calculated nitrogen hyperfine couplings constants, a^N , of the various conformations of the amido radicals are shown in Table 7-1. They are reasonable for the Π radicals but fluctuate widely from -5 to 46 gauss for the Σ radicals. The a^N values of the Π radicals are in the range of 10 to 14 gauss which is near the value of 15 gauss reported for amido Π radicals (70).

Table 7-1Summary of Calculated Electronic States of Radicals

<u>Radical</u>	<u>Conformer</u>	<u>Calculated Constants</u>		
		<u>Config-uration^a</u>	<u>Nitrogen Hyper-fine Coupling^b</u>	<u>Dipole Moment^c</u>
CH ₃ NCOCH ₃ N-Methylacetamido	trans	Π (2)	11.98	0.67
	orthogonal	Σ	14.82	3.28
	cis	Σ (2)	45.95	3.90
HCONH Formamido	transoid	Σ (2)	- 4.91	2.14
	orthogonal	Σ	14.21	2.91
	cisoid	Σ (2)	- 1.79	3.53
	reported (107) reported (115)	cisoid cisoid	Σ Π	
FCONCH ₃ N-Methylfluoro- formamido	trans	Π (2)	12.84	2.02
	orthogonal	Π	14.46	2.99
	cis	Π (2)	12.01	2.62
HCONCH ₃ N-Methylformamido	trans	Π (2)	12.19	0.41
	orthogonal	Π	14.66	2.95
	cis	Π (2)	12.02	3.25
	reported (115) reported (116)	trans trans	Π Π	
HNCCH ₃ Acetamido	transoid	Σ (2)	- 4.60	2.36
	orthogonal	Σ	14.30	3.32
	cisoid	Σ (2)	- 2.99	4.04
CH ₃ ONCOCH ₃ N-Methoxyacetamido	trans	Π (1)	10.34	2.23
	orthogonal ^d	Π	29.87 ^d	2.88 ^d
	cis	Π (2)	9.58	1.36

Table 7-1 (continued)

Radical	Conformer	Calculated Constants		
		Config- uration ^a	Nitrogen Hyper- fine Coupling ^b	Dipole Moment ^c
2-Pyrollidinono		Σ (1)	- 3.32	3.98
HCONCHO	syn	Σ (2)	41.73	3.14
N-Formylformamido	anti	Σ (2)	- 1.84	1.77
HCONCOCH ₃	syn	Σ (2)	39.07	3.78
N-Formylacetamido	anti	Σ (2)	38.82	2.05
Succinimido reported (69)		Σ (1) Σ	37.01	4.16
HNCOOCH ₃	transoid	Π (2)	13.10	1.19
N-Carbomethoxyamino	orthogonal	Σ	15.40	2.63
	cisoid	Π (2)	12.41	2.79
CH ₃ NCOOCH ₃	trans	Π (2)	12.72	0.95
N-Methyl-N-Carbo- methoxyamino	orthogonal	Π	14.47	2.60
	cis	Π (2)	12.03	2.85
HNCONH ₂	transoid	Π (2)	13.02	1.33
Urea	orthogonal	Σ	15.39	4.38
	cisoid	Π (2)	12.52	4.62
CH ₃ NCONH ₂	trans	Π (2)	12.82	1.39
N-Methylurea	orthogonal	Σ	14.75	4.34
	cis	Π (2)	12.26	4.66

- ^a The number in parenthesis refers to the orbital occupancy of the unpaired electron; (1) in HOMO, (2) in second HOMO.
- ^b In units of gauss.
- ^c In Debye units.
- ^d The programme did not converge to the 10^{-6} atomic unit limit.

Radicals such as succinimido, cis-N-methylacetamido, N-formyformamido and N-formylacetamido showed large (~ 40 gauss) a^N values as required for Σ electronic configurations (87).

Table 7-1 also lists the calculated dipole moments for each radical conformation. No general trend is evident from these values.

7-2 Structure, Configuration and Reactivity Relationships

7-2-1 Qualitative Features of Amido Radical Structure and Configuration

Careful scrutiny of the structural formulae and calculated electronic configurations of the amido radicals shown in Table 7-1 permits several tentative inferences to be made. The basic structural unit common to all radicals is



When $X=H$, the calculated electronic state of the amido radical was Σ regardless of the Y substituent. Formamido ($Y = H$) and acetamido ($Y = CH_3$) were of Σ configuration. The X substituent in amido radicals predestined the electronic configuration. When $X = CH_3$, the Y substituent may be H (N-methylformamido), F (N-methylfluoroformamido), CH_3 (trans-N-methylacetamido) or OCH_3 (N-methylacetamido). All radicals were of Π electronic configuration. An electron-withdrawing substituent at X such as CHO or $COCH_3$ ($Y = H$), resulted in the radicals being of Σ config-

uration, for example N-formylformamido and N-formylacetamido radicals. Koenig (114) has observed that the electronic ground state properties of formyloxy did not change upon replacing the hydrogen by methyl or isopropyl groups.

In the case of the related amido radicals, the generalities applicable to the amido radicals did not hold rigorously. When $Y = OCH_3$ and $X = H$ (N-carbomethoxyamino) and $X = CH_3$ (N-methyl-N-carbomethoxyamino), both were Π radicals from the INDO calculation. Likewise when $Y = NH_2$, the nature of the X substituent, $X = H$ (urea) or $X = CH_3$ (N-methylurea), did not alter the calculated Π electronic configuration of the radical. Eveleth (107) had postulated that "loading a particular parent radical with heteroatoms having non-bonded electrons should tend to favour Σ structure". The calculations performed on the related amido radicals did not support this statement.

The N-methylacetamido radical conformation is apparently important for the determination of its electronic configuration. The data of Table 6-5 show a rapid decrease of Np_z spin density between the 0° and 70° conformers. The data suggest that near 70° rotation there is a cross-over of the potential planes from Π to Σ configuration. In the urea and N-methylurea radicals there is a cross-over of configuration from Π in the cis and trans conformers to Σ in the orthogonal conformer. It may be that the conformer of altered configuration represents the excited state of the radical (115). The Σ cis-N-methylacetamido radical is structurally mimicked in the 2-pyrrolidinono radical which is also Σ from calculation. Moreover, all the cyclic radicals

investigated by calculation were of Σ electronic configuration.

7-2-2 Reactivities of Σ - Π Radicals

The differences in chemical reactivity of Σ and Π electronic ground state radicals is still academic. From the reported chemical reactions undergone by amido radicals, no apparent immutable rule exists for distinguishing between Σ and Π reactivity. As was mentioned previously there has been considerable controversy generated in even agreeing upon the electronic configuration of some radicals. However, a trend is suggested from the data available (93,96,97,103-105,117-119). Touchard and Lessard (93,97) have found that N-haloacetamides photochemically add to olefins. The yield of the 1,2-adduct increased proportionally with the electronegativity of the α -halogen substituents. The following trend was noted; $\text{CF}_3, \text{CCl}_3 > \text{CHCl}_2 > \text{CH}_2\text{F} > \text{CH}_2\text{Cl} > \text{CH}_2\text{Br} > \text{CH}_3$. NBS has also been reported to undergo addition to unsaturated bonds (103-105,118,119). Some of the NBS additions are unmistakably radical in nature (103, 119) being accelerated by the introduction of radical initiators. From the INDO calculations, all imido and those amido radicals without the nitrogen substituent were found to have Σ configuration. It may be proposed that the Σ configuration of the amido radical is a requirement for addition to unsaturated linkages.

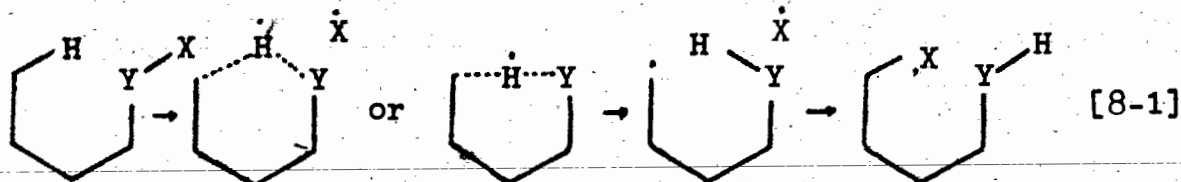
The trans-N-methylacetamido (and presumably other N-alkyl substituents) was found to have Π configuration. The N-substituted radicals react predominantly by hydrogen abstraction

(96,97,117). It was noted (97) that N-bromo-N-methylacetamide did not undergo photoaddition to cyclohexene or to 1-dodecene (a more reactive olefin toward the addition of radicals (120)) but N-chloro-N-methylacetamide did give a low yield of 1,2-adduct (~ 17 %) with the latter olefin. Two N-methyl haloamides (98,99) also underwent intramolecular photoaddition to an olefin. However, the intramolecular addition process is governed by stereochemical factors which may be of greater importance than the Σ - Π configuration of the radical. Both cis and orthogonal conformers of N-methylacetamido radical were shown by calculation to be of Σ electronic configuration.

CHAPTER 8INTRODUCTION8-1 Transition States for Hydrogen Abstraction

The transition state provides a visualization of how an assembly of atoms in reactant molecules reaches an activated complex and proceeds to product. It is intimately associated with the reaction mechanism which presupposes a definite knowledge of the role of nuclear arrangements and electronic configuration at the site of molecular transformation. In kinetic theory the transition state complex is defined as the highest potential energy point in the equilibrium between reactants and products. The structure and geometry of the transition state is deduced from the structure of the reactants and products (121).

In radical reactions proceeding through hydrogen abstraction, the source of the hydrogen atom may be inter- or intramolecular. Intermolecular transfer involves a bimolecular reaction between the radical and the hydrogen-donating solvent. The intramolecular sequence can in general be represented as in equation [8-1].



Here Y - X represents two heteroatoms which undergo homolytic cleavage and, subsequently, ligand exchange. The key step of the

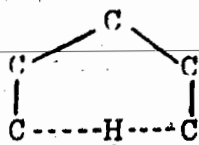
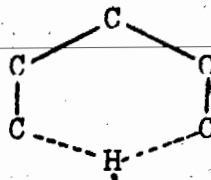
intramolecular process is the abstraction of the hydrogen from the fifth atom from the radical centre. The transition state for this hydrogen shift poses many unanswered questions and is the subject of this investigation.

8-2 Examples of 1,5-Intramolecular Hydrogen Transfer

Chemical reactions proceeding through intramolecular hydrogen abstraction can result in novel transformations. Barton (122) has reported that nitrite esters of steroidal alcohols can be photochemically decomposed and can functionalize an unactivated centre to an oxime. The photolysis of an acidified N-chloramine solution, the Hofmann-Löffler reaction, generates an aminium radical which can after undergoing 1,5 hydrogen transfer be cyclized to pyrrolidine (123,124). Intramolecular hydrogen abstraction and ligand exchange are also seen in the photolysis of long chain tertiary hypochlorites (125), of N-nitrosamides (126,127) and of N-haloamides (117,128,129).

8-3 Geometry of Transition States

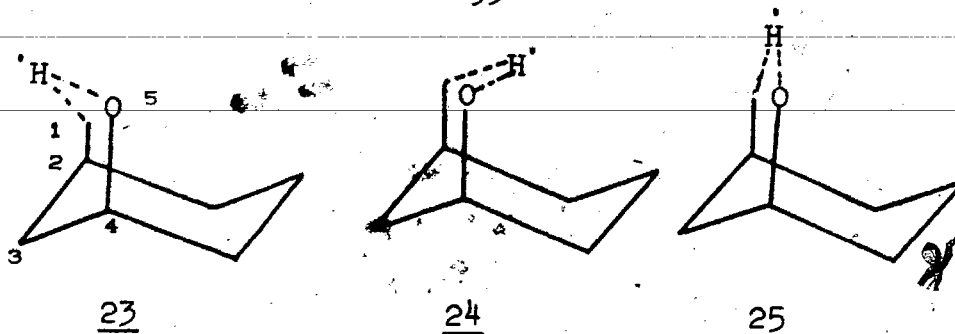
In all the examples quoted, the intramolecular hydrogen atom abstraction and, therefore, the ligand exchange, occurred at the fifth atom from the radical centre. It is expected that the transition states for these transformations should also be similar. All authors agree that the transition states have cyclic structures encompassing six atomic centres. However, there is a divergence of opinion as to whether the six nuclei form a pentagonal (five-membered) shaped structure 21 with three nuclei approximate-

2122

ly collinear as proposed by Walling and Padwa (125) or a true six-membered cyclic transition state 22 as suggested by Akhtar (130).

The pentagonal geometry 21 for the intramolecular hydrogen transfer transition state has been postulated for several acyclic radical reactions. Corey and Hertler (123) reached this conclusion for the Hofmann-Loeffler transformation as did Walling (125) for the hypochlorite photolysis. Recently there has been a report asserting that approximate quantum mechanical calculations indicate that a sigma C - H bond should be more readily attacked by a radical approaching along the collinear axis to the bond broken during hydrogen transfer (131). In the three atom hydrogen sigma bond system, the activation energy is least when H approaches H - H along the axis of the bond (132).

Rigid, geometrically constrained systems as exemplified by the steroid nucleus that undergo intramolecular hydrogen transfer are postulated (130,133,134) to have a true six-membered transition state structure as 22. Akhtar (130) pictured the transition state in the photolysis of a 6 β -steroidal nitrite as being comprised of three possible conformations; the boat 23, the chair 24 and the quasi-chair 25. The quasi-chair form was argued to be



the most favoured because it permitted maximum overlap of the orbitals in the transition state (130). The five atoms designated 1 to 5 are firmly held in place with the abstractable hydrogen residing in the various conformations between atoms 1 and 5. Models reveal that the maximum bond angle obtainable by the three participating C, H and O atoms is about 145° in 25 (130). In spite of collinearity not being attainable, the reactions proceed efficiently.

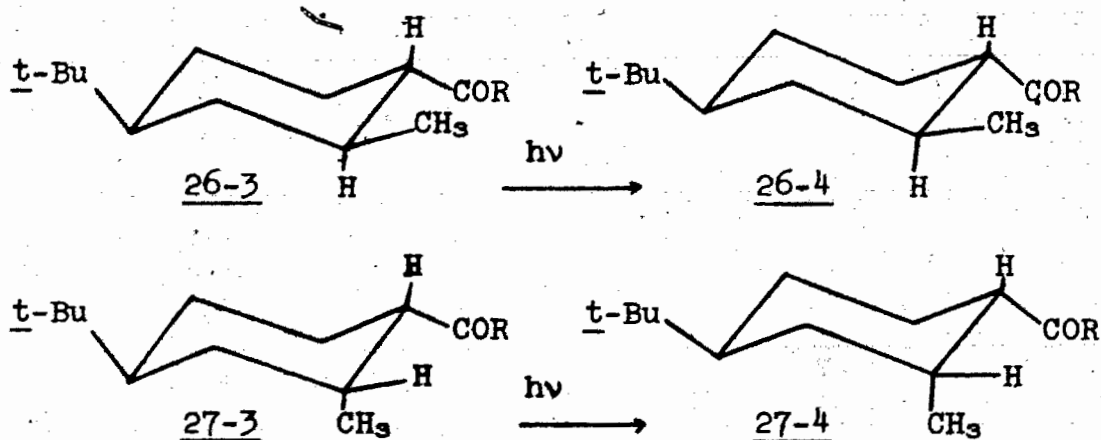
Heusler and Kalvoda (134) have critically reviewed the structural requirements of the Barton reaction in the steroidal series and made some perceptive observations. They concluded that intramolecular hydrogen abstraction occurs readily when the carbon-oxygen internuclear distance between positions 1 and 5 is between 2.5 and 2.7 \AA even when a good hydrogen donor such as cyclohexene was used as solvent. When this interatomic distance exceeded 2.8 \AA , intermolecular and/or other pathways dominated the reaction.

8-4 Objective

The objective of this investigation was to attempt to differentiate between the requirement of a pentagonal- or hexagonal-

shaped transition state geometry in the intramolecular hydrogen abstraction by an amido radical. For the five-membered transition state there is the necessity of attaining collinearity of the three involved atoms and/or coplanarity of all six atoms. For the six-membered transition state on the other hand, the prime importance is the attainment of a strain-free chair or quasi-chair conformation such as 24 or 25.

The general strategy followed was to fuse a system able to undergo intramolecular hydrogen transfer onto a semi-rigid cyclohexane ring system. The conformational driving forces can be used in an attempt to deduce the transition state structure from product analysis of the reaction mixture. The models suitable for this purpose are the amido radicals 26-4 and 27-4 which can be readily generated by the photolysis of N-bromo-trans-4-t-



26-1 R = OH
26-2 R = NHC(CH₃)₃
26-3 R = NBrC(CH₃)₃
26-4 R = $\dot{\text{N}}\text{C}(\text{CH}_3)_3$

27-1 R = OH
27-2 R = NHC(CH₃)₃
27-3 R = NBrC(CH₃)₃
27-4 R = $\dot{\text{N}}\text{C}(\text{CH}_3)_3$

butyl-trans-2-methyl-N-t-butylcyclohexanecarboxamide 26-3 and of N-bromo-trans-4-t-butyl-cis-2-methyl-N-t-butylcyclohexanecarboxamide 27-3 respectively. The bulky 4-t-butyl substituent (135) prevents inversion of the ring. Attempts to synthesize the rigid trans-decalin analogues of 26-1 and 27-1 were unsuccessful, only the diequatorial analogue of 26-1 could be isolated.

In the carboxamido radical system chosen, the N-t-butylcarboxamido group is locked in the equatorial position by the anchoring 4-t-butyl substituent. The two amido radicals 26-4 and 27-4 differ only in the orientation of the 2-methyl substituent. In the presence of a hydrogen donor, each amido radical will abstract a hydrogen either intramolecularly from the 2-methyl substituent or intermolecularly from the solvent. If the internal hydrogen transfer through a six-membered transition state prevails for both isomeric compounds, it is expected that the intramolecular ligand exchange products will not differ significantly in quantity since strain-free chair forms of transition states can be obtained for both. If the intramolecular hydrogen transfer is controlled by the five-membered transition state, the capability of the carboxamido and methyl substituents to approach coplanarity will be the controlling factor. This capability is regulated by the relative energy barriers of the cyclohexane ring toward ring flattening or toward ring puckering.

8-5 The Cyclohexane Ring System

The bond angles of cyclohexane were first considered by Sachse (136) to be strain-free tetrahedral angles of $109^{\circ}28'$.

Hassel (137), using electron diffraction techniques, determined the bond angles in unsubstituted cyclohexane to be 111.55° .

Wohl (138) has concluded from this flattened cyclohexane ring that the equatorial-equatorial (e,e) bond angles diverge to give a torsional angle of about 65° while the axial-equatorial (a,e) bonds converge to give a torsional angle of about 55° . The net result, barring mutual compression of the substituents (139), is that cis-1,2 substituents (a,e or e,a) are closer together than are the trans-1,2 substituents (e,e).

There is a paucity of information with respect to the quantitative potential energy variation during ring flattening and ring puckering. As shown in Figure 8-1 (140) there is believed to be a much steeper rise in the energy when e,e bonds approach (puckering) than when e,a bonds spread (flattening). Despite the apparent lack of quantitative numerical data (141), there does exist some proof to substantiate the above proposal.

In studies on 1,2-cyclohexanediols (142), while cis-1,2-cyclohexanediol formed an isopropylidene derivative, the corresponding trans-diol (1e,2e) did not form the cyclic ketal. This was reported to be due to greater puckering resistance of the cyclic ring in the trans isomer and would result when the interatomic distance between oxygen atoms is decreased. Similarly the cis diol was found to form a stronger intramolecular hydrogen bond than did the trans diol (143). Attraction of the hydroxyl group in the cis diol in forming a hydrogen bond will tend to produce a twist motion around the C - C bond and decrease

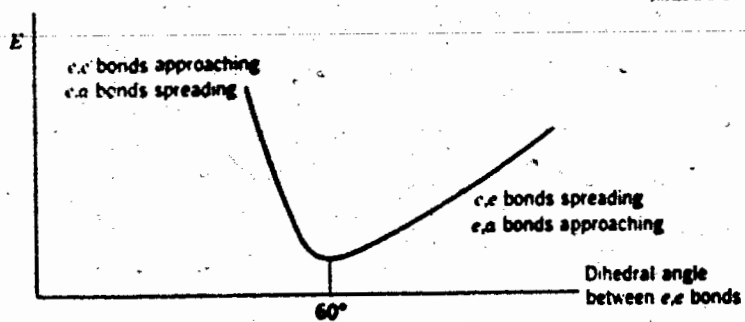


Figure 8-1 The qualitative potential energy curve of cyclohexane as a function of the dihedral angle (140)

the dihedral angle. This will cause the ring to become more planar in the cis compound and more puckered in the trans compound (143).

In the pyrolysis of acetates and xanthates the six atoms involved in cis elimination are considered to approach each other coplanarly in the transition state (144) in order to achieve the most favoured electron interactions. In pyrolysis the cis hydrogen substituent is eliminated in preference to the trans hydrogen (145). The reason for this is again the greater ease in forcing an equatorial and an axial bond into a plane in the transition state than in forcing two equatorial bonds (144).

CHAPTER 9RESULTS9-1 Interatomic Distances for Intramolecular HydrogenAbstraction

By analogy with the interatomic distance criterion for alkoxy intramolecular abstraction (134), the corresponding carbon-nitrogen interatomic distances for amido radicals 26-4 and 27-4 were calculated (146). The results are given in Table 9-1 which also has the appropriate interatomic distances resulting from changes of the dihedral angle. The carbon-nitrogen distance of the cis radical (2.60 \AA) 27-4 was within the 2.5 to 2.7 range of intramolecular hydrogen abstraction of alkoxide radicals (134). The corresponding interatomic distance of the trans radical 26-4 progressed from the borderline (2.75 \AA) to greater internuclear distances during the ring flattening process.

9-2 Physical Properties of N-Haloamides9-2-1 Preparation of N-Bromamides

The N-bromamides were smoothly prepared by the bromination of 26-2 and 27-2 with up to a ten-fold molar excess of t-butylhypobromite. The completeness of the reaction was ascertained by the disappearance of the amide hydrogen absorption at 1500 cm^{-1} . Reaction by-products such as t-butanol, methyl bromide,

Table 9-1Calculated Carbon-Nitrogen Interatomic Distances of

<u>Model Radicals</u>		
<u>Model Radical</u>	<u>Dihedral Angle</u>	<u>C...N Interatomic Distance (A°)</u>
trans	(ring flattening)	
	65.35 (normal)	2.7457
	67.35	2.7756
	69.35	2.8063
	71.35	2.8379
	73.35	2.8701
	75.35	2.9031
	(ring puckering)	
	63.35	2.7167
	61.35	2.6887
	59.35	2.6618
	57.35	2.6361
	55.35	2.6115
	cis	54.65 (normal)
52.65		2.5803
50.65		2.5588
48.65		2.5386
0.0		1.8852

acetone (ascribed to weak absorption seen at 1710 cm^{-1}) and t-butylhypobromite were removed during vacuum evaporation since they were considerably more volatile than the N-bromamides. Concentration of the reaction mixture (0° , in the dark) generally resulted in 90-100 % yields of yellow residual solid. Subsequent ir analysis of the solid demonstrated the absence of absorption at 1500 cm^{-1} due to parent amide.

9-2-2 Spectroscopic Properties of N-Haloamides

In Table 9-2 are listed the characteristic carbonyl stretchings of N-methylacetamide, N-t-butylacetamide and their respective N-halo derivatives. In both parent amides, the bulkiness of the nitrogen substituent apparently had no effect upon the carbonyl absorption. In both series the introduction of an N-bromo and an N-chloro substituent progressively increased the wavenumber of the carbonyl absorption.

Also in Table 9-2 are listed the characteristic Raman frequencies of the Amide IV band of the secondary amides and the possible corresponding bands of the N-halo compounds. The Amide IV (147) arose principally from the O=C-N bending and was observed near 630 cm^{-1} . In N,N-disubstituted amides, the O=C-N in plane deformation occurred in the 620 to 590 cm^{-1} region (147). In the N-haloamides it would appear that the N-bromo group had a greater affect on the O=C-N bending mode than did the N-chloro substituent.

Table 9-3 has tabulated the nmr chemical shifts observed for N-methylacetamide, N-t-butylacetamide and their respective

Table 9-2Infrared and Raman Absorptions of N-Halamides

Compound	Carbonyl	Vibration Frequency
	Absorption (cm^{-1})	Amide IV (cm^{-1})
$\text{CH}_3\text{CONHCH}_3$	1664	633
$\text{CH}_3\text{CONBrCH}_3$	1683	604
$\text{CH}_3\text{CONClCH}_3$	1691	637 (55), 654 (100) ^a
$\text{CH}_3\text{CONHC}(\text{CH}_3)_3$	1665	631
$\text{CH}_3\text{CONBrC}(\text{CH}_3)_3$	1675	625
$\text{CH}_3\text{CONClC}(\text{CH}_3)_3$	1687	622

^a The numbers in parentheses are relative percentage intensities of the two absorptions appearing near the 630 cm^{-1} Amide IV band of amides.

Table 9-3Nuclear Magnetic Resonance Chemical Shifts in N-Halamides

Δ cps	Chemical Shift C-Methyl (cps)	Compound	Chemical Shift N-Alkyl (cps)	Δ cps
	115	$\text{CH}_3\text{CONHCH}_3$	162	
17	132	$\text{CH}_3\text{CONBrCH}_3$	192	34
12	130	$\text{CH}_3\text{CONClCH}_3$	202	40
	114	$\text{CH}_3\text{CONHC}(\text{CH}_3)_3$	80	
32	146	$\text{CH}_3\text{CONBrC}(\text{CH}_3)_3$	87	7
16	130	$\text{CH}_3\text{CONClC}(\text{CH}_3)_3$	87	7

Table 9-4Ultraviolet Absorption Properties of N-Halamides

Compound	Concentration (moles/litre) ^a	ϵ	λ_{max} nm
$\text{CH}_3\text{CONHCH}_3$			<240
$\text{CH}_3\text{CONBrCH}_3$	2.06×10^{-3}	425	260
$\text{CH}_3\text{CONClCH}_3$	8.65×10^{-3}	~ 165	250 ^b
$\text{CH}_3\text{CONHC}(\text{CH}_3)_3$			<240
$\text{CH}_3\text{CONBrC}(\text{CH}_3)_3$	1.44×10^{-3}	765	275
$\text{CH}_3\text{CONClC}(\text{CH}_3)_3$	7.75×10^{-3}	200	258

^a CH_2Cl_2

^b shoulder

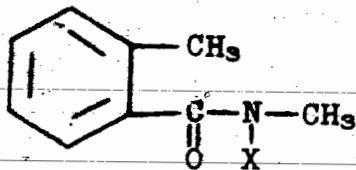
N-halo derivatives. The N-bromo substituent caused a greater downfield shift of the acetyl methyl absorption than did the N-chloro group. This shift was more pronounced in the N-t-butylacetamide series.

In Table 9-4 are summarized some uv properties of the amides of interest and their halogenated derivatives. In CH_2Cl_2 solvent, the parent amides had their λ_{max} below 240 nm. The N-bromamides shifted the λ_{max} to longer wavelength and exhibited larger extinction coefficients than did the N-chloramides. The chloramide absorption curves were broad at the base and extended to about 330 nm. The bromamides also exhibited broad absorption curves which tailed to about 360 nm.

9-3 Photolysis of N-Bromamides

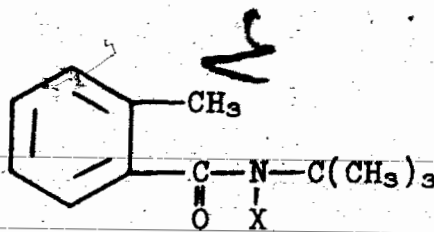
9-3-1 Photolysis of Rigid N-Bromamides - N-Bromotoluamides

The photolysis of N-bromo-N-methyl- or N-bromo-N-t-butyl-toluamide (28-2 or 29-2) with a 200 watt Hanovia medium pressure lamp through a pyrex filter in benzene solvent at 20°C proceeded smoothly and almost quantitatively to the HBr salt of the imino-lactone 30. The initially formed C-Br amide was apparently



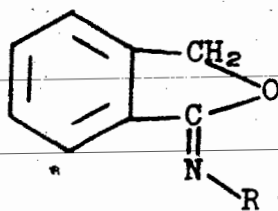
28-1 X = H

28-2 X = Br

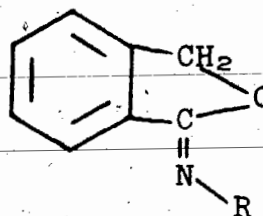


29-1 X = H

29-2 X = Br



HBr

30-1 R = CH₃30-2 R = C(CH₃)₃31-1 R = CH₃31-2 R = C(CH₃)₃

unstable and immediately cyclized during work-up. Iminolactone hydrobromide 30-2 had a strong ir absorption at 1675 cm⁻¹ whereas 30-1 had a strong absorption at 1700 cm⁻¹. Both compounds had a 2 proton broad methylene singlet at about τ 4. Both free iminolactones had strong ir absorption at 1700 cm⁻¹ (Ar-C=N stretching) and a 2 proton methylene singlet at τ 4.7. The latter compared favourably with the methylene signal of phthalide at τ 4.7 (148) as opposed to that of N-methylphthalimidine at τ 5.7 (149). Both iminolactones gave parent peaks, m/e 189 for 30-2 and m/e 147 for 30-1.

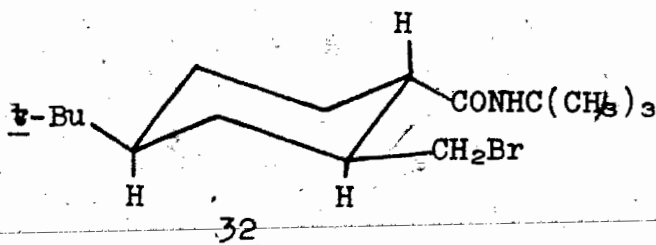
Free iminolactone 31-2 was stable to LiAlH₄ reduction but was hydrolyzed to phthalide when refluxed with 20 % H₂SO₄. Free iminolactone 31-1 on attempted column chromatography on neutral alumina resulted in almost total hydrolysis of the C=N bond to yield phthalide.

9-3-2 Photolysis of Semi-Rigid N-Bromamides

9-3-2-1 Photolysis of trans-N-Bromo-4-t-Butyl-trans-2-Methyl-

N-t-Butylcyclohexanecarboxamide (26-3)

Photolysis of 26-3 under the same conditions as described resulted in the facile formation in high yield of trans-4-t-butyl-trans-2-bromomethyl-4-t-butylcyclohexanecarboxamide 32.

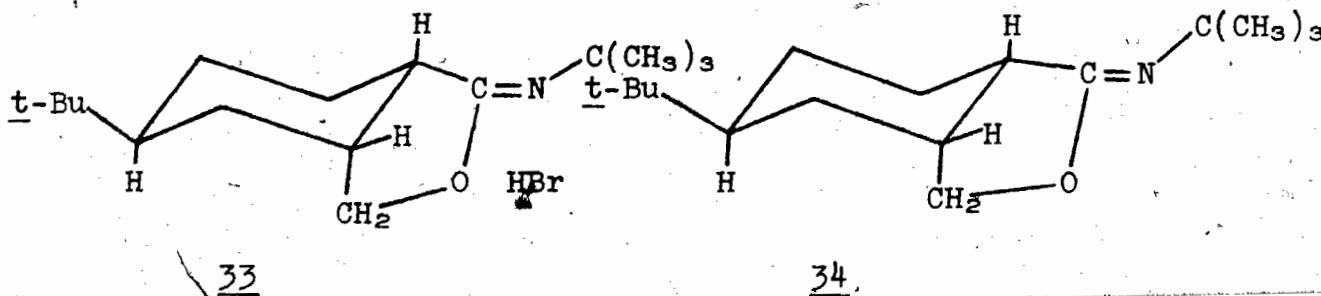


This compound had the typical amide absorptions at 3430, 1665 and 1505 cm^{-1} and a 2 proton absorption at τ 6.5. The photoproduct was stable to refluxing benzene and exhibited the characteristic bromine-containing parent peak at m/e 331 and 333 in 1:1 ratio.

9-3-2-2 Photolysis of trans-N-Bromo-4-t-Butyl-cis-2-Methyl-N-t-Butylcyclohexanecarboxamide (27-3)

Photolysis of cis-bromamide 27-3 gave as photoproduct a compound with ir absorption at 2750-2670 and 1675 cm^{-1} . In contrast to the $-\text{CH}_2\text{Br}$ signal at τ 6.5 in the photoproduct from 26-3, none was observed. After neutralization with NaCO_3 solution, the ir absorption changed to 1700 cm^{-1} and the 2750-2670 cm^{-1} region was eliminated. Nuclear magnetic resonance spectra were not too informative for structural elucidation purposes since the observed signals were broad and clustered.

By analogy with the photoproduct from 29-2, it was assumed that the iminolactone hydrobromide 33 was formed spontaneously.



Mass spectral data of 34 showed the parent peak at m/e 251 and the elemental analysis was consistent with the free iminolactone structure.

9-4 Competitive Intra- and Intermolecular Hydrogen Abstraction Processes

The isomeric bromamides 26-3 and 27-3 which were free of detectable amounts of parent amide, were photolyzed in the manner described in Chapter 11. The completion of the photoreaction was verified by the negative starch AcOH-KI test. The generated amido radical intermediates were consumed by the two major hydrogen abstraction processes. If the radical abstracted a hydrogen atom intermolecularly, the parent amide would be regenerated. If, on the other hand, the amido radical abstracted a hydrogen atom intramolecularly from the adjacent 2-methyl substituent, there would be a subsequent radical recombination to form the 2-bromomethylcarboxamide or its cyclized analogue. The trans-

bromamide 26-3 gave 32 as the intramolecularly derived photo-product while 27-3 gave the corresponding iminolactone hydrobromide 33.

Care was taken to insure that identical conditions were used for the photolysis of 26-3 and 27-3. The photolysates were quantitatively analyzed for parent amide by gas chromatography (15 % DEGS column at 180°) with added internal standard. Direct analysis of the intramolecularly derived photoproducts was not successful due to their unsymmetrical and broad-based elution characteristics. The photolysate from trans-bromamide 26-3 was analyzed directly while the solution from cis-bromamide 27-3 was first extracted with aqueous Na_2CO_3 solution to liberate the free iminolactone 34. The estimated accuracy of analysis was $\pm 2\%$. It can be seen in Table 9-5 that in benzene which lacked an easily abstractable hydrogen, the quantity of parent amide regenerated was very small. However, in cyclohexane which is a good hydrogen donor, large quantities of parent amide were formed.

In solvent mixtures of benzene and cyclohexane, an intermediate situation arose. Here there was competition between the intra- and intermolecular hydrogen abstraction processes. This competition was the phenomenon based on which the test for the requirements of the attendant transition states will be made. The N-t-butylamido radical (A^\bullet) such as 26-4 and 27-4 has been shown to undergo hydrogen abstraction exclusively as in [9-1]. Here B^\bullet is intramolecularly rearranged radical and k_1 and k_2

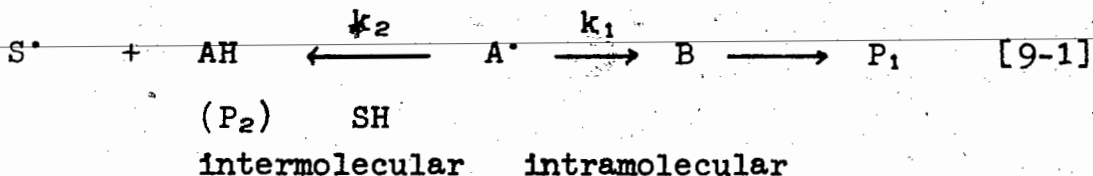
Table 9-5Solvent Composition and Hydrogen Abstraction Products

Solvent Composition % (v/v) Cyclohexane in Benzene	Percentage Recovered Amide		Intramolecular Product ^a	
	<u>trans</u>	<u>cis</u>	<u>trans</u>	<u>cis</u>
100.0 %	96.5	91.5		
26.7 %	37.2 ^b	45.8 ^b	62.8 ^b	54.2 ^b
12.0 %	32.2	16.7	67.8	83.3
8.3 %	32.2	12.5	67.8	87.5
0.0 %	< 5 ^c	0 ^c	>90 ^c	>90 ^c

^a taken as (100% - % intermolecular product), except in the last row

^b The origin of this unexpected result is not known.

^c estimated from preparative experiments



are the first order and second order rate constants for intramolecular and intermolecular hydrogen transfer respectively.

P_1 and P_2 are the respective products. It has been found that in deuterated solvent the rearranged radical B^\bullet did not incorporate deuterium (149).

For each isomeric radical [9-2] and [9-3] will hold

$$\frac{\text{rate of intramolecular transfer}}{\text{rate of intermolecular transfer}} = \frac{k_1[A^\bullet]}{k_2[A^\bullet][SH]} = \frac{k_1}{k_2[SH]} = \frac{[P_1]}{[P_2]} \quad [9-2]$$

and

$$\frac{k_1 \text{ cis}}{k_2 \text{ trans}} = \frac{\frac{[P_1]}{[P_2] \text{ cis}}}{\frac{[P_1]}{[P_2] \text{ trans}}} \quad [9-3]$$

assuming $k_2[SH]$ for cis = $k_2[SH]$ for trans. Under identical photodecomposition conditions, the rate of the intermolecular hydrogen transfer process of both cis- and trans-amido radicals 26-4 and 27-4 can be considered to be equal in comparison to the experimental error. The relative rate of intramolecular hydrogen transfer of the two isomeric amido radicals, $k_1 \text{ cis}/k_1 \text{ trans}$, was calculated to be 2.4 for the 12.0 % cyclohexane solution and 3.3 for the 8.3 % cyclohexane solution.

CHAPTER 10DISCUSSION

There is no compelling reason to believe that the interatomic distance requirements for intramolecular hydrogen abstraction are significantly different between the amido C...N and the alkoxy C...O atoms. From Table 9-1 it can be seen that both cis radical 27-4 and trans radical 26-4 have interatomic distances within the critical range (2.5 to 2.7 Å) (134) of alkoxy radical intramolecular hydrogen abstraction. The data from Table 9-5 indicates that with the amido radicals there is substantial quantity of intermolecular hydrogen abstraction in cyclohexane solvent mixture as opposed to predominantly intramolecular abstraction by alkoxy steroidal radicals in cyclohexane (134).

Since the intermolecular distance is not critical for amido radical reactivity, other factors must exert influence over the course of the reaction. It is assumed that the reactivity of these radicals occurs in the ground state. From geometrical considerations, the amido radical undergoing intramolecular hydrogen abstraction must be of Σ electronic configuration. The hybrid orbital bearing the unpaired electron is suitably oriented toward the abstractable hydrogen. If the amido radical were of Π electronic configuration, the p orbital bearing the unpaired electron would be perpendicular to the amido plane (NCO) and to the H - C axis of the abstractable hydrogen. Orbital steering (150) or the accelerated rate achieved by steering the reacting molecules in preferred orientation is of commanding importance.

Energies of activation for intermolecular hydrogen abstraction from cyclohexane by triplet state acetophenone (3.3 kcal/mole) (151) are almost identical to those for intramolecular abstraction by triplet state valerophenone (3.5 kcal/mole) (152). Assuming that the energies of activation for amido radical intra- and intermolecular hydrogen abstraction are also similar, it is conformational factors which are responsible for the differences in product quantities observed in Table 9-5.

The data of Table 9-5, although suggestive of a general trend, unfortunately is not conclusive. One would expect a monotonic increase in the amount of intramolecularly derived product as the percentage of cyclohexane in the solvent mixture decreased. This was not decisively shown by the data, especially by the trans amido radical 26-4. The reasons for this are not known. It may be that changes too small to be detected by the analytical technique employed were prevalent. Perhaps also the 4-t-butylcyclohexyl system is not the best model to demonstrate the expected conformationally induced phenomena.

The conformational control of photochemical γ - hydrogen abstraction by alkyl phenyl ketones has been documented. The cis-4-t-butylcyclohexyl phenyl ketone abstracted hydrogen exclusively while the trans-4-t-butylcyclohexyl phenyl ketone only underwent photoreduction (153). In the photochemistry of the nitrites of 20α - and 20β -hydroxysteroids, the 20α - epimer gave a much higher yield of the intramolecular hydrogen transfer product because of the absence of methyl-hydrogen interactions in the transition state which was experienced by the 20β -epimer (127).

In radical 27-4 the axial 2-methyl substituent encounters two 1,3 hydrogen-methyl interactions which are absent trans-amido radical. As a result, there is a driving force in cis-amido radical 27-4 to relieve this interaction by undergoing a partial ring flattening and, thereby, approaching a coplanar-like transition state. The trans-amido radical 26-4 lacks this driving force of steric strain relief. Even if such steric strain did exist in 26-4, it could not undergo ring inversion motion without large energy expenditure. The results of Table 9-5 show, though inconclusively, that cis-amido radical does form a greater amount of intramolecularly derived photoproduct.

CHAPTER 11EXPERIMENTAL11-1 General Techniques

The general techniques employed were the same as described in Chapter 4 except for the following special features. Infrared spectra were recorded on the Beckman IR12 spectrophotometer. Raman spectra were run on the Cary 81 instrument which was equipped with a helium-neon laser. Column chromatography was carried out using Brockmann alumina (neutral, activity 1, 80-200 mesh).

11-2 Preparation of Reagents11-2-1 Preparation of N-t-Butylacetamide

The N-t-butylacetamide was prepared from 1.5 ml t-butylamine (154). The resulting solid was sublimed (20°/0.5 mm Hg): m. p. 100-101° (sealed tube), reported (51) m. p. 101-102°. A single peak appeared on vpc analysis.

11-2-2 Preparation of t-Butylhypobromite

The t-butylhypobromite was prepared (155) from 150 ml NaOCl, 10.3 g NaBr and 9.4 ml t-butanol. The product had maximum absorption at 283 nm. Taking $\epsilon = 120$ (156), the concentration of the solution of t-butylhypobromite was 1.18 M (26 % yield).

11-2-3 Preparation of t-Butylhypochlorite

The t-butylhypochlorite was prepared (157) from 200 ml 5% NaOCl solution and 15 ml t-butanol. After work-up there resulted a yellow oil, t-butylhypochlorite (5.6 g, 47%): ir 690 cm^{-1} (m).

11-2-4 Preparation of N-t-Butyltoluamide (29-1)

From 1.3 g o-toluic acid and 7 ml t-butylamine (154) was formed crude N-t-butyltoluamide (1.48 g, 81%). Recrystallization from ethanol-H₂O, gave white solid 29-1 (0.32 g): m. p. 74-75°; ir 3420, 1675, 1485 cm^{-1} ; nmr τ 2.8 (4H, s), 4.3 (1H, b), 7.55 (3H, s), 8.55 (9H, s).

11-2-5 Preparation of trans-4-t-Butyl-trans-2-Methyl-N-t-Butylcyclohexanecarboxamide (26-2)

To 0.2 g 26-1 (158)¹ in a 25 ml flask equipped with a drying tube and reflux condenser was added 0.7 ml SOCl₂. The contents were heated for 1 h on a water bath prior to the removal of excess SOCl₂ on the water aspirator. To the residue was added 1 ml anhydrous benzene followed by dropwise addition of 0.7 ml t-butylamine in 1 ml anhydrous benzene. After heating to reflux for 1 h, 5 ml H₂O was added and the mixture was extracted with CHCl₃ (3 x 15 ml). The organic extracts were combined, dried (MgSO₄) and concentrated to give crude amide (0.24 g, 94%).

Recrystallization from cyclohexane gave white crystals of 26-2 (0.17 g): m. p. 137-138°; ir 3440, 1660 cm^{-1} .

11-2-6 Preparation of trans-4-t-Butyl-cis-2-Methyl-N-t-

Butylcyclohexanecarboxamide (27-2)

The acid 27-1 (158)¹ (0.3 g) and 1.2 ml SOCl_2 were treated in the manner previously described. To the resulting acid chloride was added 1.2 ml t-butylamine in 1.5 ml anhydrous benzene to form after work-up crude amide (0.235 g, 88 %).

This material was recrystallized from cyclohexane to form white crystals of 27-2 (0.21 g): m. p. 134-135°; ir 3440 (m), 1660 cm^{-1} .

11-3 General Procedures for N-Halogenation11-3-1 Preparation of N-Chloramides

To a 25 ml round-bottom flask equipped with a reflux condenser protected by a CaCl_2 drying tube was added 0.2 g amide, 0.6 g t-butylhypochlorite, 10 mg Na_2CO_3 and 5 ml CCl_4 . The flask, protected by Al foil, was subjected to reflux for 2.5 h on the water bath. Upon cooling, the solution was filtered in the dark. The solution in an Al protected flask was then concentrated. The absence of ir absorption at 690 cm^{-1} indicated that excess t-butylhypochlorite had been removed.

11-3-2 Preparation of N-Bromamides

Into a 25 ml erlenmeyer flask enclosed by Al foil and equipped with a magnetic stirrer was added about 150 mg

¹ This compound was kindly supplied by M. Tichy.

(~ 0.0006 moles) amide and about 5 ml 1.18 M (~ 0.006 moles) t-butylhypobromite solution. The mixture was stirred in an ice-bath for 2 h after which time an aliquot was withdrawn for ir analysis. The absence of absorption at 1500 cm^{-1} was taken as the end-point of the reaction. In the event that a weak absorption remained, the reaction time was prolonged.

Upon completion of the reaction, the solution was concentrated on the rotary evaporator in an ice-water bath. During all operations the flask was protected from light. Generally about 1 h evaporation was needed to attain a constant weight of yellow solid residue.

11-4 Spectroscopic Investigations of Substituted N-Halacetamides

The N-methylacetamide and N-t-butylacetamide were used as reference compounds. The N-chloro- and N-bromo- derivatives were made according to the procedures described. The ir, nmr, Raman and uv spectra were obtained of all the compounds.

11-4-1 Infrared Determinations

All spectra taken were approximately 10% w/v and were taken using NaCl liquid ir cells. The spectra were obtained by slowly scanning the carbonyl region ($1600\text{-}1700\text{ cm}^{-1}$) on the Beckman IR12 spectrophotometer. The results are shown in Table 9-2.

11-4-2 Nuclear Magnetic Resonance Investigations


All spectra were run in CCl_4 solution with TMS serving as the internal standard. The chemical shifts (in cps units) were taken from the parent amides. The results obtained are shown in Table 9-3.

11-4-3 Raman Investigations

The Raman spectra were run on the Cary 81 Raman spectrometer equipped with a helium-neon laser. All N-haloamide samples were concentrated to remove traces of CCl_4 . Samples were kept cold and were protected from light until use. The solids and the parent amides were placed directly into the special probe of the spectrometer. The oily N-bromo-N-methylacetamide was added into a capillary tube prior to analysis. The results are given in Table 9-3 for the absorption of the Amide IV band.

11-4-4 Ultraviolet Spectral Studies

All samples were determined in CH_2Cl_2 solvent. After formation of the appropriate N-haloamide and concentration of the solvent, an appropriate volume of CCl_4 was added to the residue for ir analysis. Lack of absorption at ~ 3400 and 1500 cm^{-1} confirmed the absence of t-butanol and unreacted amide. The CCl_4 solutions were then concentrated to a constant weight. To the flask was then added 10.0 ml CH_2Cl_2 and further suitably diluted for uv analysis. The results obtained are given in Table 9-4.



11-5 Photolysis of Substituted Toluamides11-5-1 Photolysis of N-Bromo-N-Methyltoluamide (28-2)

The haloamide 28-2 was formed from 0.23 g N-methyltoluamide 28-1 and 6 ml t-butylhypobromite in the manner previously described. Following concentration of the solution, a yellow residue (0.37 g) was left which was dissolved in 120 ml benzene and subjected to photolysis.

The photolysis cell was kept in a water bath at 20°C. The irradiation source was a 200 watt Hanovia medium pressure lamp 654A36 through a pyrex glass filter. The photolysis was permitted to continue for 1 h. The progress of the reaction was monitored with the starch AcOH-KI test solution which was negative after 0.5 h irradiation. The benzene was concentrated to give a residue of 0.31 g.

This residue was recrystallized 3 times from CHCl_3 :acetone (1:3) to give a white solid of 30-1: m. p. 205-206°; ir 3460 (m), 2700 (m), 1700 cm^{-1} ; nmr (D_2O) τ 2.1 (4H, m), 4.0 (2H, s), 6.6 (3H, s).

Anal. Calcd for $\text{C}_9\text{H}_{10}\text{NOBr}$: C, 47.39; H, 4.42; N, 6.14.

Found: C, 47.47; H, 4.51, N, 6.25.

The remainder of the photolysis residue (0.21 g) was dissolved in 20 ml saturated aqueous Na_2CO_3 . The solution was extracted with CH_2Cl_2 (3 x 20 ml). The organic extracts were combined, dried (MgSO_4) and concentrated to give solid 31-1 (0.113 g): ir 1700 cm^{-1} ; nmr τ 2.5 (4H, m), 4.7 (2H, s), 6.82

(3H, s); ms m/e 148 (M^+ , 16), 147 (100), 146 (84), 118 (77).

Attempted column chromatography of 31-1 on 10 g neutral alumina (petroleum ether 30:60 as eluant) gave a solid, phthalide: m. p. 69-71°, reported (159) m. p. 72-73°; ir 1775 cm^{-1} ; nmr τ 2.5 (4H, m), 4.7 (2H, s).

11-5-2 Photolysis of N-Bromo-N-t-Butyltoluamide (29-2)

The bromamide 29-2 was synthesized from 29-1 (0.22 g) and 6 ml t-butylhypobromite in the manner previously described. From the reaction a yellow solid (0.33 g) was obtained. This material was dissolved in 120 ml anhydrous benzene and photolyzed.

The photolysis conditions were as previously described. After 1 h irradiation, the solution was concentrated to give a residue (0.25 g) which was recrystallized (0.13 g only) from acetone: CHCl_3 (3:1) to yield white crystals of 30-2: m. p. 110-111°; ir 1675 cm^{-1} ; nmr τ 2.2 (4H, m), 4.1 (2H, s), 8.25 (9H, s).

The residue (0.12 g) was dissolved in 10 ml saturated Na_2CO_3 solution, stirred for 0.5 h and extracted with CH_2Cl_2 (3 x 10 ml). The combined organic extracts were dried (MgSO_4) and concentrated to give solid 31-2 (0.07 g): ir 1700, 1650 cm^{-1} ; nmr τ 2.2 (4H, m), 4.75 (2H, s), 8.6 (9H, s); ms m/e 189 (M^+ , 12), 174 (100), 134 (71).

Attemptes to reduce 31-2 (0.04 g, 1.6×10^{-4} moles) with a large excess of LiAlH_4 (0.15 g, 4×10^{-3} moles) in anhydrous ether for 24 h were unsuccessful and gave back only 31-2.

Into a 25 ml round-bottom flask was added 31-2 (0.05 g) and 5 ml 20% H_2SO_4 . The flask was fitted with a reflux condenser and

the contents were kept at reflux for 3 h. Upon cooling, the solution was extracted with CHCl_3 (3 x 15 ml). The organic extracts were combined, dried (MgSO_4) and concentrated to give a yellow solid, phthalide (0.03 g): m. p. 71-72°, reported (159) m. p. 72-73°; ir 1775 cm^{-1} ; nmr τ 2.5 (4H, m), 4.7 (2H, s). The ir and nmr spectra were superimposable with authentic sample.

11-6 Photolysis of Isomeric Cyclohexanecarboxamides

11-6-1 Photolysis of trans-Bromamide 26-3

To a 25 ml Al foil protected erlenmeyer flask was added 5 ml t-butylhypobromite solution and 26-2 (0.15 g). The contents were magnetically stirred for 2 h at 0°C. After 2 h reaction time, an aliquot was tested by ir spectroscopy for the absence of an amide hydrogen absorption at 1500 cm^{-1} . The solid resulting from the concentration of the solution was dissolved in 120 ml anhydrous benzene and added to the photo-cell kept at 20°C. A 200 watt medium pressure Hanovia lamp placed into a pyrex glass filter was used as the irradiation source. The photolysis was carried out for 45 minutes. However, starch AcOH-KI testing showed that the reaction was essentially complete in 0.5 h. The benzene solution was concentrated to give a solid residue (0.22 g): ir 3430, 3300, 1665, 1505 cm^{-1} ; nmr τ 4.3 (1H, b), 6.5 (2H, bs), 7.8 to 9.2 (30H, m). Vapour phase chromatography showed that the product of this reaction had one major peak in greater than 90 % quantity and 4 smaller peaks of which one was the amide 26-2.

A portion (0.180 g) of this photoproduct was subjected to preparative tlc on silica gel plates with 2% CH₃OH in CHCl₃ as the eluting solvent. The appropriate portion of the plates was scraped off and the silica gel was extracted with 15 ml CH₃OH for 1 h. After concentration of the CH₃OH solution, the resulting solid was dissolved in 2 ml CHCl₃. This solution was filtered through a short column containing 2 g neutral alumina and further eluted with 100 ml CHCl₃. Concentration of the CHCl₃ solvent left a solid (0.130 g) which was dissolved in 1 ml acetone:pet. ether 30:60 (1:2) and refrigerated. Overnight were formed white crystals of 32: m. p. 145-135°; ir 3430 (m), 1665, 1505 (m) cm⁻¹; ms m/e 333 (M⁺, 27), 331 (M⁺, 27), 318 (18), 316 (18), 276 (64), 274 (59), 252 (100).

Anal. Calcd for C₁₆H₃₀NOBr; C, 57.84; H, 9.10;
N, 4.22.

Found: C, 57.78; H, 9.04; N, 4.25.

About 30 mg of 32 was refluxed in 20 ml benzene for 2 h. No change was observed in the ir spectrum of the residue.

11-6-2 Photolysis of cis-Bromamide 27-3

The N-bromamide was formed from 27-3 (0.147 g) and 5 ml t-butylhypobromite in the usual manner. Upon removal of the solvent, yellow solid (0.232 g) resulted. This material was dissolved in 120 ml anhydrous benzene and photolyzed in the usual manner for 45 min. Upon concentration of the photolysate, there resulted a solid (0.233 g): ir 3350 (m), 1675, 1510 (w)

cm^{-1} ; a complex nmr spectrum showing no absorption at τ 6.5. Gas chromatography of a basified aliquot of the material showed one major peak ($\sim 90\%$) and three minor peaks none of which corresponded to the retention time of amide 27-2.

The photoproducts (0.160 g) were dissolved in 25 ml saturated Na_2CO_3 solution. To this was added 10 ml CHCl_3 and the mixture was stirred for 30 min. Separation of the layers, extraction of the aqueous phase with CHCl_3 (2 x 10 ml) and drying (MgSO_4) of the combined organic extracts gave upon concentration a solid (0.076 g). The resulting material was subjected to preparative tlc on silica gel adsorbant with 2% CH_3OH in CHCl_3 as eluting solvent mixture. The appropriate large band was scraped off and stirred with 20 ml CH_3OH for 1 h and then filtered. After concentration of the CH_3OH solution, the residue was dissolved in 2 ml CHCl_3 and filtered through a small column containing 2 g neutral alumina. CHCl_3 (100 ml) was used to flush the column. After concentration of the CHCl_3 solution, 0.06 g solid was left. This material was twice recrystallized from CHCl_3 :acetone (3:1) solvent mixture to yield a solid, 34: m. p. 92-93°; ir 1700 cm^{-1} ; ms m/e 251 (M^+ , 10), 237 (54), 236 (100).

Anal. Calcd for $\text{C}_{16}\text{H}_{29}\text{NO}$: C, 76.44; H, 11.63;
N, 5.57.

Found: C, 76.71; H, 11.65; N, 5.39.

11-7 Quantitative Aspects of Isomeric N-Bromocyclohexane-
carboxamide Photolysis

11-7-1 General Procedure

For the preparation of the N-bromamides, 50.0 mg amide and 4 ml t-butylhypobromite were used. The reaction conditions were as previously described. After 2 h reaction time, a quantity of solution just sufficient to take an ir spectrum was withdrawn. Once the absence of absorption at 1500 cm^{-1} had been confirmed, the solution was concentrated at 0° to a constant weight of residue while taking precautions to avoid exposure to light. The solid was then dissolved in 120 ml of the solvent or the solvent mixture in which the photolysis was to be done. The photolysis conditions were identical to those previously described. After photolysis the solutions were subjected to vpc quantitative analysis.

11-7-2 Quantitative Analysis

11-7-2-1 Photolysis of trans-Bromamide 26-3

In a typical experiment in the photolysis of 26-3, 0.2 ml internal standard N-t-butyltoluamide (9.7 mg/5.0 ml CHCl_3) was added to a 5.0 ml volumetric flask. Sufficient photolysate was added to make 5.0 ml solution which was then concentrated on the rotary evaporator (15° water bath temperature) until all the solvent was removed. Then 0.25 ml CHCl_3 was added and the resulting solution was analyzed by vpc using a 15% DEGS column and an oven temperature of 180° . The ratio of the area of 26-2 to internal standard was calculated and with the

assistance of a previously prepared calibration curve, the quantity of 26-2 in the solution was determined.

11-7-2-2 Photolysis of cis-Bromamide 27-3

In a typical experiment the solution from the photolysis of 27-3 was treated with Na_2CO_3 solution. After drying of the organic photolysis mixture, 5.0 ml were withdrawn and concentrated on the rotary evaporator (water bath at 15°). To the residue was added 0.25 ml 2-phenylpropanone internal standard solution (concentration 0.268 mg/ml). The solution was analyzed by vpc using a 15% DEGS column and an oven temperature of 180° . The ratio of the area of 27-2 to internal standard was calculated and with the assistance of a previously prepared calibration curve, the quantity of 27-2 in the solution was determined.

11-7-3 Solvents Used in The Photolyses

Photolysis experiments were performed using as solvents: cyclohexane; the mixture of 30 ml cyclohexane and 90 ml benzene; the mixture of 14.4 ml cyclohexane and 105.6 ml benzene; and the mixture of 10 ml cyclohexane and 110 ml benzene. The results obtained from the quantitative analyses were expressed as the percentage recovered amides 26-2 and 27-2. The information gleaned is summarized in Table 9-5.

REFERENCES

1. Y.L. Chow, *Tetrahedron Lett.*, 2333 (1964).
2. Y.L. Chow, *Can. J. Chem.*, 45, 53 (1967).
3. Y.L. Chow, *Accts. Chem. Res.*, 6, 354 (1973).
4. E.M. Burgess and J.M. Lavendish, *Tetrahedron Lett.*, 1227
(1964).
5. F. Minisci, *Synthesis*, 5, 1 (1973).
6. F. Minisci, R. Galli and M. Cecere, *Tetrahedron Lett.*, 3163
(1963).
7. J.M. Surzur, L. Stella and P. Tordo, *Bull. Soc. Chim. Fr.*,
115 (1970).
8. C.J. Albesetti, D.D. Coffman, F.W. Hoover, E.L. Jenner and
W.E. Mochel, *J. Amer. Chem. Soc.*, 81, 1489 (1959).
9. F. Minisci, R. Galli and M. Cecere, *Tetrahedron Lett.*, 4663
(1965).
10. J.P. Ferris, F.D. Gerwe and G.R. Gapski, *J. Org. Chem.*, 33,
3493 (1968).
11. A. Clerici, F. Minisci, M. Perchinunno and O. Porta; *J. Chem.
Soc., Perkin II*, 416 (1974).
12. R.S. Neale and E. Gross, *J. Amer. Chem. Soc.*, 89, 6579 (1967).
13. Y.L. Chow, M.P. Lau, R.A. Perry and J.N.S. Tam, *Can. J.
Chem.*, 50, 1044 (1972).
14. V. Malatesta and K.U. Ingold, *J. Amer. Chem. Soc.*, 95, 6400
(1973).
15. C.J. Colon, Ph. D. Dissertation, Simon Fraser University,
Burnaby, B.C., 1971.

16. M.P. Lau, A.J. Cessna, Y.L. Chow and R.W. Yip, J. Amer. Chem. Soc., 93, 3808 (1971).
17. J. Tanaka, J. Chem. Soc., Japan, 78, 1647 (1957).
18. W.S. Layne, H.H. Jaffe and H. Zimmer, J. Amer. Chem. Soc., 85, 435, 1815 (1963).
19. M.P. Lau, Ph. D. Dissertation, Simon Fraser University, Burnaby, B.C., 1970.
20. J. Spanswick and K.U. Ingold, Can. J. Chem., 48, 544, 546 (1969).
21. G.A. Russell, "Free Radicals", Vol. 1, J. Kochi, Ed., John Wiley, New York, 1973, p. 273.
22. H. Sakurai, S. Hayashi and A. Hosomi, Bull. Chem. Soc., Japan, 44, 1945 (1971).
23. J.I.G. Cadogan and I.H. Sadler, J. Chem. Soc., B, 1191 (1966).
24. G.A. Russell and R.C. Williamson, Jr., J. Amer. Chem. Soc., 86, 2357 (1964).
25. Y.L. Chow, C.J. Colon and S.C. Chen, J. Org. Chem., 32, 2109 (1967).
26. Y.L. Chow and C.J. Colon, Can. J. Chem., 45, 2559 (1967).
27. O.E. Edwards, D.H. Paskovich and A.H. Reddoch, Can. J. Chem., 51, 978 (1973).
28. K.B. Wiberg, "Physical Organic Chemistry", John Wiley, New York, 1964, p. 374.
29. W.C. Danen and R.C. Rickard, J. Amer. Chem. Soc., 94, 3254 (1972).
30. L.P. Hammett, Chem. Rev., 17, 125 (1935).

31. I.B. Afanas'ev, *Russ. Chem. Rev.*, 40, 216 (1971).
32. H.C. Brown and Y. Okamoto, *J. Amer. Chem. Soc.*, 79, 1913 (1957).
33. H. van Bekkum, P.E. Verkade and B.P. Wepster, *Rec. Trav. chim, Pays-Bas*, 78, 815 (1959).
34. R.W. Taft, *J. Phys. Chem.*, 64, 1805 (1960).
35. C.D. Johnson, "The Hammett Equation", University Press, Cambridge, 1973, p. 9.
36. M.M. Martin and G.J. Gleicher, *J. Amer. Chem. Soc.*, 86, 233 (1964).
37. C.J. Michejda and W.P. Hoss, *J. Amer. Chem. Soc.*, 92, 6298 (1970).
38. W.M. Schubert, B. Lam and J.R. Reefe, *J. Amer. Chem. Soc.*, 86, 4727 (1964).
39. C. Walling, E.R. Briggs, K.D. Wolfstirn and F.R. Mayo, *J. Amer. Chem. Soc.*, 70, 1537 (1948).
40. M. Imoto, K. Kinoshita and N. Nishigaki, *Makromol. Chem.*, 86, 217 (1965).
41. ref. 35, p. 20.
42. U. Klement and A. Schmidpeter, *Angew. Chem.*, 80, 444 (1968).
43. E.T. McBee, S. Resconich, L.R. Belohlav and H.P. Braendlin, *J. Org. Chem.*, 28, 3579 (1963).
44. L.A. Brooks, *J. Amer. Chem. Soc.*, 66, 1295 (1944).
45. L.H. Schwartzman and B.B. Corson, *J. Amer. Chem. Soc.*, 78, 322 (1956).
46. J.J. Johnson, *Org. Reactions*, Vol. 1, 210 (1942).
47. L.J. Kitchen and C.B. Pollard, *J. Amer. Chem. Soc.*, 69,

- 854 (1947).
48. E. Klages, Ber., 36, 3584 (1903).
 49. L. Friedman and H. Schechter, J. Org. Chem., 26, 2522 (1961).
 50. C.S. Marvel and C.G. Overberger, J. Amer. Chem. Soc., 67, 2251 (1945).
 51. "Table for Identification of Organic Compounds", Sec. Ed., The Chemical Rubber Co., Cleveland, 1964, p. 44.
 52. E.F. Pratt and J.F. Van De Castle, J. Org. Chem., 26, 2973 (1961).
 53. A.F. Titley, J. Chem. Soc., 517 (1926).
 54. E.L. Eliel, A.H. Goldkamp, L.E. Carosino and M. Eberhardt, J. Org. Chem., 26, 5188 (1961).
 55. R.H. Wiley and N.R. Smith, Organic Synthesis, 33, 62 (1953).
 56. J.M. Landesberg, L. Katz and C. Olsen, J. Org. Chem., 37, 930 (1972).
 57. P. Komppa, Ber., 26, 677 (1893).
 58. J.H. Brown and C.S. Marvel, J. Amer. Chem. Soc., 59, 1176 (1937).
 59. Y.L. Chow, S.C. Chen and D.W.L. Chang, Can. J. Chem., 48, 157 (1970).
 60. C.G. Hatchard and C.A. Parker, Proc. Roy. Soc., (London), A235, 518 (1956).
 61. J.A. Pople, D.L. Beveridge and P.A. Dobash, J. Chem. Phys., 47, 2026 (1967).
 62. Quantum Chemistry Program Exchange, program 114, University of Indiana, Bloomington, Indiana.

63. J.A. Pople and D.L. Beveridge, "Approximate Molecular Orbital Theory", McGraw-Hill, New York, 1970.
64. N.C. Baird, M.J.S. Dewar and R. Sustmann, J. Chem. Phys., 50, 1275 (1969).
65. J.W. Pensabene, W. Fiddler, C.J. Dooley, R.C. Doerr and A.E. Wasserman; J. Agr. Food Chem., 20, 274 (1972).
66. S. Hunig, G. Buttner, J. Cramer, L. Geldern, H. Hansen and E. Lucke, Chem. Ber., 102, 2093 (1963).
67. W.C. Danen, C.T. West and T.T. Kensler, J. Amer. Chem. Soc., 95, 5716 (1973).
68. B. Danieli, P. Manitto and G. Russo, Chem. Ind. (London), 329 (1969); ibid., 203 (1971).
69. E. Hedaya, R.L. Hinman, V. Schomaker, S. Theodoropoulos and L.M. Kyle, J. Amer. Chem. Soc., 89, 4875 (1967).
70. W.C. Danen and R.W. Gillert, J. Amer. Chem. Soc., 94, 6854 (1972).
71. P. Smith and P.B. Wood, Can. J. Chem., 44, 3085 (1966).
72. H. Bower, J. McRae and M.C.R. Symons, J. Chem. Soc., (A), 2400 (1971).
73. D.C. Straw and G.R. Moulton, J. Chem. Phys., 57, 2215 (1972).
74. P.W. Lau and W.C. Lin, J. Chem. Phys., 51, 5139 (1969).
75. N. Cyr and W.C. Lin, J. Chem. Phys., 50, 3701 (1969).
76. W.C. Lin, N. Cyr and K. Toriyama, J. Chem. Phys., 56, 6272 (1972).
77. L. Muszkat, Chem. Phy. Lett., 18, 414 (1973).

78. T. Koenig, J.A. Hoobler and W.R. Mabey, J. Amer. Chem. Soc., 94, 2514 (1972).
79. W.C. Danen and C.T. West, J. Amer. Chem. Soc., 93, 5582 (1971).
80. W.C. Danen and C.T. West, J. Amer. Chem. Soc., 95, 6872 (1973).
81. P.J. Krusic and T.A. Rettig, J. Amer. Chem. Soc., 92, 722 (1970).
82. N. Bersohn and J.C. Baird, "An Introduction to Electron Paramagnetic Resonance", W.J. Benjamin, Inc., New York, 1966, p. 40.
83. P. Tordo, E. Flesia and J.M. Surzur, Tetrahedron Lett., 183 (1972).
84. P. Tordo, E. Flesia, G. Labrot and J.M. Surzur, Tetrahedron Lett., 1413 (1972).
85. R. Livingston and H. Zeldes, J. Chem. Phys., 47, 4173 (1967).
86. M.C.R. Symons, J. Chem. Phys., 55, 1493 (1971).
87. R.O.C. Norman and B.C. Gilbert, J. Phys. Chem., 71, 14 (1967).
88. W.C. Lin and J.M. Nickel, J. Chem. Phys., 57, 3581 (1972).
89. W.C. Lin, J. Chem. Phys., 58, 2664 (1973).
90. H.W. Shields, P.J. Hamrick, Jr. and W. Redwine, J. Chem. Phys., 46, 2510 (1967).
91. W.M. Fox and P. Smith, J. Chem. Phys., 48, 1868 (1968).
92. G.W. Neilson and M.C.R. Symons, J. Chem. Soc., Faraday II, 68, 1582 (1972).

93. D. Touchard and J. Lessard, *Tetrahedron Lett.*, 4425 (1971).
94. S. Wolfe and D.V.C. Awang, *Can. J. Chem.*, 49, 1384 (1971).
95. H. Baer and W. Rank, *Can. J. Chem.*, 52, 2257 (1974).
96. R.S. Neale, *Synthesis*, 1, 1 (1971).
97. D. Touchard and J. Lessard, *Tetrahedron Lett.*, 3830 (1973).
98. Y.L. Chow and R.A. Perry, *Tetrahedron Lett.*, 531 (1972).
99. E. Flesia, A. Croatto, P. Tordo and J.M. Surzur, *Tetrahedron Lett.*, 535 (1972).
100. D.H.R. Barton, A.L.J. Beckwith and A. Goosen, *J. Chem. Soc.*, 181 (1965).
101. R.C. Petterson and A. Wambsgans, *J. Amer. Chem. Soc.*, 86, 1648 (1964).
102. H.J. Dauben and L.L. McCoy, *J. Amer. Chem. Soc.*, 81, 4863 (1959).
103. J.R. Shelton and C. Cialdella, *J. Org. Chem.*, 23, 1128 (1958).
104. W.J. Bailey and J. Bello, *J. Org. Chem.*, 20, 525 (1955).
105. G. Peiffer, *Bull. Soc. Chim., Fr.*, 537, 540 (1963).
106. J.A. Pople, D.P. Santry and G.A. Segal, *J. Chem. Phys.*, 43, S129 (1965).
107. E.M. Evleth, P.M. Horowitz and T.S. Lee, *J. Amer. Chem. Soc.*, 95, 7948 (1973).
108. L.F. Hamilton and S.G. Simpson, "Calculations of Analytical Chemistry", Mc-Graw-Hill, New York, 1960, p.4.
109. R.W. Fessenden and R.H. Schuler, *J. Chem. Phys.*, 39, 2147 (1963).

110. R.E. Cramer and R.S. Drago, J. Amer. Chem. Soc., 90, 4790 (1968).
111. A. Rauk, Chemistry Department, University of Calgary, private communication, 1973.
112. W.C. Danen and C.T. West, J. Amer. Chem. Soc., 96, 2447 (1974).
113. P.J. Krusic, P. Meakin and J.P. Jesson, J. Phys. Chem., 25, 3438 (1971).
114. T. Koenig, R.A. Wielessek and J.G. Huntington, Tetrahedron Lett., 2283 (1974).
115. T. Koenig, J.A. Hoobler, C.E. Klopfenstein, G. Hedden, F. Sunderman and B.R. Russell, J. Amer. Chem. Soc., 96, 4573 (1974).
116. R.N. Gillert, Ph. D. Dissertation, Kansas State University, Manhattan, Kansas.
117. Y.L. Chow and T.C. Joseph, J. Chem. Soc., Chem. Comm., 490 (1969).
118. K. Ziegler, A. Spath, E. Schaaf, W. Schumann and E. Winkelmann, Ann., 551, 80 (1942).
119. K. Sakai, N. Koya and J.P. Anselme, Tetrahedron Lett., 4543 (1970).
120. M.L. Poutsma, J. Amer. Chem. Soc., 87, 4285 (1965).
121. G.S. Hammond, J. Amer. Chem. Soc., 77, 334 (1955).
122. D.H.R. Barton, J.M. Beaton, L.E. Geller and M.M. Pecket, J. Amer. Chem. Soc., 82, 2640 (1960).
123. E.J. Corey and W.R. Hertler, J. Amer. Chem. Soc., 82, 1657 (1960).

124. M.E. Wolff, Chem. Rev., 63, 55 (1963).
125. C. Walling and A. Padwa, J. Amer. Chem. Soc., 85, 1597
(1963).
126. Y.L. Chow and A.C.H. Lee, Chem. and Ind., 827 (1967).
127. L.P. Kuhn, G.A. Kleinspehn and A.C. Duckworth, J. Amer.
Chem. Soc., 89, 3858 (1967).
128. R.S. Neale, N.L. Marcus and R.G. Schepers, J. Amer. Chem.
Soc., 88, 3051 (1966).
129. A.L.J. Beckwith and J.E. Goodrich, Aus. J. Chem., 18,
747 (1965).
130. M. Akhtar, "Advances in Photochemistry", Vol. 2, W.A. Noyes,
Jr., G.S. Hammond and J.N. Pitts, Jr., Eds.,
Interscience, New York, 1964, p. 263.
131. R. Kh. Freidlina, "Advances in Free Radical Chemistry",
Vol. 1, G.H. Williams, Ed., Logos Press, New
York, 1965, p. 271.
132. S. Glasstone, K.J. Laidler and H. Eyring, "The Theory of
Rate Processes", Mc-Graw Hill, New York, 1941,
p. 88.
133. R.H. Hesse, "Advances in Free Radical Chemistry", Vol. 3,
G.H. Williams, Ed., Logos Press, New York, 1969,
p. 83.
134. K. Heusler and J. Kalvoda, Angew. Chem. internat. Edit.,
3, 525 (1964).
135. S. Winstein and N.J. Holness, J. Amer. Chem. Soc., 77,
5562 (1955).

136. H. Sachse, Ber., 23, 1368 (1890).
137. M. Davis and O. Hassel, Acta Chem. Scan., 17, 1181 (1963).
138. R.A. Wohl, Chimia, 18, 219 (1964).
139. E.L. Eliel, S.H. Schroeter, T.J. Brett, F.J. Biros and J.C. Richler, J. Amer. Chem. Soc., 88, 3327 (1966).
140. E.L. Eliel, N.L. Allinger, S.J. Angyal and G.A. Morrison, "Conformational Analysis", John Wiley, New York, 1965, p. 78.
141. N.L. Allinger, University of Georgia, private communication, 1972.
142. S.J. Angyal and C.S. Macdonald, J. Chem. Soc., 686 (1952).
143. L.P. Kuhn, J. Amer. Chem. Soc., 74, 2492 (1952).
144. E.L. Eliel, "The Stereochemistry of Carbon Compounds", McGraw-Hill, New York, 1962, p.232.
145. D.H.R. Barton, J. Chem. Soc., 2174 (1949).
146. Quantum Chemistry Program Exchange, COORD program 136, University of Indiana, Bloomington, Indiana.
147. F.R. Dollish, W.G. Fateley and F.F. Bentley, "Characteristic Raman Frequencies of Organic Compounds", John Wiley, New York, 1974, p. 124.
148. N.M.R. Spectral Catalog, Varian Associates, Palo Alto, 1963, p. 213.
149. J.N.S. Tam, Ph. D. Dissertation, Simon Fraser University, Burnaby, B.C., 1971.
150. D.R. Storm and D.E. Koshland, Jr., J. Amer. Chem. Soc., 94, 5805 (1972).

151. L. Giering, M. Berger and C. Steel, J. Amer. Chem. Soc., 96, 953 (1974).
152. F.D. Lewis, R.W. Johnson and D.R. Korg, J. Amer. Chem. Soc., 96, 6100 (1974).
153. F.D. Lewis, R.W. Johnson and D.E. Johnson, J. Amer. Chem. Soc., 96, 6090 (1974).
154. F. Wild, "Characterization of Organic Compounds", Sec. Ed., Cambridge University Press, London, 1962, p. 218.
155. C. Walling, private communication, 1968.
156. C. Walling and A. Padwa, J. Org. Chem., 27, 2976 (1962).
157. M.J. Mintz and C. Walling, Org. Syn., 49, 9 (1969).
158. J. Sicher, F. Sipos and M. Tichy, Coll. Czech. Chem. Comm., 26, 847 (1961).
159. J.H. Gardner and C.A. Naylor, Org. Syn. 16, 71 (1936).